HELVETICA PHYSICA ACTA

SOCIETATIS PHYSICAE HELVETICAE
COMMENTARIA PUBLICA

VOLUMEN XXV

FASCICULUS TERTIUS

BASILEAE · IN AEDIBUS BIRKHAEUSER
MCMLII

NACHDRUCK 1968

Copyright 1952 by Schweizerische Physikalische Gesellschaft.
Société Suisse de Physique. - Società Fisica Svizzera.
Nachdruck verboten. - Tous droits réservés. - Printed in Switzerland.

Nuclear Spectroscopy with Harmonic Oscillator Wave-Functions

by **Igal Talmi***), Swiss Federal Institute of Technology (Zurich).

(20. IX. 1951.)

Zusammenfassung: Die Beschränkung auf harmonische Zentralpotentiale ermöglicht die Entwicklung einer neuen (vom üblichen Slaterschen Verfahren verschiedenen) Methode zur Berechnung der Matrixelemente der Wechselwirkung zwischen den äusseren Nukleonen im Schalenmodell, welche insbesondere auch den Fall nichtzentraler Kräfte in einfacher Weise zu behandeln gestattet. Als Anwendung wird gerechnet: Die Ordnung der Niveaus in der j^n-Konfiguration, für einige physikalisch interessante Fälle; die von der Spin-Bahn-Kopplung zwischen den Nukleonen herrührende Dublettaufspaltung, und die Lage der untersten Terme von Li^7 bei Berücksichtigung von Spin-Bahn-Kopplung und Tensorkräften.

Introduction.

The discovery of the "magic numbers" and the general success of the shell model in explaining many experimental facts about nuclei have led theoretical physicists to work with the methods of atomic spectroscopy in the calculation of nuclear levels. In this attempt three main difficulties are encountered:

(a) The form of the interaction potential and its exchange character are not sufficiently known. In addition, the form of the wave-functions can be only guessed. These facts make necessary the examination of various forms of the potential.

(b) There exists a lack of sufficient experimental information about nuclear spectra. There are only a few excited states for which the spin and parity assignments have been carried out. Whereas in atomic spectroscopy it was possible from the vast amount of experimental material to determine easily the several parameters used to describe the atomic levels, here these parameters must be mathematically evaluated.

(c) Non-central interactions, such as tensor forces, must here be taken into account, whereas in atomic spectra such interactions give a negligible small contribution.

*) Hebrew University, Jerusalem, Israel.

Thus, the Slater method, used in atomic spectroscopy, is not practical in nuclear spectroscopy, because:

(a) one must work with different potentials, each of which must be expanded in a series of Legendre polynomials, for which the coefficients are usually complicated functions;

(b) this fact makes impractical the calculation of the matrix elements, which now must be completely carried out; and

(c) for non-central interactions the method looses even its formal simplicity and becomes very much involved.

In the first part of this paper an alternative method is suggested and developed. Although this method is confined to the use of harmonic oscillator wave-functions, this limitation does not seem to be too serious in view of the fact that the form of the wave-functions cannot be determined if the interaction is not known. We use these wave-functions only as a model in order to learn the results for various types of interactions. That our choice of wave-functions is reasonable is seen from the rough agreement of the level order in the oscillator potential with that found experimentally. In any case, one would not expect the exact form of the wave-functions to have a decisive effect on the results. Due to the separability of the potential of two nucleons moving in the central field of a (3-dimensional) harmonic oscillator in the relative and center-of-gravity coordinates, it is possible to write the wave-functions of two interacting nucleons as a finite sum of products of functions which depend on these coordinates. This transformation makes it possible, when calculating matrix elements to integrate immediately over the center-of-gravity coordinate, of which the interaction energy is usually independent. What remains is only to calculate matrix elements of the interaction energy (which may be a complicated function of the relative coordinate and of the relative momentum), in a scheme of wave-functions written in terms of this coordinate.

After a survey of the shell model and the Slater method (§ 1, 2), the proposed method is described and discussed (§ 3). In § 4 the transformation of the wave-functions from the coordinates of the two nucleons to the relative and center-of-gravity coordinates is considered. The Slater method can be regarded as an approximation procedure in the neighbourhood of the long range limit, whereas our method can serve as a good approximation method in the short range limit, which might be looked upon as the proper approximation in the case of nuclear spectroscopy (this point is discussed in § 6).

In the second part of this paper the determination of the ground state of the j^n configuration is treated. An empirical rule, stated by MAYER[1]), is that the total angular momentum J of the ground state is equal to zero if n is even, and equal to j if n is odd. This rule was then derived theoretically by MAYER[2]) and RACAH[3]) for Majorana forces in the case of δ-type interaction, or, better said, in the short range approximation. A few cases, however, were found experimentally where this rule does not hold. KURATH[4]) and others have suggested that these deviations could be explained by considering the effect of the finite range of the forces. It has already been pointed out by the author[5]) that potentials more singular than that used by KURATH give different results. With the method described in this paper this problem can be treated quite generally. After the examination of several interaction potentials it can be concluded that for physically admissible values of the parameters (range of the forces and extension of the wave-functions), the order of levels is that given by the short range approximation. The break down of the above rule may be due to perturbations from other configurations or to the action of tensor forces.

In § 5 we present the problem and show how our method may be applied to obtain directly the values of the energy levels which are already calculated in the Slater method. The dependence of the results on the form and range of the potential is treated in § 6 for the $(d_{5/2})^3$ configuration. In § 7 the configuration $(f_{7/2})^3$ is treated and discussed. The configuration $(g_{9/2})^3$ is treated in § 8. In several nuclei in which these configurations appear (according to the shell model), the spin of the ground state is not that predicted by the jj-coupling scheme in the short range limit. These cases are especially interesting as they may give direct information about the nuclear interactions (in contrast to the other odd-even nuclei whose level schemes have been classified, in which only the states of the single nucleon are observed, thus giving information about the central field only and providing no direct information about the nuclear forces).

The third part of this paper deals with mutual spin-orbit interactions. An interesting problem is whether the spin-orbit interaction, introduced by CASE and PAIS[6]) in order to explain the results of scattering experiments, can give for heavier nuclei sufficientsplitting between the states $j = l + 1/2$ and $j = l - 1/2$ (of a single nucleon) to satisfy the requirements of the shell model. We state the problem and calculate matrix elements of the mutual spin-orbit interaction in § 9. A few cases of a single nucleon outside closed shells are treated

in § 10, and the resulting doublet splitting is calculated. With reasonable values of the parameters an order of magnitude of a few MeV is obtained. The results are, however, very sensitive to the nuclear radius in the interesting region.

In the fourth part of the paper the Li^7 nucleus is discussed. In this nucleus only one excited state has been found in the energy region between the ground state and several MeV. As early experiments showed that this excited level has a compound nature, it was suggested by INGLIS[7]) that it may be composed of the four excited levels of the jj-coupling configuration $(p_{3/2})^3_N\, p_{3/2\,P}$ which may perhaps coincide (but he was not able, using only central forces, to obtain such a coincidence). Our method was used to take account also of tensor forces and to check whether their contribution may bring coincidence of those excited levels. The $(p_{3/2})_N\, p_{3/2\,P}$ configuration is treated in § 12 for the case of central interactions with tne various exchange operators. The term values were calculated by the sum method combined with the use of the quantum number of the total isotopic spin. In § 13 the matrix elements of the tensor forces interaction for this configuration are calculated. The results (§ 14) show that, for reasonable values of the interaction parameters it is possible to obtain such a coincidence.

As recent experiments have shown that a spin 1/2 for the excited level is compatible with the known facts[8]), the natural explanation arose that the two lowest states are the components of a ^2P state (in LS-coupling). LS-coupling for Li^7 is not in contradiction with the shell model, as Li^7 is a light nucleus; it is believed that only for heavier nuclei does jj-coupling take place. It is known that neither the Thomas interaction nor the magnetic spin-orbit interaction can give sufficient splitting between the components of the ^2P ground state. The splitting which results from the Case and Pais interaction is calculated for the ^2P state of the configuration $p^3_N\, p_P$ (§ 15). The result is of the right order of magnitude but the splitting obtained is again very sensitive to the nuclear dimensions.

I. The Method of the Harmonic Oscillator Wave-Functions.

§ 1. *The shell model.*

The term "nuclear spectroscopy" is well defined in experimental physics; it means the measurement of nuclear spectra, their classification, and level assignment. On the other hand in theoretical physics this term does not usually mean "the theory of nuclear spectra", but is more limited. It is mostly used in the sense of "the use of the methods of atomic spectroscopy in explaining nuclear spectra".

In the past many attempts have been made to apply the methods of atomic spectroscopy to the calculation of nuclear energy levels. Meanwhile more experimental material has been gathered, especially in the region of high excitation energies, and the theories which successfully explained these facts were statistical in their nature. Only in the last few years has it become clear that there are regularities in the nuclei which are not of a statistical nature (magic numbers). Various "shell models" (which are in fact the former Hartree approximations) have been proposed, the most successful of which is the one based on the strong spin-orbit interaction[1])[9]). This model does not only explain the magic numbers and the spins of the ground states of nuclei, but can also be applied to the classification of level schemes in the low energy region[10]). It appears that experiment now forces the theoretician to accept a theory which he earlier abandoned and for the validity of which there are not yet sufficient theoretical grounds.

The basic assumption of any shell model is that the average field which acts on a single nucleon can be approximated by a central field in which the nucleon has a definite state (characterized by quantum numbers n and l). The nucleons occupy the lowest states and may form closed shells. A magic nucleus is a nucleus which contains closed shells only. The characteristics of the ground state are determined by the interaction of the nucleons outside the closed shells. This interaction energy is usually taken as a perturbation on the zero order energy, which is the sum of the energies of the single nucleon in the central field. The zero order energy is the same for all the states of a given configuration (i.e., the nucleons outside closed shells occupy definite states of the central field). In addition to the central field acting on the nucleons there can also be an interaction of the spin of a nucleon with its orbital angular momentum (the usual spin-orbit interaction). If this is large compared to the mutual interaction of the nucleons, the spins (i.e. total angular momenta) of the nucleons j are good quantum numbers. Thus every nucleon has a definite n, l, and j. This is the jj-coupling scheme which is postulated in the shell model of M. G. MAYER.

To the zeroth order the wave-functions of the nucleons are products of the wave functions of the single nucleon in the central field. The wave-functions of the nucleons in the states $n_1 l_1$, $n_2 l_2$, ..., $n_m l_m$, with other quantum numbers a_1, a_2, ..., a_m (where a, for example, could be the magnetic quantum number m) is:

$$\psi_A(x_1, x_2, \ldots, x_m) = \psi_{a_1 n_1 l_1}(x_1)\, \psi_{a_2 n_2 l_2}(x_2) \ldots \psi_{a_m n_m l_m}(x_m). \qquad (1)$$

The zero order energy is degenerate, since it is the same for all the states of the configuration. If the mutual interaction of the nucleons is taken into account this degeneracy is partly removed, as known from perturbation theory. The first order energies are then the eigenvalues of that part of the interaction energy which belongs to the configuration.

The appropriate zero-order wave-functions are definite linear combinations of the wave functions ψ_A determined by the quantum numbers of the interaction energy (these are, for example L and S in the case of Russel Saunders coupling, J in the case of jj-coupling, etc.). Therefore the matrix elements of the interaction energy is a sum of matrix elements $(A \mid V \mid B)$. The interaction energy has the form $\sum_{i<j} V_{ij}$ where $V_{ij} = V_{ij}(x_i, x_j)$ describes the interaction of the i-th and j-th nucleons. In evaluating the matrix elements of one of these terms we can integrate over the coordinates x_l, $l \neq i, l \neq j$, and obtain:

$$\left.\begin{aligned} &\int\int \cdots \int \psi^*_{a_1}(x_1)\, \psi^*_{a_2}(x_2) \ldots \psi^*_{a_m}(x_m)\, V_{ij}(x_i, x_j)\, \psi_{b_1}(x_1)\, \psi_{b_2}(x_2) \ldots \\ &\quad \ldots \psi_{b_m}(x_m)\, dx_1\, dx_2 \ldots dx_m = \delta_{a_1 b_1}\, \delta_{a_2 b_2} \ldots \\ &\quad \ldots \delta_{a_{i-1} b_{i-1}}\, \delta_{a_{i+1} b_{i+1}} \ldots \delta_{a_{j-1} b_{j-1}}\, \delta_{a_{j+1} b_{j+1}} \ldots \delta_{a_m b_m} \times \\ &\quad \times \int\int \psi^*_{a_i}(x_i)\, \psi^*_{a_j}(x_j)\, V_{ij}(x_i, x_j)\, \psi_{b_i}(x_i)\, \psi_{b_j}(x_j)\, dx_i\, dx_j . \end{aligned}\right\} \quad (2)$$

Therefore the matrix elements of V in the zero-order scheme are the sums of matrix elements of the type (2). The coefficients depend only on the operators commuting with the interaction energy (quantum numbers) and may be calculated without the explicit knowledge of the interaction, as they are independent of the exact form of the wave functions. There are well developed methods for obtaining them, as given by CONDON and SHORTLEY[11]), G. RACAH[12]) and others. The explicit dependence on the form of the interaction is contained in the matrix elements which we shall consider in some detail.

§ 2. *Survey of the Slater Method.*

The important feature of the matrix element

$$\int\int \psi^*_{a_1}(\vec{r}_1)\, \psi^*_{a_2}(\vec{r}_2)\, V_{12}(\vec{r}_1 - \vec{r}_2)\, \psi_{b_1}(\vec{r}_1)\, \psi_{b_2}(\vec{r}_2)\, d^3 r_1\, d^3 r_2 \quad (3)$$

is that the ψ are functions of $\vec{r}_1$ and $\vec{r}_2$, and V_{12} is a function of $\vec{r}_1 - \vec{r}_2$. The usual way of treating such expressions in atomic spectroscopy was developed by J. SLATER[13]), who expressed $V(\vec{r}_1 - \vec{r}_2)$ as

a function of $\vec{r}_1$ and $\vec{r}_2$. The procedure is to expand $V(\vec{r}_1 - \vec{r}_2)$ in a series of Legendre polynomials, the argument of which is the angle ω_{12} between $\vec{r}_1$ and $\vec{r}_2$ with coefficients which are functions of $|\vec{r}_1|$ and $|\vec{r}_2|$:

$$V(\vec{r}_1 - \vec{r}_2) = \sum_{k=0}^{\infty} f_k(r_1, r_2)\ P_k(\cos \omega_{12})\,. \tag{4}$$

$P_k(\cos \omega_{12})$ can be expanded in a finite sum of products of spherical harmonics which are functions of ϑ_1, φ_1 and ϑ_2, φ_2 respectively (these are the polar angles of $\vec{r}_1$ and $\vec{r}_2$). At this stage the angular integrations can be performed, and a sum of radial integrals

$$R^k(a_1, a_2, b_1, b_2) = \int\int R_{a_1}(r_1)\, R_{a_2}(r_2)\, f_k(r_1, r_2)\, R_{b_1}(r_1)\, R_{b_2}(r_2)\, dr_1 dr_2 \tag{5}$$

remains, the coefficients of which are products of two integrals of the type $\int \Theta_k\, \Theta_l\, \Theta_{l'}\, d\cos\vartheta$ (only finite number of these coefficients do not vanish for definite a_1, a_2, b_1, b_2). We shall mention in this work the F^k only, but all the considerations are true mutatis mutandis for the G^k too

$$[F^k(a_1, a_2) = R^k(a_1, a_2, a_1, a_2) \quad G^k(a_1, a_2) = R^k(a_1, a_2, a_2, a_1)]\,.$$

This procedure is very useful in atomic spectroscopy because there the interaction is given by $V_{12} = e^2/|\vec{r}_1 - \vec{r}_2|$ and there exists the simple expansion:

$$\frac{1}{|\vec{r}_1 - \vec{r}_2|} = \sum_{k=0}^{\infty} \frac{r_<^k}{r_>^{k+1}} P_k(\cos \omega_{12}) \qquad r_< = \mathrm{Min}\,(r_1, r_2) \qquad r_> = \mathrm{Max}\,(r_1, r_2).$$

The wave functions are not easy to compute, and their radial part is the only indeterminate factor of the F^k. In fact, the atomic spectroscopists did not bother themselves with the calculations of the F^k, as in any case many energy levels were measured, so that it was easy to evaluate the F^k from some of them, and check whether these values of the Slater parameters really gave the other levels as well. In nuclear spectroscopy, on the other hand, this is impossible as there are usually only very few levels measured and classified. Therefore if one is to use the Slater-method, the F^k must be mathematically evaluated. Even for the central forces, however, we do not know the exact form of the potential. We should therefore calculate the energy levels for different forms of the potential. However even in simple cases such as the Yukawa potential, the calculation of the F_k is so complicated that Slater-method is of little practical value.

For complicated interactions, such as tensor forces and mutual spin-orbit interaction, the expansion is very complicated and of practically no value (an example of such an expansion is given in a paper of MARVIN[14]).

§ 3. *The alternative method for the oscillator wave functions.*

To overcome these difficulties we make use of the fact that the interaction energy depends only on the relative coordinate $\vec{r} = \vec{r}_2 - \vec{r}_1$, and our procedure is to express also the wave functions as functions of $\vec{r} = \vec{r}_2 - \vec{r}_1$ and the other coordinate $\vec{R} = (\vec{r}_1 + \vec{r}_2)/2$ (the coordinate of the center of gravity of the 1st and 2nd nucleons). This transformation enables us, when calculating matrix elements, to integrate immediately with respect to R, and we are left with a single integration of $\int \psi_1^*(\vec{r})\, V(\vec{r})\, \psi_2(\vec{r})\, d^3r$ which can usually be carried out without difficulties.

This coordinate transformation is always possible, but the functions of $\vec{r}$ and $\vec{R}$ generally turn out to be very complicated. The success of this procedure depends on the proper choice of the wave-functions. The best choice would be that one which allows us to expand the wave-function $\psi_{a_1}(\vec{r}_1)\, \psi_{a_2}(\vec{r}_2)$ in a finite sum of products of functions which depend on $\vec{r}$ and $\vec{R}$ respectively. This would certainly be the case if the potential of the central field, which is the sum $V_c(r_1^2) + V_c(r_2^2)$, is also separable in the coordinates r and R.

The condition for such a decomposition is:

$$V_c(r_1^2) + V_c(r_2^2) = U(R^2) + W(r^2)\,. \tag{6}$$

Putting $r = 0$ we obtain:

$$2\, V_c(R^2) = U(R^2) + \text{const.}$$

and putting $R = 0$ we obtain:

$$2\, V_c(r^2) = W(4\, r^2) + \text{const.}$$

If we now put in (6) $r_1^2 = r_2^2$ so that $R^2 = r_1^2 \cos^2\alpha$, $r^2 = 4\, r_1 \sin^2\alpha$ where $2\,\alpha$ is the angle between $\vec{r}_1$ and $\vec{r}_2$ we obtain:

$$2\, V_c(r_1^2) = 2\, V_c(r_1^2 \cos^2\alpha) + 2\, V_c\left(\frac{4\, r_1^2 \sin^2\alpha}{4}\right) + \text{const.}$$

Differentiation with respect to α yields:

$$0 = -2\, r_1^2 \cos\alpha \sin\alpha\, V_c'(r_1^2 \cos^2\alpha) + 2\, r_1^2 \sin\alpha \cos\alpha\, V_c'(r_1^2 \sin^2\alpha)$$

or:

$$V_c'(r_1^2 \cos^2\alpha) = V_c'(r_1^2 \sin^2\alpha)$$

which means $V_c'(r^2) = \text{const.} = A$, i.e. $V_c(r^2) = A\,r^2 + \text{const.}$ Therefore the only potential (possessing a derivative) which satisfies this condition is the harmonic oscillator potential:

$$\omega\,r_1^2 + \omega\,r_2^2 = \frac{1}{2}\,(4\,\omega^2\,R^2 + \omega^2\,r^2)\,.$$

Taking the wave functions of the harmonic oscillator we can decompose every wave-function $\psi_{a_1}(\vec{r_1})\,\psi_{a_2}(\vec{r_2})$ into a finite sum of terms of the form $\psi_1(\vec{R})\,\psi_2(\vec{r})$ (where ψ_1, ψ_2 are essentially functions of the same kind as ψ_{a_1}, ψ_{a_2}).

In order to utilize this method we must, therefore, use a very special form of the wave functions. This is not such a serious limitation, however, as the exact form of the potential and hence of the wave-functions, is not accurately known. We shall therefore be satisfied with the harmonic oscillator wave-functions, using them as model wave-functions, in order to learn the behaviour of, say, the energy levels in terms of the nuclear radius, range, magnitude and form of the potential.

Compared with other model wave-functions, it seems that, physically, those of the harmonic oscillator are quite good, as the order of levels in the shell model is roughly that of an oscillator potential well.

The potential of a single nucleon bound harmonically, besides being in a central potential, is separable also in Cartesian coordinates. Therefore every function of the three dimensional oscillator can be given as a product of three wave-functions of the one dimensional oscillator depending on the Cartesian coordinates x, y, and z. This representation of the wave-functions has been extensively used[15][16]. The coordinates used in this work are, however, the polar coordinates, and the wave functions are therefore a product of a function of r and a spherical harmonic.

The radial parts of the wave functions

$$\psi\,(r, \vartheta, \varphi) = \frac{R(r)}{r}\,Y_l^{(m)}\,(\vartheta, \varphi)$$

are easily calculated, and can be shown to be of the form:

$$R_{nl}(r) = N_{nl}\,e^{-\frac{\nu}{2}\,r^2}\,r^{l+1}\,v_{nl}\,(r)$$

where N_{nl} is a normalization factor, and v_{nl} is an associated Laguerre polynomial[17] (properly normalized):

$$v_{nl}\,(r) = L_{n+l+\frac{1}{2}}^{l+\frac{1}{2}}\,(\nu\,r^2)$$

ν is given by $\nu = \omega m/h$, and m and ω appear in the Hamiltonian of the harmonic oscillator:

$$H = \frac{1}{2m}(p^2 + m^2\omega^2 r^2).$$

The explicit expression for these $L^{l+1/2}_{n+l+1/2}$ is

$$L^{l+\frac{1}{2}}_{n+l+\frac{1}{2}}(\varrho) = \sum_{k=0}^{n}(-1)^k 2^k \binom{n}{k} \frac{(2l+1)!!}{(2l+2k+1)!!}\varrho^k.$$

With this definition the normalization factor becomes:

$$N^2_{nl} = \frac{2^{l-n+2}(2l+2n+1)!!\,\nu^{l+3/2}}{\sqrt{\pi}\,n!\,[(2l+1)!!]^2}.$$

The first few functions are:

for $n = 0$

$$R_l(r) = N_l e^{-\frac{\nu}{2}r^2} r^{l+1} \qquad \text{and} \quad N^2_l = \frac{\sqrt{\nu}\,\nu^{l+1}\,2^{l+2}}{\sqrt{\pi}\,1\cdot 3\cdots(1+2l)},$$

for $n = 1$

$$v_{1l} = 1 - \frac{2\nu}{2l+3}r^2 \qquad \text{and} \quad N^2_{1l} = \frac{\sqrt{\nu}\,\nu^{l+1}\,2^{l+1}\,(2l+3)}{\sqrt{\pi}\,1\cdot 3\cdots(1+2l)},$$

for $n = 2$

$$v_{2l} = 1 - \frac{4\nu}{2l+3}r^2 + \frac{4\nu^2}{(2l+3)(2l+5)}r^4$$

$$\text{and } N^2_{2l} = \frac{\sqrt{\nu}\,\nu^{l+1}\,2^{l-1}\,(2l+3)(2l+5)}{\sqrt{\pi}\,1\cdot 3\cdots(1+2l)}.$$

These are the only wave-functions which will be used in the following. All of them satisfy:

$$\int_0^\infty R^2_{nl}(r)\,dr = 1;$$

the $Y^{(m)}_l(\vartheta, \varphi)$ should therefore also be normalized to unity.

We shall have to calculate integrals of the form

$$I_{nl} = \int_0^\infty R^2_{nl}(r)\,V(r)\,dr$$

The integrals I_{nl} with $n \neq 0$ can be expressed as sums of integrals I_{0l} which we shall write simply as I_l. The respective formulae are:

$$I_{1l} = \frac{2l+3}{2}I_l - (2l+3)I_{l+1} + \frac{2l+5}{2}I_{l+2}$$

$$I_{2l} = \frac{(2l+3)(2l+5)}{8}I_l - \frac{(2l+3)(2l+5)}{2}I_{l+1} + \frac{(2l+5)(6l+13)}{4}\times$$

$$\times I_{l+2} - \frac{(2l+5)(2l+7)}{2}I_{l+3} + \frac{(2l+7)(2l+9)}{8}I_{l+4}.$$

We shall not need here formulae for higher n, but they can be easily calculated. These I_l, as we shall see later, replace the F_k of the Slater method, but unlike the latter can be calculated by a simple integration.

§ 4. *The transformation to the relative and center of gravity coordinates.*

The zero-order Hamiltonian of two nucleons moving in the field of the oscillator potential is:

$$H = \frac{1}{2m}(p_1^2 + m^2\omega^2 r_1^2) + \frac{1}{2m}(p_2^2 + m^2\omega^2 r_2^2) .$$

We make now the canonical coordinate transformation:

$$\vec{r} = \vec{r}_2 - \vec{r}_1 \qquad \vec{p} = \frac{\vec{p}_2 - \vec{p}_1}{2}$$

$$\vec{R} = \frac{\vec{r}_2 + \vec{r}_1}{2} \qquad \vec{P} = \vec{p}_2 + \vec{p}_1$$

which introduces the relative coordinate and the center of gravity coordinate of the two nucleons, with the respective momenta. The Hamiltonian expressed in terms of the new variables is:

$$H = \frac{1}{2M}(P^2 + M^2\omega^2 R^2) + \frac{1}{2\mu}(p^2 + \mu^2\omega^2 r^2)$$

where:

$$M = 2m, \qquad \mu = \frac{1}{2}m .$$

This is the Hamiltonian of two harmonic oscillators with masses M and μ. The solution of the corresponding wave-equation can be written as a product of wave-functions of the two oscillator potentials depending on R and r respectively. The angular momenta and the number of nodes which characterize these wave functions will be called L, Λ and N, n respectively.

If we want to express the wave-function $\psi^{m_1}_{n_1 l_1}(\vec{r}_1)\,\psi^{m_2}_{n_2 l_2}(\vec{r}_2)$ of two nucleons with definite quantum numbers $n_1\, l_1\, m_1$ and $n_2\, l_2\, m_2$, as a sum of products $\psi^{M}_{NL}(\vec{R})\,\psi^{m}_{n\Lambda}(\vec{r})$ we must find out what values of N, L, M and n, Λ, m should be taken into account. It is obvious that the integrals (quantum numbers) of the system must have the same values on both sides. We thus have the following restrictions:

(1) The z-component of the orbital angular momentum.

$$m_1 + m_2 = M + m .$$

(2) The energy.

$$\hbar\,\omega\,(2\,n_1+l_1+2\,n_2+l_2+3)=\hbar\,\omega\,(2\,N+L+2\,n+\Lambda+3)$$

which implies

$$2\,n_1+2\,n_2+l_1+l_2=2\,N+2\,n+L+\Lambda\,.$$

(3) The symmetry. Instead of the wave-function $\psi^{m_1}_{n_1 l_1}(\vec{r}_1)\,\psi^{m_2}_{n_2 l_2}(\vec{r}_2)$ (in the case that n_1, l_1, m_1, differ from n_2, l_2, m_2) it is useful to take the symmetric and anti-symmetric combinations:

$$\frac{1}{\sqrt{2}}\left(\psi^{m_1}_{n_1 l_1}(\vec{r}_1)\,\psi^{m_2}_{n_2 l_2}(\vec{r}_2)+\psi^{m_1}_{n_1 l_1}(\vec{r}_2)\,\psi^{m_2}_{n_2 l_2}(\vec{r}_1)\right) \tag{7}$$

$$\frac{1}{\sqrt{2}}\left(\psi^{m_1}_{n_1 l_1}(\vec{r}_1)\,\psi^{m_2}_{n_2 l_2}(\vec{r}_2)-\psi^{m_1}_{n_1 l_1}(\vec{r}_2)\,\psi^{m_2}_{n_2 l_2}(\vec{r}_1)\right) \tag{8}$$

which are multiplied by $+1$ and (-1) respectively under the transformation $\vec{r}_1\to\vec{r}_2$, $\vec{r}_2\to\vec{r}_1$ (which induces the transformation $\vec{r}\to-\vec{r}$, $\vec{R}\to\vec{r}$), and therefore $\psi_L(\vec{R})\,\psi_\Lambda(\vec{r})$ is multiplied by $(-1)^\Lambda$ (the parity of $\psi_\Lambda(r)$]. Therefore:

Symmetrical (antisymmetrical) wave-functions contain only even (odd) values of Λ in their expansion.

(4) Parity. The transformation $\vec{r}_1\to-\vec{r}_1$ corresponds to $\vec{r}\to 2\vec{R}$, $\vec{R}\to\vec{r}/2$. The radial part of the function $\psi_L(\vec{R})\,\psi_\Lambda(\vec{r})$, which is the only part that changes, is $f(\sqrt{2\nu}\,R)\,g(\sqrt{\nu}\,r/\sqrt{2})$ (the factors 2 and 1/2 multiplying the ν of the oscillator potential come from $M=2\,m$, $\mu=m/2$). Therefore it is changed under the transformation according to:

$$f(\sqrt{2\,\nu}\,R)\,g\left(\sqrt{\frac{\nu}{2}}\,r\right)\to f\left(\sqrt{2\,\nu}\,\frac{r}{2}\right)g\left(\sqrt{\frac{\nu}{2}}\,2\,R\right)=f\left(\sqrt{\frac{\nu}{2}}\,r\right)g\,(\sqrt{2\,\nu}\,R)$$

and consequently:

$$\psi_L(\vec{R})\,\psi_\Lambda(\vec{r})\to\psi_L(\vec{r})\,\psi_\Lambda(\vec{R})\,.$$

In the same way it is seen that the transformation $\vec{r}_2\to-\vec{r}_2$ or $\vec{r}\to-2\,\vec{R}$, $\vec{R}\to-\vec{r}/2$ results in:

$$\psi_L(\vec{r}_1)\,\psi_\Lambda(\vec{r})\to(-1)^{L+\Lambda}\,\psi_L(\vec{r})\,\psi_\Lambda(\vec{R})\,.$$

As a result, the expansion of $\psi_{l_1}(\vec{r}_1)\,\psi_{l_2}(\vec{r}_2)$ should contain $\psi_L(\vec{R})\,\psi_\Lambda(\vec{r})$ and $\psi_L(\vec{r})\,\psi_\Lambda(\vec{R})$ only in the combination:

$$\psi_L(\vec{R})\,\psi_\Lambda(\vec{r})+(-1)^{l_1}\,\psi_L(\vec{r})\,\psi_\Lambda(\vec{R})\,. \tag{9}$$

It is multiplied in the transformation $\vec{r}_1 \to -\vec{r}_1$ by $(-1)^{l_1}$, and in the transformation $\vec{r}_2 \to -\vec{r}_2$ by

$$(-1)^{L+\Lambda}(-1)^{l_1} = (-1)^{l_1+l_2}(-1)^{l_1} = (-1)^{l_2}$$

(as $2N + 2n + L + \Lambda = 2n_1 + 2n_2 + l_1 + l_2$).

When we build the symmetric and antisymmetric functions, we see that if l_1 and l_2 are both even or both odd (and hence L and Λ have the same property) both $\psi_L(\vec{R})\,\psi_\Lambda(\vec{r})$ and $\psi_L(\vec{r})\,\psi_\Lambda(\vec{R})$ may enter into those functions, and therefore only in the combination (9). If one of l_1, l_2 is even and the other is odd, the symmetric function contains only $\psi_L(\vec{R})\,\psi_\Lambda(\vec{r})$ (with Λ even and L odd) and the antisymmetric function contain only $\psi_\Lambda(\vec{R})\,\psi_L(\vec{r})$. Therefore the coefficient of $\psi_L(\vec{R})\,\psi_\Lambda(\vec{r})$ in the symmetric function should be $(-1)^{l_2}$ times the coefficient of $\psi_\Lambda(\vec{R})\,\psi_L(\vec{r})$ in the antisymmetric function.

Subject to the above conditions, the transformation is most conveniently calculated in the following manner. The wave-functions (7) and (8) are written down in the case $\varphi_1 = \varphi_2 = \varphi = \Phi$. It is then easy to express them as functions of $\vec{R}$ and $\vec{r}$ and compare these expressions with a linear combination of the admissible wave-functions $\psi^M_{NL}(\vec{R})\,\psi^m_{n\Lambda}(\vec{r})$ (according to the above conditions). By equating respective coefficients, the factors of this expansion may be easily found. When doing so no account should be taken of the exponential factor, as

$$e^{-\frac{\nu}{2}r_1^2} e^{-\frac{\nu}{2}r_2^2} = e^{-\frac{\nu}{2}(r_1^2+r_2^2)} = e^{-\frac{\nu}{2}\left(\frac{4R^2+r^2}{2}\right)} = e^{-\frac{2\nu}{2}R^2} e^{-\frac{\nu/2}{2}r^2}$$

II. On the Order of Levels in j^n Configurations.

§ 5. *The evaluation of Slater parameters for the harmonic oscillator wave-functions.*

The method described in I will now be used to obtain some results on level spacings and especially on the order of levels in a few interesting cases together with a discussion of their dependence on the range and form of the potential. An important problem in the shell model based on strong spin-orbit coupling, which leads to the jj-coupling scheme, is the determination of the spin (total angular momentum) of the ground state of the j^n configuration. It was pointed out by FEENBERG[18]) that for $n = 2$ the spin of the ground state is zero (for Majorana forces). His argument was generalized by RACAH[19]) who showed that for any n the ground state has the

minimum spin allowed by the Pauli principle, namely (for an odd n) 3/2 in the case of three particles (or holes) in a shell, and 1/2 in other cases. This result is apparently in contradiction with the empirical rule that the spin of the ground state is equal to the spin of the odd nucleon. However, RACAH's argument was based (as that of FEENBERG) on the long range approximation, in which one assumes that the interaction potential can be approximated by a square well in the region where the amplitudes of the wave-functions are important. On the other hand, results of MAYER[2]) showed that with a δ-potential the spin of the ground state is $J = j$ if n is odd and $J = 0$ if n is even. (This is in fact a short-range approximation, where one assumes that the potential is different from zero only in a region so small that the change of the wave-functions in that region is small compared to the wave-functions themselves.) This result was subsequently proved by RACAH[3]) in a general way.

If we pass continuously (i.e. by a continuous change of some parameters) from the short range limit to that of the long range, we see that the order of levels changes continuously, and for different values of the parameters one obtains different spins of the ground state. The dependence of the spin of the ground state on the range of the potential has been treated in some special cases by KURATH[4]) and the author[5]). In the following, our method is used to obtain general results which are applicable to every potential, and additional interesting forms of the potential are treated.

The method of the harmonic oscillator wave functions can be combined with the vast amount of results calculated in atomic spectroscopy: in these results all the energy levels are expressed in terms of the F_k; on the other hand it is possible to express them in terms of the integrals I_l. It is therefore always possible to write down the F_k as functions of the I_l. This allows us to calculate the values of the F_k, when using any potential, by first computing the values of the I_l by direct integration. The use of this procedure makes all the formulae derived in the F_k formalism useful for calculations of the energy levels.

If one is interested in central interactions only, it is not necessary to calculate the wave-functions of the configuration in terms of $\vec{R}$ and $\vec{r}$, as only the Slater parameters F_k are required and with the above transformation they can be directly calculated in terms of the I_l.

The F^k (which differ only by a constant factor from the F_k) are defined by:

$$F^k(a_1, a_2) = \int_0^\infty \int_0^\infty R^2_{a_1}(r_1)\, R^2_{a_2}(r_2)\, f_k(r_1, r_2)\, dr_1\, dr_2$$

where the $f_k(r_1, r_2)$ are the coefficients of the expansion (4). The f_k are therefore given by

$$f_k(r_1, r_2) = \frac{2k+1}{2} \int_{-1}^{+1} V(|\vec{r}_2 - \vec{r}_1|)\, P_k(\cos \omega_{12})\, d \cos \omega_{12}$$

(the factor $2/2\, k + 1$ is the square of the normalization factor of the Legendre polynomials), and thus:

$$F^k = \frac{2k+1}{2} \int_{-1}^{+1} \int_0^\infty \int_0^\infty V(|\vec{r}_2 - \vec{r}_1|) \frac{R^2_{a_1}(r_1)}{r_1^2} \frac{R^2_{a_2}(r_2)}{r_2^2} \times$$
$$\times P_k(\cos \omega_{12})\, r_1^2\, dr_1\, r_2^2\, dr_2\, d \cos \omega_{12}\,.$$

This expression can be integrated also over other angles $d\Omega$ of which the integrand is independent, thus completing $r_1^2\, r_2^2\, dr_1\, dr_2\, d \cos\omega_{12}$ to the differential of the volume element in the space of the vectors $\vec{r}_1$ and $\vec{r}_2$. We obtain, after multiplication by a proper normalization factor N_Ω,

$$F^k(a_1, a_2) = N_\Omega \frac{2k+1}{2} \int\int V(|\vec{r}_2 - \vec{r}_1|) \frac{R^2_{a_1}(r_1)}{r_1^2} \frac{R\ \ (r_2)}{r_2^2} \times$$
$$\times P_k\,(\cos \omega_{12})\, d^3 r_1\, d^3 r_2\,. \qquad (10)$$

This integral can now be transformed to an integral over $\vec{R}$ and $\vec{r}$. As $V(|\vec{r}_2 - \vec{r}_1|)$ is a function of $|\vec{r}\,|$ only, it remains to express

$$\frac{R^2_{a_1}(r_1)}{r_1^2} \frac{R^2_{a_2}(r_2)}{r_2^2}\, P_k\,(\cos \omega_{12})$$

in terms of $\vec{R}$ and $\vec{r}$. This is always possible with the help of the relation

$$r_1\, r_2 \cos \omega_{12} = (\vec{r}_1, \vec{r}_2) = \frac{1}{4}\,(4\, R^2 - r^2)\,.$$

The result is a function of R, r and the angle α between the vectors $\vec{R}$ and $\vec{r}$ — $\varphi_k(R, r, \alpha)$. So the above expression becomes:

$$F^k = \frac{2k+1}{2} N_\Omega \int\int V(r)\, \varphi_k(R, r, \alpha)\, d^3 R\, d^3 r = \frac{2k+1}{2} N_\Omega \times$$
$$\times \int_{\Omega'} \int_{-1}^{+1} \int_0^\infty \int_0^\infty V(r)\, \varphi_k(R, r, \alpha)\, R^2\, d\, R\, r^2\, dr\, d \cos \alpha\, d\, \Omega' = \frac{2k+1}{2} \times$$
$$\times \int_{-1}^{+1} \int_0^\infty \int_0^\infty V(r)\, \varphi_k(R, r, \alpha)\, R^2\, d\, R\, r^2\, dr\, d \cos \alpha\,. \qquad (11)$$

Where $d\Omega'$ stands for the differentials which form with $R^2\,dR r^2\,dr \times d\cos\alpha$ the volume element $d^3R\,d^3r$; the integrand is independent of them and the integration results merely in the dropping of the normalization constant N_Ω. The integration over α can be easily done and it is then possible to carry out the R-integration, which leaves F^k expressed in terms of the r-integrals $-I_l$. In this way the Slater parameters are calculated in terms of simple integrals without bothering about the expansion of the potential in a series of Legendre polynomials and without the complicated integrations in which such an expansion results.

In order to see how this procedure works, we give explicitly the expression of $r_1^k\, r_2^k\, P_k(\cos\omega_{12})$ in terms of R, r and α. This expression results from the calculation of a configuration in which $l_1 = l_2$ (and therefore k is even). Putting

$$P_k(\cos\omega_{12}) = \sum_{n=0}^{\infty} c_{2n}\cos^{2n}\omega_{12}$$

$k = 2m$, we obtain:

$$r_1^k\, r_2^k\, P_k(\cos\omega_{12}) = \sum_{n=0}^{m} c_{2n}\, r_1^{k-2n}\, r_2^{k-2n}\, r_1^{2n}\, r_2^{2n}\cos^{2n}\omega_{12} =$$

$$= \sum_{n=0}^{m} c_{2n}\,(r_1^2\, r_2^2)^{m-n}\left(\frac{4R^2-r^2}{4}\right)^{2n} = \sum_{n=0}^{m} c_{2n}\left(\frac{4R^2-r^2}{4}\right)^{2n}\times$$

$$\times\left[\left(\frac{4R^2-r^2}{4}\right)^2 + R^2 r^2 - (\vec{R},\vec{r})^2\right]^{m-n}.$$

Use was made here of the relation

$$r_1^2\, r_2^2 = \left(\frac{4R^2-r^2}{4}\right)^2 + R^2 r^2 - (\vec{R},\vec{r})^2 = \left(\frac{4R^2-r^2}{4}\right) + R^2 r^2\sin^2\alpha\,.$$

As an example we evaluate in detail F^2 of the configuration p^2:

$$F^2 = N_1^4\,\frac{5}{2}\int_{-1}^{+1}\int_0^\infty\int_0^\infty V(r)\, e^{-\nu(r_1^2+r_2^2)}\, r_1^2\, r_2^2\left(\frac{3}{2}\cos^2\omega_{12} - \frac{1}{2}\right)\times$$

$$\times\, r_1^2\, dr_1\, r_2^2\, dr_2\, d\cos\omega_{12} =$$

$$= \left(\frac{\sqrt{\nu}\,\nu^2\,8}{\sqrt{\pi}\cdot 3}\right)^2\frac{5}{2}\int_{-1}^{+1}\int_0^\infty\int_0^\infty V(r)\, e^{-\nu\frac{4R^2+r^2}{2}}\left[\frac{3}{2}\left(\frac{4R^2-r^2}{4}\right)^2 -\right.$$

$$\left. -\,\frac{1}{2}\left(\left(\frac{4R^2-r^2}{4}\right)^2 + R^2 r^2\sin^2\alpha\right)\right] R^2\, dR\, r^2\, dr\, d\cos\alpha =$$

$$= \left(\frac{\sqrt{\nu}\,\nu^2\,8}{\sqrt{\pi}\cdot 3}\right)^2 5 \int_0^\infty V(r)\, e^{-\frac{\nu}{2}r^2}\left[\frac{1}{4}\left(\frac{4\sqrt{\pi}\,15}{\sqrt{2\,\nu}\,(2\,\nu)^3\,16}+\frac{\sqrt{\pi}}{4\sqrt{2\,\nu}\cdot 2\,\nu\cdot 4}\,r^4\right)-\right.$$

$$\left.-\frac{5\sqrt{\pi}\cdot 3}{6\sqrt{2\,\nu}\,(2\,\nu)^2\,8}\,r^2\right] r^2\,dr = \left(\frac{\sqrt{\nu}\,\nu^2\,8}{\sqrt{\pi}\cdot 3}\right)^2 \times$$

$$\times 5\left[\frac{1}{4}\left(\frac{4\sqrt{\pi}\cdot 15}{\sqrt{2\,\nu}\,(2\,\nu)^3\,16}\cdot\frac{\sqrt{\pi}}{\sqrt{\nu/2}\cdot\nu/2\cdot 4}I_0+\frac{\sqrt{\pi}}{4\sqrt{2\,\nu}\cdot 2\,\nu\cdot 4}\cdot\frac{\sqrt{\pi}\cdot 15}{\sqrt{\nu/2}\,(\nu/2)^3\,16}I_2\right)-\right.$$

$$\left.-\frac{5\sqrt{\pi}\,3}{6\sqrt{2\,\nu}\,(2\,\nu)^2\,8}\cdot\frac{\sqrt{\pi}\,3}{\sqrt{\nu/2}\,(\nu/2)^2\,8}\,I_1\right] = \frac{25}{12}\left[(I_0+I_2)-2\,I_1\right].$$

In this way the F^k for the configurations d^n, f^n, and g^n were obtained; these are later used in the discussion of the jj-coupling configurations $(d_{5/2})^3$, $(f_{7/2})^3$, and $(g_{5/2})^3$.

§ 6. *The $(d_{5/2})^3$ configuration with various potentials.*

The simplest configuration where the short and long range approximations give different results is $(d_{5/2})^3$. In the δ-limit the state with $J = 5/2$ is the ground state, and in the long range limit the state with $J = 3/2$ is the lowest. If one passes from one limit to the other a cross-over of these two levels occurs. This case is also of an experimental interest as a $J = 3/2$ state of the configuration is postulated[1]) for the ground state of Na^{21}. This case was treated by KURATH[4]) who used oscillator wave-functions and a Gaussian potential. It was also calculated by the author[5]) using the Slater method with Coulomb field wave-functions and a Yukawa potential. The results were different, since the Gaussian potential can be well approximated by a square well when its range is increased, whereas the Yukawa potential has a singularity at the origin and does not yield the long range limit when its range tends to infinity. We shall discuss in this paragraph the cross-over and its dependence on the range and form of the potential.

The energy states of the configuration $(d_{5/2})^n$ were calculated by INGLIS[20]) in the case of ordinary (WIGNER) forces between the particles. The calculation of the levels in the case of Majorana interaction can be carried out in the same manner (an example of such a calculation is given later in the case of Li^7).

The results are:

$$E_{9/2} = \frac{36}{25} F^0 - \frac{72}{5 \cdot 49} F^2 - \frac{1329}{25 \cdot 441} F^4$$

$$E_{5/2} = \frac{4}{5} F^0 - \frac{56}{5 \cdot 49} F^2 - \frac{651}{5 \cdot 441} F^4$$

$$E_{3/2} = \frac{3}{5} F^0 + \frac{12}{5 \cdot 49} F^2 - \frac{627}{5 \cdot 441} F^4.$$

The sign convention is that the F_k are positive and the Majorana potential is attractive (negative) in symmetrical states.

From the definition of the F_k it follows that in the short range limit $F^k = (2k+1) F_0$, while in the long range approximation $F^k \ll F_0$. From these relations the order of the levels $J = 5/2$ and $J = 3/2$ in the two limits can be immediately seen. We calculated the F^k in terms of the I_l using the procedure of § 5 with the following results:

$$3 \cdot 5 F^0 = \frac{63}{16} (I_0 + I_4) + \frac{7}{4} (I_1 + I_3) + \frac{29}{8} I_2$$

$$7 \cdot 3 \frac{1}{49} F^2 = \frac{9}{16} (I_0 + I_4) - \frac{1}{2} (I_1 + I_3) - \frac{1}{8} I_2$$

$$7 \cdot 5 \frac{1}{49} F^4 = \frac{3}{16} (I_0 + I_4) - \frac{3}{4} (I_1 + I_3) + \frac{9}{8} I_2.$$

Remark: In the above results only the combination $(I_0 + I_4)$, $(I_1 + I_3)$ appear, thus forming with I_2 three independent parameters which replace F_0, F_2, and F_4 of the Slater method. The reason for this fact can be seen as follows: In the wave-function $\psi_{l_1}(r_1)\, \psi_{l_2}(r_2)$ the product $r_1^{l_1} \cdot r_2^{l_2}$ appears as a factor, and therefore when we express it as a function of $\vec{r}$ and $\vec{R}$ the sum of the powers of R and r in every term is equal to $l_1 + l_2$. The transformation $\vec{r}_1 \to -\vec{r}_1$ which induces $\vec{r} \to 2\vec{R}$, $\vec{R} \to \vec{r}/2$ transforms, as we have already seen, $f(\sqrt{2\nu}\, R)\; g(\sqrt{\nu/2}\, r)$ into $f(\sqrt{\nu/2}\, r)\; g(\sqrt{2\nu}\, R)$. As a result, to every term in which $R^m\, r^{l_1+l_2-m}$ appears there corresponds another term which has the same angular part and contains $r^m\, R^{l_1+l_2-m}$ as a factor. When the angular and R-integrations are performed these two terms give in the r-integration the integrals $I_{l_1+l_2-m}$ and I_m with the same factors. Therefore only the combination $(I_m + I_{l_1+l_2-m})$ appears in the result. It should be remembered that there exists only one set of the I_l the combinations of which form the F_k and G_k of the various configurations.

Putting these values in the above formulae we obtain the energy levels expressed by the I_l:

$$E_{9/2} = \frac{1}{25} \left(-\frac{117}{16} (I_0 + I_4) + \frac{165}{4} (I_1 + I_3) - \frac{255}{8} I_2 \right)$$

$$E_{5/2} = \frac{1}{5} \left(-\frac{63}{16} (I_0 + I_4) + \frac{63}{4} (I_1 + I_3) - \frac{157}{8} I_2 \right)$$

$$E_{3/2} = \frac{1}{5} \left(-\frac{36}{16} (I_0 + I_4) + \frac{54}{4} (I_1 + I_3) - \frac{156}{8} I_2 \right).$$

From the definition of the I_l it is seen that in the short range approximation $I_l \ll I_0$ $(l > 0)$ (because for $l > 0$, R_l vanishes at the origin), and in the long range limit all the I_l are equal.

This property of the I_l makes our method useful for approximations in the short range limit. In the first approximation only the coefficient of I_0 should be calculated (use is made of this fact in § 15). On the other hand the Slater method can serve as an approximation in the long range limit. Near this limit $F^k \ll F^0$ $(k > 0)$, so that the first approximation is given by F^0. From this point of view these two methods are complementary, and hence it is natural to work with the I_l in nuclear spectroscopy where there are good reasons to believe that the short range approximation is justified.

We have mentioned before that the cross-over should depend not only on the range of the potential but also strongly on its form. A flat potential like a square well or the Gaussian potential give the long range limit as its range tends to infinity, but a potential which is singular at the origin does not yield the long range limit even if its range tends to infinity (the important parts of the potential are in the neighbourhood of the origin). The I_l $(l > 0)$, though they are no longer zero, do not approach the value of I_0 (alternatively the F^k, $k > 0$, are smaller than F^0 but do not tend to zero). As far as the order of the levels is considered, such potentials represent an intermediate case between the two limits.

We shall compare potentials in which the range parameter appears in the same manner but their forms are different, namely:

(a) the Gaussian potential $V\, e^{-r^2/r_0^2}$ which for $r_0 \to \infty$ gives the long range limit (this potential was used by KURATH[4]));

(b) the potential $V\, e^{-r^2/r_0^2}/r/r_0$ which gives in the limit $r_0 \to \infty$ the Coulomb potential, and,

(c) the potential $V\, e^{-r^2/r_0^2}/r^2/r_0^2$ which is still more singular at the origin.

Although the difference in behaviour was already noted[5]), we discuss it again as we shall use here the same wave-functions for all of them. The I_l corresponding to these potentials are calculated to be:

$$\text{(a)} \quad I_l = N_l^2 \int_0^\infty e^{-\nu r^2} V(r)\, r^{2l+2}\, dr = N_l^2\, V \int_0^\infty e^{-\left(\nu + \frac{1}{r_0^2}\right) r^2} r^{2l+2}\, dr =$$

$$= V \left(\frac{\lambda^2}{1+\lambda^2}\right)^{l+3/2}$$

$$\text{(b)}\quad I_l = N_l^2 \int_0^\infty e^{-\nu r^2} V(r)\, r^{2l+2}\, dr = N_l^2\, V r_0 \int_0^\infty e^{-\left(\nu+\frac{1}{r_0^2}\right) r^2} r^{2l+1}\, dr =$$

$$= V\lambda \frac{n_l^2\, l!}{2\sqrt{\pi}} \left(\frac{\lambda^2}{1+\lambda^2}\right)^{l+1} \qquad n_l^2 = \frac{\sqrt{\pi}}{\sqrt{\nu}\,\nu^{l+1}} N_l^2$$

$$\text{(c)}\quad I_l = N_l^2 \int_0^\infty e^{-\nu r^2} V(r)\, r^{2l+2}\, dr = N_l^2\, V r_0^2 \int_0^\infty e^{-\left(\nu+\frac{1}{r_0^2}\right) r^2} r^{2l}\, dr =$$

$$= V\lambda^2 \frac{2}{2l+1} \left(\frac{\lambda^2}{1+\lambda^2}\right)^{l+\frac{1}{2}}.$$

λ is defined by $\lambda = r_0\sqrt{\nu}$; it is the ratio of the potential range to $1/\sqrt{\nu}$ which determines the extension of the wave-function. If λ tends to infinity it may be seen that I_l of the Gaussian potential are all equal, while in the limit $\lambda \to \infty$ for the case (b) (which gives the Coulomb potential), I_l is proportional to $n_l^2\, l!$; and in case (c) I_l is proportional to $2/2\,l+1$.

The cross over of the levels $J = 5/2$ and $J = 3/2$ occurs where the I fulfil the equation:

$$27\,(I_0 + I_4) - 36\,(I_1 + I_3) + 2\,I_2 = 0\,. \tag{13}$$

Relative to the value of I, the values of the I in the three cases are:

$$\text{(a)}\quad I_l \sim \left(\frac{\lambda^2}{1+\lambda^2}\right)^l$$

$$\text{(b)}\quad I_l \sim \frac{n_l^2\, l!}{4} \left(\frac{\lambda^2}{1+\lambda^2}\right)^l$$

and

$$\text{(c)}\quad I_l \sim \frac{1}{2l+1} \left(\frac{\lambda^2}{1+\lambda^2}\right)^l$$

Using these relations we find that the cross over occurs in case (a) at the value $\lambda = 1{\cdot}326$, whereas in case (b) it occurs only at $\lambda = 4{\cdot}34$. The effect of the form of the potential appears more pronounced in case (c); in this case no cross-over occurs as λ varies from zero to infinity. [For the left hand side of (13) for $\lambda = 0$ is positive, and it remains so even when the I_l attain their maximum value $\sim 1/(2\,l+1)$.]

This strong dependence on the form shows that for such problems it is not enough to consider the range only. Potentials of different forms which may be adjusted to fit some condition will not usually give here the same results.

In the preceding section we discussed the effect of the form of the potential on the order of the levels and the place of the cross-

over, using the same wave-functions; we shall now give the results for the Yukawa potential using harmonic oscillator wave-functions and compare them to those obtained with the Coulomb field wave-functions[5]).

For the Yukawa potential, $V(r) = V e^{-r/r_0}/r/r_0$, the I_l are calculated as follows:

$$I_l = N_l^2 \int_0^\infty V(r)\, e^{-\nu r^2} r^{2l+2}\, dr = N_l^2\, V r_0 \int_0^\infty e^{-\nu r^2 - r/r_0} r^{2l+1} dr =$$

$$= \frac{N_l^2}{\sqrt{\nu}\, \nu^{l+1}} V\lambda \int_0^\infty e^{-\xi^2 - \xi/\lambda} \xi^{2l+1} d\xi$$

where $\xi = \sqrt{\nu}\, r$ and $\lambda = \sqrt{\nu}\, r_0$. We introduce the constant $\mu = 1/2\,\lambda$ and $x = \xi + \mu$, and obtain:

$$I_l = \frac{N_l^2}{\sqrt{\nu}\, \nu^{l+1}} V\lambda\, e^{\mu^2} \int_\mu^\infty e^{-x^2} (x-\mu)^{2l+1}\, dx\,.$$

This gives for the integrals which we need:

$$I_0 = V\lambda \left[\frac{2}{\sqrt{\pi}} - 2\,\mu\,(1 - \Phi(\mu))\, e^{\mu^2}\right]$$

$$I_1 = \frac{2}{3} V\lambda \left[\frac{2}{\sqrt{\pi}} (1+\mu^2) - 2\,\mu \left(\frac{3}{2} + \mu^2\right)(1-\Phi(\mu))\, e^{\mu^2}\right]$$

$$I_2 = \frac{8}{15} V\lambda \left[\frac{2}{\sqrt{\pi}} \left(1 + \frac{9}{4}\mu^2 + \frac{1}{2}\mu^4\right) - 2\,\mu \left(\frac{15}{8} + \frac{5}{2}\mu^2 + \frac{1}{2}\mu^4\right) \times \right.$$
$$\left. \times \left(1 - \Phi(\mu)\right) e^{\mu^2}\right]$$

$$I_3 = \frac{16}{35} V\lambda \left[\frac{2}{\sqrt{\pi}} \left(1 + \frac{29}{8}\mu^2 + \frac{5}{3}\mu^4 + \frac{1}{6}\mu^6\right) - \right.$$
$$\left. - 2\,\mu \left(\frac{35}{16} + \frac{35}{8}\mu^2 + \frac{7}{4}\mu^4 + \frac{1}{6}\mu^6\right)\left(1 - \Phi(\mu)\right) e^{\mu^2}\right]$$

$$I_4 = \frac{128}{315} V\lambda \left[\frac{2}{\sqrt{\pi}} \left(1 + \frac{325}{64}\mu^2 + \frac{115}{32}\mu^4 + \frac{35}{48}\mu^6 + \frac{1}{24}\mu^8\right) - \right.$$
$$\left. - 2\,\mu \left(\frac{315}{128} + \frac{105}{16}\mu^2 + \frac{63}{16}\mu^4 + \frac{3}{4}\mu^6 + \frac{1}{24}\mu^8\right)\left(1 - \Phi(\mu)\right) e^{\mu^2}\right]$$

Φ is the error function

$$\Phi(x) = \frac{2}{\sqrt{\pi}} \int_0^x e^{-t^2} dt\,.$$

These values of I_l for various values of μ were substituted into formulae (12), (13) to give the level spacings corresponding to each μ.

The cross-over of the levels $J = 5/2$ and $J = 3/2$ occurs at a value $\lambda = 9$, i.e. for $r_0/r_l = 9\sqrt{2} \sim 13$ where $r_l = \sqrt{2\nu}$ is the parameter appearing in the wave function of a single d-nucleon. This should be compared to the value $r_0/r_l \sim 10$, obtained with the use of the Coulomb field wave-functions, where r appears in these functions in the exponent: $R_l(r) = N_l\, r^{l+1}\, e^{-r/r_l}$.

It is interesting to see that the results are essentially the same, thus supporting the opinion that the exact form of the wave-function is not very important.

The results of this paragraph show that the appearence of the spin 3/2 in the ground state of Na^{21} is unlikely to be due only to the effect of Majorana forces, as the value of λ which should then be assumed is too big, especially if we assume that the potential is a "deep hole" potential, such as that of YUKAWA, rather that a flat one.

§ 7. *The configuration* $(f_{7/2})^3$.

This configuration [and equivalently $(f_{7/2})^5$] has six states with spins $J = 15/2,\ 11/2,\ 9/2,\ 7/2,\ 5/2,\ 3/2$. For Majorana forces in the short range approximation the state with $J = 7/2$ is the ground state, and in the long range limit the state with $J = 3/2$ is the lowest; above it lies $J = 5/2$ and the state with $J = 7/2$ is next to it. The cross-over of these three states was found by KURATH[4]) who used a Gaussian potential. We shall in the following discuss this configuration using also other forms of the potential.

The matrix elements of the Majorana interaction in the $(j_1,\ j_2,\ m_{j_1},\ m_{j_2})$ scheme were found in the way described in § 12. The integrals $J(m_1,\ m_2;\ m_3,\ m_4)$ were calculated in terms of the Slater parameters F_k by the usual method. As there are no two states with equal J in this case the sum method was used to obtain the energies of the various states with the following results:

$$\left.\begin{aligned}
E_{15/2} &= -90\,F_0 + 2700\,F_2 + 7020\,F_4 + 7974\,F_6 \\
E_{11/2} &= -62\,F_0 + 1580\,F_2 + 2736\,F_4 + 42302\,F_6 \\
E_{9/2} &= -51\,F_0 + 425\,F_2 + 6201\,F_4 + 32765\,F_6 \\
E_{7/2} &= -42\,F_0 + 1610\,F_2 + 6930\,F_4 + 82082\,F_6 \\
E_{5/2} &= -35\,F_0 + 665\,F_2 - 2583\,F_4 + 80717\,F_6 \\
E_{3/2} &= -30\,F_0 - 660\,F_2 + 4752\,F_4 + 50622\,F_6
\end{aligned}\right\} \qquad (14)$$

The F_k in the above expressions are defined by:

$$F_0 = \frac{F^0}{7^2}, \quad F_2 = \frac{F^2}{3^2 5^2 7^2}, \quad F_4 = \frac{F^4}{3^2 7^2 11^2}, \quad F_6 = \frac{5^2 F^6}{3^2 7^2 11^2 13^2}.$$

Using the method described above, these F^k are expressed in the terms of I_l as is given in the following formulae:

$$F^6 = \frac{5577}{2240}[I_0 + I_6) - 6\,(I_1 + I_5) + 15\,(I_2 + I_4) - 20\,I_3]$$

$$F^4 = \frac{297}{2240}[13\,(I_0 + I_6) - 34\,(I_1 + I_5) + 19\,(I_2 + I_4) + 4\,I_3]$$

$$F^2 = \frac{3}{448}[143\,(I_0 + I_6) - 66\,(I_1 + I_5) - 15\,(I_2 + I_4) - 124\,I_3)]$$

$$F^0 = \frac{1}{2240}[429\,(I_0 + I_6) + 198\,(I_1 + I_5) + 387\,(I_2 + I_4) + 212\,I_3].$$

Taking the Gaussian potential we obtain the following results which are in agreement with those of KURATH: for $\lambda < 1{\cdot}27$ the lowest state is $J = 7/2$; at $\lambda = 1{\cdot}27$ the level with $J = 5/2$ becomes the ground level and is the lowest one in the region $1{\cdot}27 < \lambda < 1{\cdot}35$; for $\lambda > 1{\cdot}35$ the $J = 3/2$ state is the ground state. Thus there is a region where the ground state has the spin 5/2. The configuration $(f_{7/2})^n$ is predicted by the shell model for all nuclei having N or Z (neutron or proton number) between 20 and 28. The only odd-even nuclei in this region, of which the spins have been measured are the following odd-proton nuclei: ${}_{21}Sc^{45}$ and ${}_{27}Co^{59}$ have the spin 7/2 as required by the shell model, ${}_{23}V^{51}$ has also the spin 7/2 whereas ${}_{25}Mn^{55}$ has the spin 5/2. It was suggested[1]) that the ground state of the last nucleus is a $J = 5/2$ state of the $(f_{7/2})^5$ configuration. KURATH[4]) tries to explain the occurrence of the 5/2 ground state by suggesting that r_0 of the nuclear forces and r_l of the nucleon orbit satisfy $1{\cdot}27 < \lambda < 1{\cdot}35$. Even for the Gaussian potential such a value of r_0 is too big if one determines r_l roughly from the nuclear radius, but a more serious objection is raised if we consider potentials which are singular at the origin. Taking the potential $V(r) = Ve^{-r^2/r_0^2}/r/r_0$ we find that for $\lambda < 3{\cdot}3$ the ground state is $J = 7/2$, at $\lambda = 3{\cdot}3$ a cross-over of this with the $J = 3/2$ level occurs and for $\lambda > 3{\cdot}3$ the ground state is $J = 3/2$. The level $J = 5/2$ crosses the level $J = 7/2$ only at $\lambda = 9{\cdot}5$ where $J = 3/2$ is already lower. We see that here the use of a $\sim 1/r$ potential not only shifted the points of cross-over but changes completely the situation: there is no more any region of λ where $J = 5/2$ is the ground state. As far as scattering experiments are concerned, there is no indication that the Gaussian potential is better than the Yukawa potential. If one considers it

just as a model the above calculations show that the results depend strongly on the model used and it is a little bit early to draw from them any physical conclusions. We must conclude that it is not likely that the effect of Majorana forces can alone explain the appearance of the 5/2 ground state of Mn^{55}.

§ 8. *The configuration* $(g_{9/2})^3$.

This is the simplest configuration j^n in which two states with the same J appear. The states of the $(g_{9/2})^3$ configuration are: two states with $J = 9/2$ and eight more states with $J = 21/2, 17/2, 15/2, 13/2, 11/2, 7/2, 5/2$, and $3/2$. The sum method cannot give the term values of the two $J = 9/2$ states but only their sum. The separation of these energies can be done by diagonalization of the energy matrix, but with the elaborate methods of RACAH[12]) this becomes much easier. One can define two states with $J = 9/2$, one with the Seniority $v = 1$ and the other with $v = 3$. As the interaction energy does not commute with the Seniority operator, there is a non-vanishing matrix element connecting these states and the energies of the ground $J = 9/2$ and of the excited $J = 9/2$ states can be found by diagonalization of the two-rowed matrix.

The energy levels with $J \neq 9/2$ and $J = 9/2$, $v = 1$, $J = 9/2$, $v=3$ as well as the matrix element V connecting the last two states were calculated by RACAH[21] in terms of the Slater's F_k. We write here down only the results for $J \leqslant 9/2$ as the other levels lie above these and are of less physical interest.

State	Type of force									
	Wigner forces factors of					Majorana forces factors of				
	F_0	F_2	F_4	F_6	F_8	F_0	F_2	F_4	F_6	F_8
$J=9/2$ $v=1$	3	33	1287	429	2431	− 8/9	407/14	24453/14	1144	24739/18
$J=9/2$ $v=3$	3	−43	− 93	−163	−3417	− 8/9	75/14	3153/14	1014	7879/18
$V/\sqrt{429}$	0	− 1	105	− 31	51	0	1/2	− 105/2	31/2	− 51/2
$J=7/2$	3	56	−1488	−595	−2295	− 7/9	100/7	3336/7	542	12379/9
$J=5/2$	3	−14	962	−728	−2652	−56/81	613/63	−4693/7	5629/9	69992/81
$J=3/2$	3	−24	−1488	417	−4947	−17/27	−284/21	4272/7	2518/3	15089/27

The F_k are defined by:

$$F_0 = F^0,$$

$$F_2 = \frac{4F^2}{3^2 11^2}, \quad F_4 = \frac{F^4}{11^2 13^2}, \quad F_6 = \frac{16F^6}{3^2 11^2 13^2}, \quad F_8 = \frac{7^2 F^8}{11^2 13^2 17^2}.$$

The two states with $J = 9/2$ are given by the solutions of the secular equation as follows:

$$E^g_{9/2} = \frac{1}{2}(E^1_{9/2} + E^3_{9/2}) - \frac{1}{2}[(E^1_{9/2} - E^3_{9/2})^2 + 4\,V^2]^{1/2}$$

$$E^e_{9/2} = \frac{1}{2}(E^1_{9/2} + E^3_{9/2}) + \frac{1}{2}[(E^1_{9/2} - E^3_{9/2})^2 + 4\,V^2]^{1/2}.$$

If one examines the values given above it appears that $|V|$ is small in comparison to $|E^1_{9/2} - E^3_{9/2}|$ (it vanishes both in the short range and the long range limits where $v = 1$ and $v = 3$ are exactly the ground and excited states with $J = 9/2$). Therefore it is sufficient to take only the first term of the expansion in powers of $V/|E^1_{9/2} - E^3_{9/2}|$ (which is the second approximation of perturbation theory). This gives:

$$E^g_{9/2} = E^1_{9/2} - \frac{V^2}{|E^1_{9/2} - E^3_{9/2}|} = E^1_{9/2} + \frac{V^2}{E^1_{9/2} - E^3_{9/2}};$$

$$E^e_{9/2} = E^3_{9/2} + \frac{V^2}{|E^1_{9/2} - E^3_{9/2}|} = E^3_{9/2} - \frac{V^2}{E^1_{9/2} - E^3_{9/2}}.$$

The $(g_{9/2})^{3,5,7}$ configurations are of a special interest, since it was observed by GOLDHABER and SUNYAR[22]) that in nuclei which have such a configuration according to the shell model there is a state with spin 7/2 and even parity. This state, 7/2+, lies in a few cases under the level $J = 9/2$ which is usually observed in these nuclei (and described as $g_{9/2}$ according to the shell model) and above it in the other cases. An assignment $g_{7/2}$ for this level is in contrast with the shell model as this state (of the single nucleon) should lie 1–2 MeV above the $g_{9/2}$ state (because of the strong spin-orbit interaction). GOLDHABER and SUNYAR[22]) assume therefore that this state is the $J = 7/2$ state of the $(g_{9/2})^n$ configuration.

The general method described in § 5 was used to obtain the F^k expressed in terms of the I_i; the results are:

$$F^8 = \frac{2431}{16128}[(I_0 + I_8) - 8\,(I_1 + I_7) + 28\,(I_2 + I_6) - \\ - 56(I_3 + I_5) + 70\,I_4]$$

$$F^6 = \frac{1759}{16128}[17\,(I_0 + I_8) - 76\,(I_1 + I_7) + 116\,(I_2 + I_6) - \\ - 52\,(I_3 + I_5) - 10\,I_4]$$

$$F^4 = \frac{143}{26880}[255\,(I_0 + I_8) - 480\,(I_1 + I_7) + 68\,(I_2 + I_6) - \\ - 32\,(I_3 + I_5) + 378\,I_4]$$

$$F^2 = \frac{11}{16128}[1105\,(I_0 + I_8) - 260\,(I_1 + I_7) + 52\,(I_2 + I_6) - \\ - 764\,(I_3 + I_5) - 266\,I_4]$$

$$F^0 = \frac{1}{80640}[12155\,(I_0 + I_8) + 5720\,(I_1 + I_7) + 10868\,(I_2 + I_6) + \\ + 6248\,(I_3 + I_5) + 10658\,I_4].$$

With the help of these formulae we calculated the order of the levels, for Wigner and Majorana forces with the potential $V(r) = Ve^{-r^2/r_0^2}/r/r_0$. As is seen in the table above, the coefficient of F_2 in the case of Wigner forces, is larger for the state $J = 7/2$ than for the other states. Therefore in the long range approximation this is the lowest state up to the long range limit where all the levels coincide. As the potential used does not yield this limit, the resulting order of the levels is: $9/2^g$, 7/2, 5/2, 3/2, $9/2^e$. The spacing of the levels $9/2^g$ and 7/2 is, for $\lambda \leqslant 1{\cdot}5$, smaller by a factor ~ 4 than the distance between the $9/2^g$ and the 5/2 levels. For Majorana forces with the same potential the lowest state is $9/2^g$ up to $\lambda = 3{\cdot}2$ where a cross-over of this level occurs with the $J = 3/2$ level, which is the ground level for $\lambda > 3{\cdot}2$. The 7/2 level does not cross the $9/2^g$ for any λ. When a potential of the form $(1 + P_x)\,V(r)/2$ is used (equal Wigner and Majorana forces), the situation is like that in the case of Wigner forces, except that the levels $9/2^g$ and 7/2 are not so close. Also for the Gaussian potential $V(r) = V\,e^{-r^2/r_0^2}$ there is in the case of Majorana forces no region of λ in which the ground state has $J = 7/2$.

The question of the relative spacings of the other levels $J = 5/2$ and $J = 3/2$ is critical in this case because they should be found experimentally if they are not much higher. In order to clarify this point, we shall refer to an interesting case discussed by GOLDHABER and SUNYAR[22]). ${}_{36}Kr^{83}$ has an even number of protons and 47 neutrons which are equivalent to three holes in the $g_{9/2}$ sub-shell. The spin of the ground state is measured to be 9/2. The isomeric transition is from a $p_{1/2}$ state not to the ground state but to a low lying 7/2+ state, 9 keV above the ground 9/2 state. The distance between the levels $p_{1/2}$ and 7/2+ is 32·2 keV. If a state with $J = 5/2$ or $J = 3/2$ were lying in this spacing, not too close to the upper state, a transition to it would have been preferred upon the observed transition.

It is interesting that the 7/2 state is close to the ground state also for small λ, so that perturbations from other configurations or tensor forces and other non-central interactions may bring it still lower. This question, however, should be considered in more detail.

III. Mutual Spin-Orbit Interactions.

§ 9. *Matrix elements of the mutual spin-orbit interaction.*

It is well known that neither the Thomas interaction nor the magnetic spin-orbit interaction are big enough to account for the wide separation between the states $j = l + 1/2$ and $j = l - 1/2$ of an odd nucleon as required by Mayer's shell model. CASE and PAIS[6]) introduced in a phenomenological way a strong spin-orbit interaction, in order to preserve charge symmetry of the nuclear forces in analyzing high energy nucleon-nucleon scattering. They also made a very rough estimation and found that this interaction could give a doublet splitting of the right order of magnitude necessary for the shell model.

Although there is not yet a conclusive evidence for the existence of such a strong spin-orbit interaction, it is interesting to calculate the effects of such an interaction in cases of a single nucleon outside closed shells.

The spin-orbit interaction of CASE and PAIS was assumed to be of the form:

$$V_{12} = V(|\vec{r}_2 - \vec{r}_1|)\ (\vec{s}^{(1)} + \vec{s}^{(2)},\ \vec{L}_{12}) \tag{17}$$

where $\vec{s}^{(1)}$ and $\vec{s}^{(2)}$ are the spins of the two interacting nucleons, and $\vec{L}_{12}$ is their relative angular momentum

$$\hbar\,\vec{L}_{12} = (\vec{p}_2 - \vec{p}_1) \times (\vec{r}_2 - \vec{r}_1)\,.$$

It is immediately seen why it is extremely difficult to use here the Slater method. Such interactions were generally treated[8]) with the simplification of summation over all nucleons but one, so that $\sum_{i \neq 1} V(|r_i - r_1|)\ (\vec{s}^{(i)} + \vec{s}^{(1)},\ \vec{L}_{i,1})$ became $\vec{V}(r_1)\ (\vec{s}^{(1)},\ \vec{L}_1)$ (in the case of an odd number of nucleons).

Using the method described above the solution of the problem becomes very simple, as $\vec{L}_{12}$ is exactly the $\vec{\Lambda}$ introduced before. To obtain the matrix elements, the operator $(\vec{s}^{(1)} + \vec{s}^{(2)},\ \vec{L}_{12})$ is applied to a wave-function $\psi_{L_1}(\vec{R})\ \psi_{\Lambda_1}(\vec{r})$; this yields a sum of functions of the same type. When we multiply this sum by another wave-function $\psi_{L_2}(\vec{R})\ \psi_{\Lambda_2}(\vec{r})$ and integrate (the integration on the R-coordinate can be immediately done) we obtain the result as a sum of the integrals I_1 [of course, I_0 will not appear as $\vec{\Lambda}\ \psi^0_{n0}(\vec{r})$ vanishes].

In order to calculate the matrix elements of (17) it is more convenient not to work with the A_x and A_y components of a vector,

but instead with the combinations $A_\pm = A_x \pm i\,A_y$. With this notation (17) can be written in the form:

$$V(r)\Big[\tfrac{1}{2}\,(s_+^{(1)}+s_+^{(2)})\,\Lambda_- + \tfrac{1}{2}\,(s_-^{(1)}+s_-^{(2)})\,\Lambda_+ + (s_z^{(1)}+s_z^{(2)})\,\Lambda_z\Big]. \quad (18)$$

The wave-functions with definite n_1, l_1 and n_2, l_2 in the (m_l, m_s)-scheme are:

$$(m_1^\pm, m_2^\pm) = (m_1, m_2)\;\delta\left(\pm\tfrac{1}{2}\middle|\sigma_1\right)\delta\left(\pm\tfrac{1}{2}\middle|\sigma_2\right) =$$
$$= \psi^{m_1}(r_1)\;\psi^{m_2}(r_2)\;\delta\left(\pm\tfrac{1}{2}\middle|\sigma_1\right)\delta\left(\pm\tfrac{1}{2}\middle|\sigma_2\right)$$

where σ_1 and σ_2 are the spin coordinates of the nucleons 1 and 2. The operators s_+, s_-, and s_z, when applied on these functions, give, as is well known:

$$s_+\,\delta(m_s|\sigma) = \left(\tfrac{1}{2} - m_s\right)\delta(-m_s|\sigma)$$
$$s_-\,\delta(m_s|\sigma) = \left(\tfrac{1}{2} + m_s\right)\delta(-m_s|\sigma) \qquad s_z\,\delta(m_s|\sigma) = m_s\,\delta(m_s|\sigma).$$

The corresponding equations for a general L are:

$$L_\pm\,\psi_l^m = (l \mp m)^{\frac{1}{2}}\,(l \pm m + 1)^{\frac{1}{2}}\,\psi_l^{m\pm 1} \qquad L_z\psi_l^m = m\,\psi_l^m.$$

As (17) is linear in $\vec{s}^{(1)}$ and $\vec{s}^{(2)}$, the only non-vanishing matrix elements are those which connect states differing at most in one of the spin eigenvalues. As an example we calculate

$$\left.\begin{aligned}
J(m_1^+, m_2^-) &= \sum_{\sigma_1,\sigma_2}\int\int (m_1, m_2)^*\,\delta\left(\tfrac{1}{2}\middle|\sigma_1\right)\delta\left(-\tfrac{1}{2}\middle|\sigma_2\right)V_{12}(m_1,m_2)\times \\
&\quad\times\delta\left(\tfrac{1}{2}\middle|\sigma_1\right)\delta\left(-\tfrac{1}{2}\middle|\sigma_2\right)d^3r_1\,d^3r_2 = \\
&= \sum_{\sigma_1,\sigma_2}\int\int (m_1, m_2)^*\,\delta\left(\tfrac{1}{2}\middle|\sigma_1\right)\delta\left(-\tfrac{1}{2}\middle|\sigma_2\right)V(r)\left(\tfrac{1}{2}-\tfrac{1}{2}\right) \\
&\quad\times\Lambda_z(m_1, m_2)\;\delta\left(\tfrac{1}{2}\middle|\sigma_1\right)\delta\left(\tfrac{1}{2}\middle|\sigma_2\right)d^3r_1\,d^3r_2 = 0 \\
J(m_1^+, m_2^+) &= \int\int V(r)\;(m_1, m_2)^*\,\Lambda_z(m_1, m_2)\,d^3r_1\,d^3r_2 \\
K(m_1^+, m_2^+) &= \int\int V(r)\;(m_1, m_2)^*\,\Lambda_z(m_2, m_1)\,d^3r_1\,d^3r_2 \\
J(m_1^-, m_2^-) &= -\int\int V(r)\;(m_1, m_2)^*\,\Lambda_z(m_1, m_2)\,d^3r_1\,d^3r_2 \\
K(m_1^-, m_2^-) &= -\int\int V(r)\;(m_1, m_2)^*\,\Lambda_z(m_2, m_1)\,d^3r_1\,d^3r_2.
\end{aligned}\right\} \quad (19)$$

These matrix elements will be used later on. If there is a difference in one of the spin values, Λ_+ and Λ_- may appear; for example:

$$\sum_{\sigma_1,\sigma_2}\int\int(m_1^{\pm}, m_2^{-})^* V_{12}(m_1^{\pm}, m_2^{+})\, d^3r_1\, d^3r_2 = \\ = \int\int V(r)\,(m_1, m_2)^* \frac{1}{2}\Lambda_+(m_1, m_2)\, d^3r_1\, d^3r_2\,.$$

§ 10. *Doublet splitting for a nucleon outside closed shells.*

We shall have to calculate matrix elements of 18) in the (m_l, m_s)-scheme and make applications for the doublet splitting for a nucleon outside closed shells (the effect of this interaction on the energy levels of Li^7 will be treated later). If the doublet splitting in such a case is large compared to the interaction energy between two nucleons in this unfilled shell, the jj-coupling scheme would result.

We start from the (m_l, m_s)-scheme and use the sum method to obtain the energies of the doublet components. We use the fact that M_J (as well as J) is an integral, and also the Landé interval rule which holds for these interactions. This rule states that the energy of the state $^{2S+1}L_J$ is equal to

$$\zeta(S, L)\,\frac{J(J+1)-L(L+1)-S(S+1)}{2}.$$

The expansion of the wave-functions (7), (8) in terms of the wave-functions $\psi_L(\vec{R})\,\psi_\Lambda(\vec{r})$ is easily calculated by the method described above. The results we need are given in the Appendix. We treat the following cases:

A. A single p-nucleon outside the closed s-shell.

The wave-functions are $(m^{\pm};\ 0^+0^-;\ 0^+0^-)$ where the last two quantum numbers refer to two s-protons, the other two to two s-neutrons and the $m^{\pm}$ refers to the odd p-nucleon. When computing the diagonal matrix elements which belong to these functions we see that the only non-vanishing contributions come from the ps-terms. These are exchange terms if the two nucleons have the same charge, and ordinary terms otherwise. The matrix elements were calculated with the help of formulae (19). For example:

$$J(\pm 1^+, 0^+) - K(\pm 1^+, 0^+) = \int\int V(r)\,(1,0)^*\Lambda_z(1,0)\, d^3r_1\, d^3r_2 = \\ = \int\int V(r)\,\psi_1^{\pm 1}(r)^*\,\psi_0^0(R)^*\,\Lambda_z\,\psi_1^{\pm 1}(r)\,\psi_0^0(R)\, d^3r\, d^3R = \\ = \int V(r)\,\psi_1^{\pm 1}(r)^*\,\Lambda_z\,\psi_1^{\pm 1}(r)\, d^3r = \\ = \pm\int V(r)\,\psi_1^{\pm 1}(r)^*\,\psi_1^{\pm 1}(r)\, d^3r = \pm I_1$$

and similar calculations for other matrix elements. The results for the *ps*-diagonal elements are:

$$J(\pm 1^+,0^+)-K(\pm 1^+,0^+)=\pm I_1 \qquad J(\pm 1^+,0^+)=\pm\tfrac{1}{2}I_1$$
$$J(0^+,0^+)=K(0^+,0^+)=0$$
$$J(\pm 1^-,0^-)-K(\pm 1^-,0^-)=\mp I_1 \qquad J(\pm 1^-,0^-)=\mp\tfrac{1}{2}I_1$$
$$J(0^-,0^-)=K(0^-,0^-)=0\,.$$

With these results we build the following table:

M_J	Wave-functions	*ps* diagonal matrix elements		Sum of the energies
		ordinary	exchange	
$\frac{3}{2}$	$(1^+;0^+0^-;0^+0^-)$	$(1^+,0^+)$	$(1^+,0^+)$	$\frac{3}{2}I_1$
$\frac{1}{2}$	$(0^+;0^+0^-;0^+0^-)$ $(1^-;0^+0^-;0^+0^-)$	$(0^+,0^+)$ $(1^-,0^-)$	$(0^+,0^+)$ $(1^-,0^-)$	$-\frac{3}{2}I_1$

As M_J is an integral the following equations can be written:

$$E(^3P_{3/2})=\frac{3}{2}I_1$$
$$E(^3P_{3/2})+E(^3P_{1/2})=-\frac{3}{2}I_1$$

from which it follows:

$$E(^3P_{3/2})=\frac{3}{2}I_1$$
$$E(^3P_{1/2})=-3\,I_1$$

in accordance with the interval rule. The splitting is accordingly:

$$\Delta E=\frac{9}{2}I_1\,.$$

B. A hole in the *p*-shell and a closed *s*-shell.

The relevant *pp*-matrix elements are calculated to be:

$$J(\pm 1^+,0^+)-K(\pm 1^+,0^+)=\pm\frac{1}{2}I_1$$
$$J(0^+,0^+)-K(0^+,0^+)=0=J(\pm 1^+,\mp 1^+)-K(\pm 1^+,\mp 1^+)\,.$$

For the configuration $s^4 p^5$ the corresponding table is:

M_J	Wave-functions	Diagonal matrix elements			Sum of the energies		Total
		ps ordinary	*ps* exchange	*pp* exchange	*ps*	*pp*	
$\frac{3}{2}$	$(1^+, 1^-, -1^+, 0^+, 0^-; 0^+0^-; 0^+0^-)$	$(1^+, 0^+)$	$(1^+, 0^+)$	$(1^+, 0^+)$			
		$(1^-, 0^-)$	$(1^-, 0^-)$	$(1^-, 0^-)$	$-\frac{3}{2} I_1$	$-\frac{1}{2} I_1$	$-2 I_1$
		$(-1^+, 0^+)$	$(-1^+, 0^+)$	$(-1^+, 0^+)$			

From this table we obtain $E(^2P_{3/2}) = -2 I_1$, and with the help of the interval rule $E(^2P_{1/2}) = 4 I_1$. The doublet is inverted and the splitting is:

$$\Delta E = 6 I_1.$$

C. A single p-proton outside a closed s-shell and a closed neutron p-shell.

The additional matrix elements for this case are (ordinary):

$$J(1^+, 1^+) = I_2 \quad J(1^+, 0^+) = \frac{1}{4} I_1 + \frac{1}{4} I_2 \quad J(0^+, 0^+) = J(1^+, -1^+) = 0$$

from which we obtain:

M_J	Wave-functions	*pp* (ordinary) diagonal elements	sum of energies		Total
			pp	*ps*	
$\frac{3}{2}$	$(1^+; 1^+, 1^-, 0^+, 0^-, -1^+, -1^-; 0^+, 0^-; 0^+0^-)$	$(1^+1^+)\,(1^+0^+)$	$\frac{1}{4} I_1 + \frac{5}{4} I_2$	$\frac{3}{2} I_1$	$\frac{7}{4} I_1 + \frac{5}{4} I_2$

This table gives

$$E(^2P_{3/2}) = \frac{7}{4} I_1 + \frac{5}{4} I_2,$$

and

$$E(^2P_{1/2}) = -\frac{7}{2} I_1 - \frac{5}{2} I_2.$$

Hence the splitting is:

$$\Delta E = \frac{21}{4} I_1 + \frac{15}{4} I_2.$$

D. A single d-nucleon outside the closed s- and p-shells.

The relevant matrix elements are:

$$J(2^+, 0^+) - K(2^+, 0^+) = I_1 \qquad J^{ds}(2^+, 0^+) = \frac{1}{2} I_1 + \frac{1}{2} I_2$$

$$dp$$

$$J(2^+,1^+)-K(2^+,1^+)=\frac{1}{4}I_1+\frac{9}{4}I_3 \qquad J(2^+,1^+)=\frac{1}{8}I_1+\frac{1}{4}I_2+\frac{9}{8}I_3$$

$$J(2^+,0^+)-K(2^+,0^+)=\frac{1}{2}I_1+\frac{1}{2}I_3 \qquad J(2^+,0^+)=\frac{1}{4}I_1+\frac{1}{2}I_2+\frac{1}{4}I_3$$

$$J(2^+,-1^+)-K(2^+,-1^+)=\frac{1}{4}I_1+\frac{1}{5}I_{11}+\frac{1}{20}I_3=\frac{3}{4}I_1-I_2+\frac{3}{4}I_3$$

$$J(2^+,-1^+)=\frac{3}{8}I_1-\frac{1}{4}I_2+\frac{3}{8}I_3$$

with the help of which we obtain:

M_J	Wave-functions	diagonal matrix elements				sum of energies		Total sum
		ds		*dp*				
		ord.	exch.	ord.	exch.	*ds*	*dp*	
$\frac{5}{2}$	$(2^+;1^+,1^-,0^+,0^-,-1^+,-1^-;1^+,1^-,0^+,0^-,-1^+,-1^-;0^+,0^-;0^+0^-)$	$(2^+,0^+)$	$(2^+,0^+)$	$(2^+,1^+)$	$(2^+,1^+)$			
				$(2^+,0^+)$	$(2^+,0^+)$	$\frac{3}{2}I_1+\frac{1}{2}I_2$	$\frac{9}{4}I_1-\frac{1}{2}I_2+\frac{21}{4}I_3$	$\frac{15}{4}I_1+\frac{21}{4}I_3$
				$(2^+,-1^+)$	$(2^+,-1^+)$			

Therefore

$$E(^2D_{5/2})=\frac{15}{4}I_1+\frac{21}{4}I_3, \qquad E(^2D_{3/2})=-\frac{45}{8}I_1-\frac{63}{8}I_3,$$

and the splitting is:

$$\Delta E=\frac{75}{8}I_1+\frac{105}{8}I_3.$$

We thus see that:

for p-nucleon interacting with the 4 s-nucleons, the splitting is

$$\frac{9}{2}I_1;$$

for p-proton interacting with the 4 s-nucleons and the 6 p-neutrons, the splitting is

$$\frac{21}{4}I_1+\frac{15}{4}I_2;$$

for d-nucleon interacting with the 4 s-nucleons and the 12 p-nucleons, the splitting is

$$\frac{75}{8}I_1+\frac{105}{8}I_3.$$

CASE and PAIS gave in their paper[6]) an estimated form of the potential $V(r)$ to suit the experimental data of the scattering:

$$V(r) = V_0 \frac{1}{x} \frac{d}{dx} \frac{e^{-x}}{x}$$

where $x = r/r_0$.

The values of r_0 and V_0 were given roughly as $r_0 \sim 1{,}1 \times 10^{-13}$ cm, $V_0 \sim 24$ MeV. Using this potential the I_1 can be easily calculated. The result is:

$$I_1 = \frac{V_0}{3}\left[\frac{2}{\sqrt{\pi}} \frac{2\mu^2-1}{4\mu^3} - \left(1 - \Phi(\mu)\right) e^{\mu^2}\right]$$

where

$$\mu = \frac{1}{2\sqrt{\nu}\, r_0}.$$

For this value of r_0 and reasonable value of $\sqrt{\nu}$ the I_l, $l \geqslant 2$, are much smaller than I_1. The integral is very sensitive to the value of μ (and for a fixed value of r_0—to the value of $\sqrt{\nu}$). Some interesting values are:

μ =	1,0	1,2	1,3	1,4	2,0
I_1 =	1,16	0,57	0,40	0,31	0,07 MeV

We can fix the value of ν by determining the nuclear radius in terms of it:

$$R^2 = \overline{r^2} = N_l^2 \int_0^\infty e^{-2\nu r^2} r^{2l+4}\, dr = \frac{2l+3}{4\nu}.$$

Using the relation $R \sim 1{\cdot}5 \times A^{1/3} \times 10^{-13}$ cm we obtain for the cases considered:

A. $\Delta E \sim 4$ MeV **C.** $\Delta E \sim 2$ MeV **D.** $\Delta E \sim 3{\cdot}5$ MeV.

The first case cannot give any information on He^5 or Li^5 as there are no bound states for these nuclei. It is interesting to see that with the parameters roughly determined from the scattering experiments the order of magnitude of a few MeV may be obtained as required by the shell model (although this calculation should not be considered more than an estimate).

IV. The Low States of Li^7.

§ 11. *The Li^7 nucleus.*

The most striking fact about the Li^7 nucleus is the existence of only one low lying level, 0·48 MeV above the ground state, and the absence of any other level up to a few MeV. The most natural explanation of such a situation is that of the LS-coupling scheme, where the ground state and the first excited level are assumed to be the components of a ^2P. However, various reactions were believed to point out that the excited level has a more complicated character and in certain reactions it behaves like a level with a spin 5/2. It was therefore suggested by INGLIS[7]) that the jj-coupling scheme might give the right explanation. In this scheme the ground level of the configuration $(p_{3/2})^3_N\, p_{3/2\,P}$ has $J = 3/2$ and there are four higher levels with the spins 1/2, 5/2, 7/2 and another 3/2 (which lies somewhat higher than the other three). If there are only Wigner forces between the nucleons the levels $J = 1/2$, 5/2, 7/2 coincide, and it was assumed by INGLIS that the excited level might be such a compound one. However, even a rough coincidence did not result from his calculations and the situation became still worse when Majorana forces were included too[23]). There exists, however, another possibility, that such a coincidence of the first excited levels would result from the effect of non-central forces, such as tensor forces, and hence in the next sections the calculation of the configuration $(p_{3/2})^3_N\, p_{3/2\,P}$ is carried out in the extreme jj-coupling, taking into account tensor forces and mutual spin-orbit interactions in addition to the central forces.

Recent experimental results show that the assignment $J = 1/2$ to the excited level of Li^7 is very probable[8]), and therefore the explanation could be once again based on the LS-coupling scheme[24]). The splitting of the two levels should then arise from the spin-orbit interactions. As the Thomas term gives too small a contribution, we calculate the splitting due to the Case and Pais interaction. It should be mentioned that the lack of other levels below 5 MeV is not very well understood in either coupling scheme. Such calculations should therefore, not be interpreted as successful explanation but only as a preliminary survey of the various possibilities.

§ 12. *The configuration $(p_{3/2})^3_N\, p_{3/2\,P}$ with central forces.*

The energy values of the various states of the jj-coupling scheme can be calculated by the sum method from the diagonal matrix elements of the $(j_1, j_2, m_{j_1}, m_{j_2})$-scheme, in the same way as in

atomic spectroscopy. The wave-function of a single nucleon with given n, l, $j = l + 1/2$ and m_j is given by:

$$u(n\,l\,j\,m_j|1) = (2l+1)^{-\frac{1}{2}}\left[\left(l+m_j+\tfrac{1}{2}\right)^{\frac{1}{2}} u\left(n\,l\,m_j-\tfrac{1}{2}\middle|1\right)\delta\left(\tfrac{1}{2}\middle|\sigma_1\right)+\right.$$
$$\left.+\left(l-m_j+\tfrac{1}{2}\right)^{\frac{1}{2}} u\left(n\,l\,m_j+\tfrac{1}{2}\middle|1\right)\delta\left(-\tfrac{1}{2}\middle|\sigma_1\right)\right] \qquad (20)$$

(the phases are fixed according to CONDON and SHORTLEY[25]), or briefly:

$$u(n\,l\,j\,m_j|1) = f\,u\left(n\,l\,m_j-\tfrac{1}{2}\middle|1\right)\delta\left(\tfrac{1}{2}\middle|\sigma_1\right)+g\,u\left(n\,l\,m_j+\tfrac{1}{2}\middle|1\right)\delta\left(-\tfrac{1}{2}\middle|\sigma_1\right).$$

For $l = 1$ and $j = 3/2$ the f and g are:

m_j	$\frac{3}{2}$	$\frac{1}{2}$	$-\frac{1}{2}$	$-\frac{3}{2}$
f	1	$\sqrt{\frac{2}{3}}$	$\sqrt{\frac{1}{3}}$	0
g	0	$\sqrt{\frac{1}{3}}$	$\sqrt{\frac{2}{3}}$	1

We define the integral J and the exchange integral K of the interaction by:

$$\left.\begin{aligned} J(n\,l\,j\,m_j, n'\,l'\,j'\,m_j') &= \sum_{\sigma_1\,\sigma_2}\int\int u^*(n\,l\,j\,m_j|1)\,u^*(n'\,l'\,j'\,m_j'|2)\times \\ &\times V_{12}\,u(n\,l\,j\,m_j|1)\,u(n'\,l'\,j'\,m_j'|2)\,d^3r_1\,d^3r_2 \\ K(n\,l\,j\,m_j, n'\,l'\,j'\,m_j') &= \sum_{\sigma_1\,\sigma_2}\int\int u^*(n\,l\,j\,m_j|1)\,u^*(n'\,l'\,j'\,m_j'|2)\times \\ &\times V_{12}\,u(n\,l\,j\,m_j|2)\,u(n'\,l'\,j\,m_j'|1)\,d^3r_1\,d^3r_2\,. \end{aligned}\right\} \qquad (21)$$

Exchange operators can be defined for the various central interactions in terms of the spin-exchange operator P_σ and the space-exchange operator P_x.

Type of force			
WIGNER (ordinary)	MAJORANA	HEISENBERG (char. exch.)	BARTLET
1	P_x	$-P_x P_\sigma$	P_σ

When the summation over the spin coordinates is carried out there remains a sum of integrals on space coordinates only, the coefficients

of which are products of f, g (of m_j), and of f', g' (of m_j). For ordinary (Wigner) interaction we obtain (the common n, l, and j were dropped out):

$$\left.\begin{aligned} J(m_j, m_j') &= f^2 f'^2 J\left(m_j - \tfrac{1}{2}, m_j' - \tfrac{1}{2};\ m_j - \tfrac{1}{2}, m_j' - \tfrac{1}{2}\right) + \\ &+ f^2 g'^2 J\left(m_j - \tfrac{1}{2}, m_j' + \tfrac{1}{2};\ m_j - \tfrac{1}{2}, m_j' + \tfrac{1}{2}\right) + \\ &+ f'^2 g^2 J\left(m_j + \tfrac{1}{2}, m_j' - \tfrac{1}{2};\ m_j + \tfrac{1}{2}, m_j' - \tfrac{1}{2}\right) + \\ &+ g^2 g'^2 J\left(m_j + \tfrac{1}{2}, m_j' + \tfrac{1}{2};\ m_j + \tfrac{1}{2}, m_j' + \tfrac{1}{2}\right) \\ K(m_j, m_j') &= f^2 f'^2 J\left(m_j - \tfrac{1}{2}, m_j' - \tfrac{1}{2};\ m_j' - \tfrac{1}{2}, m_j - \tfrac{1}{2}\right) + \\ &+ 2 f f' g g' J\left(m_j - \tfrac{1}{2}, m_j' + \tfrac{1}{2};\ m_j' - \tfrac{1}{2}, m_j + \tfrac{1}{2}\right) + \\ &+ g^2 g'^2 J\left(m_j + \tfrac{1}{2}, m_j' + \tfrac{1}{2};\ m'_j + \tfrac{1}{2}, m_j + \tfrac{1}{2}\right) \end{aligned}\right\} \quad (22)$$

where J are the integrals on space coordinates defined by:

$$J(m_1, m_2; m_3, m_4) = \int\int V(r)\, u^*(m_1|1)\, u^*(m_2|2)\, u(m_3|1)\, u(m_4|2)\, d^3r_1\, d^3r_2 \quad (23)$$

some of them are the integrals encountered with among the matrix elements in the (m_l, m_l')-scheme, e.g.

$$J(m_1, m_2; m_1, m_2) = J(m_1, m_2)$$
$$J(m_1, m_2; m_2, m_1) = K(m_1, m_2)\,.$$

It is easy to see that in order to obtain the matrix elements of the Majorana interaction, which is spin-independent in the above representation, we must take the same coefficients as in (22) and only multiply $V(r)$ in (23) by the operator P_x. This results in a change in the order of the last two quantum numbers in $J(m_1, m_2, m_3, m_4)$ which thus becomes $J(m_1, m_2, m_4, m_3)$. [This therefore transforms $J(m_1, m_2)$ into $K(m_1, m_2)$ and vice versa.]

In order to obtain the matrix elements of the Bartlet interaction, we must exchange the spin coordinates in (21). This can be achieved by first doing an exchange of both the space and the spin coordinates and then another space exchange. As a result J^B has the same coefficients as K^W but the last two quantum numbers are exchanged. This means:

$$J^B = K^M \quad \text{and} \quad K^B = J^M\,.$$

The matrix elements of the Heisenberg interaction should be related to those of the Wigner interaction in the same way, but for a change in sign:

$$J^H = -K^W \quad \text{and} \quad K^H = -J^W.$$

It is therefore enough to calculate the case of ordinary forces. This gives the matrix elements in the $(j_1, j_2, m_{j_1}, m_{j_2})$-scheme:

$$J\left(\tfrac{3}{2}, \tfrac{3}{2}\right) = J(1,1) \qquad K\left(\tfrac{3}{2}, \tfrac{3}{2}\right) = K(1,1)$$

$$J\left(\tfrac{3}{2}, \tfrac{1}{2}\right) = \tfrac{2}{3} J(1,0) + \tfrac{1}{3} J(1,1) \qquad K\left(\tfrac{3}{2}, \tfrac{1}{2}\right) = \tfrac{2}{3} K(1,0)$$

$$J\left(\tfrac{3}{2}, -\tfrac{1}{2}\right) = \tfrac{1}{3} J(1,-1) + \tfrac{2}{3} J(1,0) \qquad K\left(\tfrac{3}{2}, -\tfrac{1}{2}\right) = \tfrac{1}{3} K(1,-1)$$

$$J\left(\tfrac{3}{2}, -\tfrac{3}{2}\right) = J(1,-1) \qquad K\left(\tfrac{3}{2}, -\tfrac{3}{2}\right) = 0$$

$$J\left(\tfrac{1}{2}, \tfrac{1}{2}\right) = \tfrac{4}{9} J(0,0) + \tfrac{4}{9} J(1,0) + \tfrac{1}{9} J(1,1)$$

$$K\left(\tfrac{1}{2}, \tfrac{1}{2}\right) = \tfrac{4}{9} K(0,0) + \tfrac{4}{9} J(1,0) + \tfrac{1}{9} K(1,1)$$

$$J\left(\tfrac{1}{2}, -\tfrac{1}{2}\right) = \tfrac{4}{9} J(0,0) + \tfrac{2}{9} J(1,0) + \tfrac{2}{9} J(0,-1) + \tfrac{1}{9} J(1,-1)$$

$$K\left(\tfrac{1}{2}, -\tfrac{1}{2}\right) = \tfrac{2}{9} K(1,0) + \tfrac{2}{9} K(0,-1) + \tfrac{4}{9} J(0,0;-1,1).$$

The matrix elements in the scheme (m_l, m_l'), i.e. $J(m_1, m_2, m_3, m_4)$ are easily calculated in terms of the I_l from the wave-functions of the pp-configuration A 3; they are (for ordinary forces):

$$J(1,1) = \tfrac{1}{2}(I_0 + I_2) \qquad J(1,0) = \tfrac{1}{4}(I_0 + I_2) + \tfrac{1}{2} I_1$$

$$J(0,0) = \tfrac{3}{4}(I_0 + I_2) - \tfrac{1}{2} I_1 \qquad J(1,-1) = \tfrac{1}{2}(I_0 + I_2)$$

$$K(1,1) = \tfrac{1}{2}(I_0 + I_2) \qquad K(1,0) = \tfrac{1}{4}(I_0 + I_2) - \tfrac{1}{2} I_1$$

$$K(0,0) = \tfrac{3}{4}(I_0 + I_2) - \tfrac{1}{2} I_1 \qquad K(1,-1) = \tfrac{1}{2}(I_0 + I_2) - I_1$$

$$J(0,0;-1,1) = -\tfrac{1}{4}(I_0 + I_2) + \tfrac{1}{2} I_1.$$

To pass from a direct to an exchange integral in this scheme the integrals I which arise from functions symmetric in the (space) coordinates of the two nucleons (those of even Λ, like I_0, I_2, I_{10}, etc.) should be kept unchanged, while those arising from antisymmetric functions (odd Λ, like I_1) should be multiplied by -1. In

terms of these matrix elements the diagonal elements of the $(j_1, j_2, m_{j_1}, m_{j_2})$-scheme can be written down.

In order to calculate the energy levels we write down the matrix elements corresponding to the various M_J [when writing $(m_{j_1}, m_{j_2}; m_{j_3})$ — m_{j_1} and m_{j_2} are the two neutrons' quantum numbers and m_{j_3} is the proton quantum number]. We obtain the following table:

M_J	States in the $(m_{j_1}, m_{j_2}; m_{j_3})$-scheme	Diagonal matrix elements	
		exchange	ordinary
$\frac{7}{2}$	$(\frac{3}{2}, \frac{1}{2}; \frac{3}{2})$	$(\frac{3}{2}, \frac{1}{2})$	$(\frac{3}{2}, \frac{3}{2})(\frac{3}{2}, \frac{1}{2})$
$\frac{5}{2}$	$(\frac{3}{2}, -\frac{1}{2}; \frac{3}{2})(\frac{3}{2}, \frac{1}{2}; -\frac{1}{2})$	$(\frac{3}{2}, \frac{1}{2})(\frac{3}{2}, -\frac{1}{2})$	$(\frac{3}{2}, \frac{3}{2})\ (\frac{3}{2}, \frac{1}{2})\ (\frac{3}{2}, -\frac{1}{2})\ (\frac{1}{2}, \frac{1}{2})$
$\frac{3}{2}$	$(\frac{3}{2}, -\frac{3}{2}; \frac{3}{2})(\frac{3}{2}, -\frac{1}{2}; \frac{1}{2})(\frac{3}{2}, \frac{1}{2}; -\frac{1}{2})(\frac{1}{2}, -\frac{1}{2}; \frac{3}{2})$	$(\frac{3}{2}, \frac{1}{2})(\frac{3}{2}, -\frac{1}{2})$ $(\frac{3}{2}, -\frac{3}{2})(\frac{1}{2}, -\frac{1}{2})$	$(\frac{3}{2}, \frac{3}{2})(\frac{3}{2}, \frac{1}{2})(\frac{3}{2}, -\frac{1}{2})(\frac{1}{2}, -\frac{1}{2})$ $(\frac{3}{2}, -\frac{3}{2})(\frac{3}{2}, -\frac{1}{2})(\frac{3}{2}, \frac{1}{2})(\frac{1}{2}, -\frac{1}{2})$
$\frac{1}{2}$	$(\frac{3}{2}, -\frac{3}{2}; \frac{1}{2})(\frac{1}{2}, -\frac{1}{2}; \frac{1}{2})(\frac{3}{2}, -\frac{1}{2}; -\frac{1}{2})(\frac{3}{2}, \frac{1}{2}; -\frac{3}{2})$ $(\frac{1}{2}, -\frac{3}{2}; \frac{3}{2})$	$(\frac{3}{2}, \frac{1}{2})(\frac{3}{2}, -\frac{1}{2})$ $(\frac{3}{2}, -\frac{3}{2})(\frac{1}{2}, -\frac{1}{2})$ $(\frac{1}{2}, -\frac{3}{2})$	$(\frac{3}{2}, -\frac{3}{2})(\frac{3}{2}, \frac{1}{2})(\frac{3}{2}, -\frac{1}{2})(\frac{1}{2}, \frac{1}{2})$ $(\frac{3}{2}, -\frac{3}{2})(\frac{3}{2}, \frac{1}{2})(\frac{3}{2}, -\frac{1}{2})(\frac{1}{2}, \frac{1}{2})$ $(\frac{1}{2}, -\frac{1}{2})(\frac{3}{2}, -\frac{1}{2})$

Thus we see that there are 5 independent states, namely those with $J = 7/2$ and $J = 5/2$, the two with $J = 3/2$ and the one with $J = 1/2$. The sum method can only give the sum of the two states with $J = 3/2$ but here we can separate the two levels with the help of another quantum number—the isotopic spin τ. 2 neutrons and 1 proton have the projection $\tau_z = -1/2$ of the isotopic spin $\vec{\tau}$, and therefore the states may have either $\tau = 1/2$ or $\tau = 3/2$. The states which have $\tau = 3/2$ are also the states of the configuration $(p_{3/2})^3_P$ $(\tau_z = 3/2)$. Now $(p_{3/2})^3_P$ has only one state—$J = 3/2$ $(\tau = 3/2)$ the energy of which can be immediately obtained from an analogous table:

M_J	States in the $(m_{j_1}, m_{j_2}, m_{j_3})$-scheme	Diagonal matrix elements	
		exchange	ordinary
$\frac{3}{2}$	$(\frac{3}{2}, \frac{1}{2}, -\frac{1}{2})$	$(\frac{3}{2}, \frac{1}{2})(\frac{3}{2}, -\frac{1}{2})(\frac{1}{2}, -\frac{1}{2})$	—

The sum of these energies is the energy of the state $J = 3/2$, $\tau = 3/2$. When this energy is subtracted from the energies of the two states with $J = 3/2$, which is obtained from the other table, the value of the level $J = 3/2$, $\tau = 1/2$ is left.

Using the values given above for the matrix elements we obtain the following values of the energy levels:

State	Type of force	WIGNER	MAJORANA	HEISENBERG	BARTLET
$J=\frac{9}{2}$	$\tau=\frac{3}{2}$	$\frac{5}{6}(I_0+I_2)+\frac{4}{3}I_1$	$\frac{5}{6}(I_0+I_2)-\frac{7}{3}I_1$	$\frac{5}{6}(I_0+I_2)+\frac{4}{3}I_1$	$-\frac{5}{6}(I_0+I_2)+\frac{7}{3}I_1$
$J=\frac{7}{2}$	$\tau=\frac{1}{2}$	$I_0+I_2+I_1$	$I_0+I_2-I_1$	$-\frac{1}{2}(I_0+I_2)+I_1$	$\frac{1}{2}(I_0+I_2)+I_1$
$J=\frac{5}{2}$	$\tau=\frac{1}{2}$	$I_0+I_2+I_1$	$I_0+I_2-\frac{16}{9}I_1$	$-\frac{1}{2}(I_0+I_2)+I_1$	$\frac{1}{2}(I_0+I_2)+\frac{2}{9}I_1$
$J=\frac{1}{2}$	$\tau=\frac{1}{2}$	$I_0+I_2+I_1$	$I_0+I_2-\frac{8}{3}I_1$	$-\frac{1}{2}(I_0+I_2)+I_1$	$\frac{1}{2}(I_0+I_2)-\frac{2}{3}I_1$
$J=\frac{3}{2}$	$\tau=\frac{1}{2}$	$\frac{11}{6}(I_0+I_2)-\frac{2}{3}I_1$	$\frac{11}{6}(I_0+I_2)-\frac{7}{3}I_1$	$\frac{1}{3}(I_0+I_2)-\frac{2}{3}I_1$	$-\frac{1}{3}(I_0+I_2)+\frac{4}{3}I_1$

The same results expressed in terms of the Slater integrals are:

State	Type of force	WIGNER	MAJORANA	HEISENBERG	BARTLET
$J=\frac{3}{2}$	$\tau=\frac{3}{2}$	$3F_0-5F_2$	$-\frac{2}{3}F_0+\frac{40}{3}F_2$	$3F_0-5F_2$	$\frac{2}{3}F_0-\frac{40}{3}F_2$
$J=\frac{7}{2}$	$\tau=\frac{1}{2}$	$3F_0-3F_2$	F_0+7F_2	$-6F_2$	$2F_0-4F_2$
$J=\frac{5}{2}$	$\tau=\frac{1}{2}$	$3F_0-3F_2$	$\frac{2}{9}F_0+\frac{98}{9}F_2$	$-6F_2$	$\frac{11}{9}F_0-\frac{1}{9}F_2$
$J=\frac{3}{2}$	$\tau=\frac{1}{2}$	$3F_0-3F_2$	$-\frac{2}{3}F_0+\frac{46}{3}F_2$	$-6F_2$	$\frac{1}{3}F_0+\frac{13}{3}F_2$
$J=\frac{8}{2}$	$\tau=\frac{1}{2}$	$3F_0+7F_2$	$\frac{4}{3}F_0+\frac{46}{3}F_2$	$+4F_2$	$\frac{2}{3}F_0-\frac{22}{3}F_2$

The connection between the I_l and the F_k is given by:

$$I_0+I_2=2F_0+2F_2 \qquad F_0=\frac{5}{12}(I_0+I_2)+\frac{1}{6}I_1 \qquad F_0=F^0$$

or

$$I_1=F_0-5F_2 \qquad F_2=\frac{1}{12}(I_0+I_2)-\frac{1}{6}I_1 \qquad F_2=F^2/25\,.$$

(Only the combinations I_0+I_2 appears, and thus there are only two parameters I_0+I_2 and I_1 replacing F_0 and F_2.)

In the short range limit — $I_l=0, l>0$ (or $F^2=5F_0$), the results for Wigner forces and Majorana forces coincide, because then only space-symmetric functions contribute to the energy (the same applies for HEISENBERG and BARTLET, except for a change in sign).

It is interesting to note that in the long range limit, when all the I_l are equal ($F^k=0,\ k>0$), the term values of the Heisenberg interaction vanish for $\tau=1/2$. This fact can be explained in a general way. With the help of the isotopic spin $\vec{\tau}$ the Heisenberg interaction can be written as:

$$\sum_{i<k}V_{ik}=\sum_{i<k}\frac{1+4\,(\vec{\tau}^{(i)},\vec{\tau}^{(k)})}{2}V(|\vec{r}_i-\vec{r}_k|)\,.$$

If $V(|\vec{r}_i - \vec{r}_k|)$ has a constant value in the region where the wave-functions differ from zero, we can put it out of the integral sign when calculating the energy, and what remains is the diagonal value of the operator $\sum_{i<k} [1+4(\vec{\tau}^{(i)}, \vec{\tau}^{(k)})]/2$ belonging to the state considered. This value can be immediately found as follows (it is an eigenvalue if the total isotopic spin τ is a quantum number of the given state):

$$T = \sum_{i<k} \frac{1}{2}\left(1+4(\vec{\tau}^{(i)}, \vec{\tau}^{(k)})\right) = \sum_{i<k} \frac{1}{2} + \sum_{i<k} 2(\vec{\tau}^{(i)}, \vec{\tau}^{(k)}) = \frac{n(n-1)}{4} +$$

$$+\tau(\tau+1) - n\tau^{(i)}(\tau^{(i)}+1) = \tau(\tau+1) + \frac{n^2}{4} - n$$

$$\tau^{(i)}(\tau^{(i)}+1) = \frac{3}{4}.$$

This is the factor of F_0 or I_0 when $I_l = I_0$, in any state with given n and τ. In the above case $n = 3$ and we obtain:

$$\tau = \frac{3}{2} \qquad T = 3; \qquad \tau = \frac{1}{2} \qquad T = 0.$$

The coefficients of F_0 for Bartlet forces (and jj-coupling) can be evaluated in the same way was used by RACAH[19]). He evaluated the diagonal value of $\sum_{i<k}(1 - P_\sigma^{ik})/2$, and therefore, in order to obtain the diagonal value of $\sum_{i<k} P_\sigma^{ik}$, the value he obtained should be multiplied by -2 and to it $n(n-1)/4$ should be added. The result is:

$$\frac{n(n-1)}{4} - \frac{n\,j(j+1) - J(J+1)}{(2l+1)^2}.$$

§ 13. *Matrix elements of the Tensor Forces Interaction.*

The interaction energy in the case of tensor forces is:

$$V_{12} = S_{12}V(r) = \left[\frac{(\vec{s}^{(1)}, \vec{r})\,(\vec{s}^{(2)}, \vec{r})}{r^2} - \frac{1}{3}(\vec{s}^{(1)}, \vec{s}^{(2)})\right] V(r) \quad \vec{r} = \vec{r}_2 - \vec{r}_1. \quad (24)$$

It appears also in atomic spectroscopy as the magnetic spin-spin interaction. Also here the development in a series of spherical harmonics is complicated and would not be practical to work with. The tensor forces play an important role in nuclear physics. They have been used to explain the quadrupole moment of the Deutron and, very extensively, in the analysis of scattering experiments. They may also give, in second approximation, a contribution to the doublet splitting.

By our method it is quite a simple matter to obtain matrix elements of the interaction (24). It consists, in fact, only of the

computation of matrix elements of spherical harmonics with $l = 2$, which can be done generally by the use of the Gaunt formula[26]), or else by direct integration. The operator S_{12} of (24) can be written as:

$$\left.\begin{aligned}
&\left(\vec{s}^{(1)}, \frac{\vec{r}}{r}\right)\left(\vec{s}^{(2)}, \frac{\vec{r}}{r}\right) - \frac{1}{3}(\vec{s}^{(1)}, \vec{s}^{(2)}) = (s_+^{(1)} s_-^{(2)} + s_-^{(1)} s_+^{(2)})\left(\frac{1}{4}\sin^2\vartheta - \frac{1}{6}\right) + \\
&+ s_z^{1)} s_z^{(2)}\left(\cos^2\vartheta - \frac{1}{3}\right) + \frac{1}{2}(s_z^{(1)} s_-^{(2)} + s_-^{(1)} s_z^{(2)}) \sin\vartheta\cos\vartheta\, e^{i\varphi} + \\
&+ \frac{1}{2}(s_z^{(1)} s_+^{(2)} + s_+^{(1)} s_z^{(2)}) \sin\vartheta\cos\vartheta\, e^{-i\varphi} + \frac{1}{4} s_-^{(1)} s_-^{(2)} \times \\
&\times \sin^2\vartheta\, e^{2i\varphi} + \frac{1}{4} s_+^{(1)} s_+^{(2)} \sin^2\vartheta\, e^{-2i\varphi} = \\
&= \sqrt{\frac{8}{45}}\left[s_z^{(1)} s_z^{(2)} - \frac{1}{4}\left(s_+^{(1)} s_-^{(2)} + s_-^{(1)} s_+^{(2)}\right)\right] Y_2^{(0)}(\vartheta\,\varphi) - \\
&- \frac{1}{\sqrt{15}}(s_z^{(1)} s_-^{(2)} + s_-^{(1)} s_z^{(2)})\, Y_2^{(1)}(\vartheta, \varphi) + \\
&+ \frac{1}{\sqrt{15}}(s_z^{(1)} s_+^{(2)} + s_+^{(1)} s_z^{(2)})\, Y_2^{(-1)}(\vartheta, \varphi) + \\
&+ \frac{1}{\sqrt{15}} s_-^{(1)} s_-^{(2)}\, Y_2^{(2)}(\vartheta, \varphi) + \frac{1}{\sqrt{15}} s_+^{(1)} s_+^{(2)}\, Y_2^{(-2)}(\vartheta, \varphi)\,.
\end{aligned}\right\} \quad (25)$$

In order to obtain the matrix elements in the $(j_1, j_2, m_{j_1}, m_{j_2})$-scheme we use the wave-functions A 3. S_{12} operates on the spin coordinates of the two nucleons, with respect to which the summation can then be carried out, and what remains is a sum of integrals on the r-coordinate with products of f, g, f', g' as coefficients. The angular integration can be easily done and the radial integrals can be expressed in terms of the I_l. In addition to the integrals met with before, there appears also:

$$I_{2,10} = N_2\, N_{10} \int_0^\infty V(r)\, R_2(r)\, R_{10}(r)\, dr = \sqrt{\frac{2}{5}}\left(\frac{3}{2} I_1 - \frac{5}{2} I_2\right).$$

I_0 does not appear in these sums because S_{12} contains only spherical harmonics of order 2 [as a result of subtracting $(\vec{s}^{(1)}, \vec{s}^{(2)})/3$].

We shall give here the results for the configuration $(p_{3/2})_N^2\, p_{3/2\,P}$. The exchange integrals K are easily derived from the direct integrals J by an exchange of only the space coordinates of the two nucleons (multiplication with P_x). This means that integrals arising from symmetric functions (even Λ, like I_2, $I_{2,10}$, etc.) remain unchanged, while those which arise from antisymmetric functions (odd Λ, like I_1) are multiplied by -1. This is a result of the fact that the operator S_{12} is diagonal with respect to the total spin (of the two nucleons) S, and that its eigenvalue for the singlet state ($S = 0$) is zero. There-

fore only that part of the wave-function which is in the triplet state contributes to the matrix elements, and that part is symmetrical with respect to the two spin coordinates. Thus instead of spin and space exchange, space exchange alone is sufficient to obtain the K from the J integral. This is clearly seen in the results:

$$J\left(\frac{3}{2},\frac{3}{2}\right)=-\frac{1}{42}I_2$$

$$J\left(\frac{3}{2},\frac{1}{2}\right)=\frac{1}{180}I_1-\frac{1}{84}I_2$$

$$J\left(\frac{3}{2},-\frac{1}{2}\right)=\frac{1}{180}I_1-\frac{5}{756}I_2-\frac{1}{135}\sqrt{\frac{5}{2}}I_{2,10}=-\frac{1}{180}I_1+\frac{1}{84}I_2$$

$$J\left(\frac{3}{2},-\frac{3}{2}\right)=\frac{1}{60}I_1-\frac{1}{252}I_2-\frac{1}{90}\sqrt{\frac{5}{2}}I_{2,10}=\frac{1}{42}I_2$$

$$J\left(\frac{1}{2},\frac{1}{2}\right)=-\frac{19}{1134}I_2-\frac{4}{405}\sqrt{\frac{5}{2}}I_{2,10}=-\frac{2}{135}I_1+\frac{1}{126}I_2$$

$$J\left(\frac{1}{2},-\frac{1}{2}\right)=\frac{1}{60}I_1-\frac{25}{2268}I_2-\frac{1}{810}\sqrt{\frac{5}{2}}I_{2,10}=\frac{2}{135}I_1-\frac{1}{126}I_2$$

$$K\left(\frac{3}{2},\frac{3}{2}\right)=-\frac{1}{42}I_2$$

$$K\left(\frac{3}{2},\frac{1}{2}\right)=-\frac{1}{180}I_1-\frac{1}{84}I_2$$

$$K\left(\frac{3}{2},-\frac{1}{2}\right)=-\frac{1}{180}I_1-\frac{5}{756}I_2-\frac{1}{135}\sqrt{\frac{5}{2}}I_{2,10}=-\frac{1}{60}I_1+\frac{1}{84}I_2$$

$$K\left(\frac{3}{2},-\frac{3}{2}\right)=-\frac{1}{60}I_1-\frac{1}{252}I_2-\frac{1}{90}\sqrt{\frac{5}{2}}I_{2,10}=-\frac{1}{30}I_1+\frac{1}{42}I_2$$

$$K\left(\frac{1}{2},\frac{1}{2}\right)=-\frac{2}{135}I_1+\frac{1}{126}I_2$$

$$K\left(\frac{1}{2},-\frac{1}{2}\right)=-\frac{1}{60}I_1-\frac{25}{2268}I_2-\frac{1}{810}\sqrt{\frac{5}{2}}I_{2,10}=-\frac{1}{54}I_1-\frac{1}{126}I_2.$$

When treating the tensor forces as a perturbation on the strong spin-orbit interaction which gives rise to the jj-coupling scheme, the sum method can be used to determine the first order contributions to the energy levels. This is done in the same manner as in the case of central forces. We give here the results for an ordinary potential and a potential which is multiplied by the operator P_x (this simply replaces J by K and vice versa). The I_t in the following table are 12 times those defined above, as it is customary to define S_{12} as

$3/r^2(\vec{\sigma}^{(1)}, \vec{r})(\vec{\sigma}^{(2)}, \vec{r}) - (\vec{\sigma}^{(1)}, \vec{\sigma}^{(2)})$ which is $3 \cdot 4 = 12$ times the operator S_{12} in (24).

State		Ordinary potential	Potential with space exchange
$J=\frac{3}{2}$	$\tau=\frac{3}{2}$	$\frac{2}{3} I_1$	$-\frac{2}{3} I_1$
$J=\frac{7}{2}$	$\tau=\frac{1}{2}$	$\frac{1}{3} I_1 - \frac{3}{7} I_2$	$-\frac{1}{3} I_1 - \frac{3}{7} I_2$
$J=\frac{5}{2}$	$\tau=\frac{1}{2}$	$-\frac{1}{9} I_1 + \frac{5}{21} I_2$	$-\frac{2}{45} I_1 + \frac{5}{21} I_2$
$J=\frac{1}{2}$	$\tau=\frac{1}{2}$	$-\frac{7}{15} I_1 + I_2$	$-\frac{13}{15} I_1 + I_2$
$J=\frac{3}{2}$	$\tau=\frac{1}{2}$	$\frac{2}{3} I_1$	$-\frac{16}{15} I_1$

The matrix elements of the mutual spin-orbit interaction (17) can be calculated with the help of those in the (m_l', m_l)-scheme. The wave-functions (20) are used and the matrix elements are the sums of matrix elements in the (m_l, m_l')-scheme, with coefficients which are products of f, g, f', and g'. Here it is seen, much better than in the (m_l, m_l')-scheme that the K integrals differ from the J only by the sign of the I_l arising from space antisymmetric functions. The reason for it is the same as in the case of the tensor forces. The operator $(\vec{s}^{(1)}+\vec{s}^{(2)}, \vec{l})$ is diagonal with respect to the magnitude of the total spin S ($\vec{S} = \vec{s}^{(1)} + \vec{s}^{(2)}$) and its eigenvalue in the singlet state is zero. [In the (m_l, m_l')-scheme this fact manifests itself in the vanishing of the matrix elements when $m_{s_1} = \pm 1/2$ $m_{s_2} = \mp 1/2$]. The results are:

$$J\left(\frac{3}{2}, \frac{3}{2}\right) = I_2 \qquad J\left(\frac{3}{2}, \frac{1}{2}\right) = \frac{1}{6} I_1 + \frac{1}{2} I_2 \qquad J\left(\frac{3}{2}, -\frac{1}{2}\right) = \frac{1}{6} I_1 + \frac{1}{6} I_2$$

$$J\left(\frac{3}{2}, -\frac{3}{2}\right) = 0 \qquad J\left(\frac{1}{2}, \frac{1}{2}\right) = \frac{5}{9} I_2 \qquad J\left(\frac{1}{2}, -\frac{1}{2}\right) = \frac{4}{9} I_2$$

$$K\left(\frac{3}{2}, \frac{3}{2}\right) = I_2 \qquad K\left(\frac{3}{2}, \frac{1}{2}\right) = -\frac{1}{6} I_1 + \frac{1}{2} I_2 \qquad K\left(\frac{3}{2}, -\frac{1}{2}\right) = -\frac{1}{6} I_1 + \frac{1}{6} I_2$$

$$K\left(\frac{3}{2}, -\frac{3}{2}\right) = 0 \qquad K\left(\frac{1}{2}, \frac{1}{2}\right) = \frac{5}{9} I_2 \qquad K\left(\frac{1}{2}, -\frac{1}{2}\right) = \frac{4}{9} I_2.$$

From these matrix elements the first order contributions to the energy levels of the configuration $(p_{3/2})^2_N \, p_{3/2\,P}$ can be calculated with the help of the sum method. These contributions are:

τ \ J	$\frac{7}{2}$	$\frac{5}{2}$	$\frac{3}{2}$	$\frac{1}{2}$
$\frac{3}{2}$			$\frac{2}{3} I_1$	
$\frac{1}{2}$	$\frac{1}{2} I_1 + \frac{3}{2} I_2$	$\frac{1}{2} I_1 + \frac{13}{18} I_2$	$-\frac{1}{3} I_1 + I_2$	$\frac{1}{2} I_1 - \frac{1}{6} I_2$

§ 14. *Numerical results.*

In order to obtain numerical results we have to evaluate the I_l. We assume that the potential of the interaction between the nucleons has the radial dependence of the Yukawa potential. The general formulas for the I_l in this case were given in § 6.

The value of $\sqrt{\nu}$, which measures the extension of the wave-functions, can be roughly determined from the Li^7-Be^7 Coulomb energy difference. This gives: $1/\sqrt{\nu} \sim 2{\cdot}4 \times 10^{-13}$ cm.

The value of r_0 of the Yukawa potential can be taken from the analysis of scattering experiments; it is between 1·1 and $1{\cdot}4 \times 10^{-13}$ cm. This determines roughly $\lambda \sim 0{\cdot}5$, $\mu \sim 1$. For $\lambda = 0{\cdot}5$, $\mu = 1$ the following values are obtained:

$$I_0 = 0{\cdot}137\ V \qquad I_1 = 0{\cdot}040\ V \qquad I_2 = 0{\cdot}014\ V.$$

For the tensor forces we take the same radial dependence as for the central interactions, with the same results for the I_l.

We shall now show that there are certain values of the interaction parameters for which the four excited states (or three of them) nearly coincide. Such a possibility can only mean that the interpretation in terms of the jj-coupling scheme could have been consistent with the existence of a low-lying compound level, if this were experimentally verified.

State	Exchange operator $(1+P_x)/2$			Exchange operator $(1+P_x)(\frac{1}{3}+\frac{1}{3}P_\sigma)/2$		
	$\gamma=0$	$\gamma=3$	$\gamma=4$	$\gamma=0$	$\gamma=6$	$\gamma=8$
$J=\frac{3}{2}\ \tau=\frac{3}{2}$	0·68	1·28 (1·98)	1·48 (2·18)	0·68	1·88 (2·55)	2·28 (2·98)
$J=\frac{7}{2}$	1·00	1·30 (1·80)	1·40 (1·90)	1·50	2·10 (2·60)	2·30 (2·80)
$J=\frac{5}{2}$	0·88	1·26 (1·76)	1·38 (1·88)	1·30	2·05 (2·55)	2·30 (2·80)
$J=\frac{1}{2}$	0·75	1·23 (1·73)	1·39 (1·89)	1·10	2·06 (2·56)	2·38 (2·88)
$J=\frac{3}{2}\ \tau=\frac{1}{2}$	1·38	2·34 (2·04)	2·66 (2·36)	1·86	3·80 (3·50)	4·40 (4·10)

For the case in which an exchange operator $(1 + P_x)/2$ multiplies the potential, the coincidence of the higher levels can be achieved by adding a tensor force with an exchange operator $-P_x$. If we take the exchange operator of the central forces to be

$$\frac{1}{2}(1+P_x)\left(\frac{4}{3}+\frac{1}{3}P_\sigma\right)=\frac{1}{2}\left(\frac{4}{3}W+\frac{4}{3}M-\frac{1}{3}H+\frac{1}{3}B\right)$$

where W, M, H, and B are the exchange operators of the Wigner, Majorana, Heisenberg, and Bartlet interactions respectively, a co-

incidence can also be attained with the same form of the tensor forces. The results are given in the preceding table where the energy values are expressed in units of $V/7$ and V is the constant of the Yukawa potential in the case of central forces. The corresponding constant for tensor forces is γV.

If V is equal to 7 MeV the above energies are in units of MeV. The spacing between the ground state and the excited (compound) level is then of the right order of magnitude but bigger than the observed 0·48 MeV. If the contribution of the mutual spin-orbit interaction is added, this difference decreases. The term values so corrected are given in the above table in parentheses.

Obviously there are enough parameters to explain the coincidence and the level spacing. The above calculation points out that with reasonable values of them agreement can be achieved, but as long as more exact values of the interaction parameters (magnitude and range of the potential, exchange character, etc.) cannot be fixed with the help of other experiments, no decisive conclusion can be drawn.

§ 15. *Splitting of the* $(p_N^2\, p_P)^{2}{}^{2}P$ *ground state due to spin-orbit interaction.*

As already noted the new experiments favour the assignment $J = 1/2$ for the first excited level of Li^7. It became also clear that the level is quite sharp and there are no other levels in its close neighbourhood[8]). The explanation in terms of the LS-coupling scheme seems therefore plausible. There is also some evidence that the ground state of Li^6 is $^3S_1$ which means that in that nucleus LS-coupling exists. The configuration $p_N^2\, p_P$ in the LS-coupling scheme was treated by WIGNER & FEENBERG[27])[28]), and by HUND[29]). For Wigner and Majorana forces the lowest state is a ^2P with $\tau = 1/2$. According to this the two lowest levels of Li^7 should be interpreted as the two components of this doublet with $J = 3/2$ and $J = 1/2$. With this interpretation the problem still exists where are the other levels of this configuration, specially the next ^2F ($\tau = 1/2$) which should not be as high as 5 MeV (for reasonable values of the parameters). We shall calculate the splitting of the ground ^2P, arising from the mutual spin-orbit interaction of the type introduced by CASE and PAIS, as it is well known that the Thomas interaction and the magnetic spin-orbit interaction give too small a contribution (a splitting can arise also from tensor forces, but only in the second approximation).

The energy of the ground ^2P is for Wigner and Majorana forces:

$$3F_0+18F_2=\frac{11}{4}(I_0+I_2)-\frac{5}{2}I_1$$

(in the notation of HUND it is $3A+2B$ where $A=F_0+4F_2$ and $B=3F_2$). This energy is not degenerate (some of the energy values of higher states are twice and thrice degenerate), and thus it is possible to find the wave-function of the ground state by direct diagonalization of the energy matrix in the scheme $(m_{l_1}, m_{l_2}; m_{l_3})$. The energy is not degenerate also in the short range limit, so that we may calculate the energy matrix in this limit, which makes the calculation simpler.

The wave-function of the ground ^2P (or the ground ^{22}P in the notation $^{(2l+1)(2S+1)}L_J$) in the state $M_J=3/2$ is a linear combination of those wave-functions $(m_{l_1}^{\pm}, m_{l_2}^{\pm}; m_{l_3}^{\pm})$ for which

$$M_S=m_{s_1}+m_{s_2}+m_{s_3}=+\frac{1}{2} \quad \text{and} \quad M_L=m_{l_1}+m_{l_2}+m_{l_3}=+1.$$

There are 8 such functions [in the notation $(m_{l_1}^{m_{s_1}}, m_{l_2}^{m_{s_2}}; m_{l_3}^{m_{s_3}})$ 1 and 2 are the neutrons numbers and 3 is the proton number] and they are listed below:

$\psi_1=(1^+,-1^+;1^-)$ $\quad$ $\psi_4=(1^-,-1^+;1^+)$ $\quad$ $\psi_7=(1^-,0^+;0^+)$

$\psi_2=(1^+,0^+;0^-)$ $\quad$ $\psi_5=(1^+,1^-;-1^+)$ $\quad$ $\psi_8=(0^+,0^-;1^+)$

$\psi_3=(1^+,-1^-;1^+)$ $\quad$ $\psi_6=(1^+,0^-;0^+)$

With these functions the energy matrix in the short range limit, where only I_0 is different from zero, can be built and the diagonalization carried out.

The energy matrix in units of $1/4\,I_0$.

4	−1						
−1	4						
		6	−2	2	−1	0	−1
		−2	6	−2	0	−1	1
		2	−2	6	−1	1	0
		−1	0	−1	5	−1	1
		0	−1	1	−1	5	−1
		−1	1	0	1	−1	5

The matrix is already reduced and the value of $11/4\, I_0$ of the energy of the ground ^2P is an eigenvalue of the 6-row matrix. The corresponding wave-function is a linear combination of the 6 functions ψ_3, ψ_4, ψ_5, ψ_6, ψ_7, ψ_8 the coefficients of which are the components of the eigenvector of the 6-row matrix which belongs to the eigenvalue 11. The linear equations are easily solved with the following results for the coefficients (after normalization to unity):

$$\psi\left(^{22}P^g_{3/2};\, M_J = \frac{3}{2}\right) = \frac{2}{\sqrt{15}}(1^+, -1^-; 1^+) - \frac{2}{\sqrt{15}}(1^-, -1^+; 1^+) +$$
$$+ \frac{2}{\sqrt{15}}(1^+, 1^-, -1^+) - \frac{1}{\sqrt{15}}(1^+, 0^-; 0^+) + \frac{1}{\sqrt{15}}(1^-, 0^+; 0^+) -$$
$$- \frac{1}{\sqrt{15}}(0^+, 0^-; 1^+)\,.$$

The diagonal matrix elements of the mutual spin-orbit interaction which belongs to this wave-function can be now calculated with the help of the matrix elements in the (m_l, m_i)-scheme. In order to obtain the total splitting this function should be multiplied by the wave-functions of the 4 s-nucleons and so the contribution of the interaction of the p- with the s-nucleons will be added to the interaction of the 3 p-nucleons themselves. The calculation is performed in the same way as in cases B and C above. The results are:

Energy of the sp-interaction	Energy of the pp-interaction	Total
$\frac{1}{15} \cdot \frac{15}{2} I_1 = \frac{1}{2} I_1$	$1\frac{1}{5} \cdot 5\, I_2 = \frac{1}{3} I_2$	$\frac{1}{2} I_1 + \frac{1}{3} I_2$

This is the energy of the state $^{22}P_{3/2}$:

$$E(^{22}P^g_{3/2}) = \frac{1}{2} I + \frac{1}{3} I$$

the Landé interval rule yields

$$E(^{22}P^g_{1/2}) = -I - \frac{2}{3} I$$

so that the splitting is:

$$\Delta E = \frac{3}{2} I_1 + I_2\,.$$

The integral I_1 was already calculated with the potential given by Case and Pais. The value of $\sqrt{\nu}$ can be roughly fixed by the determination of the Coulomb energy difference between Li^7 and

Be^7 in terms of it. This gives for the splitting the order of magnitude of ~ 1 MeV. The smaller level spacing in Be^7 can be explained by considering the Coulomb expansion. It is not possible to make more exact statements as the value of I_1 is very sensitive to the values of the parameters. Although this should not be considered as an exact determination of the energies, it is interesting to see that the right order of magnitude is obtained.

The author would like to express his deep gratitude to Prof. W. Pauli, under whose guidance this work has been carried out, and also to Prof. M. Verde and Dr. M. R. Schafroth for helpful discussions.

Appendix.

Expansion of the wave-functions of two nucleons.

ss.

$$(0,0) = \psi_0^0(R)\,\psi_0^0(r) \qquad \text{A 1}$$

ps.

$$\left.\begin{aligned}(\pm 1,0)_s &= \frac{1}{\sqrt{2}}\{(\pm 1,0) + (0,\pm 1)\} = \psi_1^{\pm 1}(R)\,\psi_0^0(r)\\ (0,0)_s &= \psi_1^0(R)\,\psi_0^0(r)\\ (\pm 1,0)_a &= \frac{1}{\sqrt{2}}\{(\pm 1,0) - (0,\pm 1)\} = -\psi_1^{\pm 1}(r)\,\psi_0^0(R)\\ (0,0)_a &= -\psi_1^0(r)\,\psi_0^0(R)\end{aligned}\right\} \qquad \text{A 2}$$

pp.

$$\left.\begin{aligned}(\pm 1,\pm 1) &= \frac{1}{\sqrt{2}}\left(\psi_2^{\pm 2}(R)\,\psi_0^0(r) - \psi_2^{\pm 2}(r)\,\psi_0^0(R)\right)\\ (\pm 1,0)_s &= \frac{1}{\sqrt{2}}\left(\psi_2^{\pm 1}(R)\,\psi_0^0(r) - \psi_2^{\pm 1}(r)\,\psi_0^0(R)\right)\\ (\pm 1,0)_a &= \frac{1}{\sqrt{2}}\left(\psi_1^{\pm 1}(R)\,\psi_1^0(r) - \psi_1^{\pm 1}(r)\,\psi_1^0(R)\right)\\ (0,0) &= \frac{1}{\sqrt{3}}\left(\psi_2^0(R)\,\psi_0^0(r) - \psi_2^0(r)\,\psi_0^0(R)\right) -\\ &\quad -\frac{1}{\sqrt{6}}\left(\psi_{10}^0(R)\,\psi_0^0(r) - \psi_{10}^0(r)\,\psi_0^0(R)\right)\\ (\pm 1,\mp 1)_s &= \frac{1}{\sqrt{6}}\left(\psi_2^0(R)\,\psi_0^0(r) - \psi_2^0(r)\,\psi_0^0(R)\right) +\\ &\quad +\frac{1}{\sqrt{3}}\left(\psi_{10}^0(R)\,\psi_0^0(r) - \psi_{10}^0(r)\,\psi_0^0(R)\right)\\ (\pm 1,\mp 1)_a &= \frac{1}{\sqrt{2}}\left(\psi_1^{\pm 1}(R)\,\psi_1^{\mp 1}(r) - \psi_1^{\pm 1}(r)\,\psi_1^{\mp 1}(R)\right)\end{aligned}\right\} \qquad \text{A 3}$$

ds.

$$
\left.\begin{aligned}
(m,0)_s &= \frac{1}{\sqrt{2}}\left(\psi_2^m(R)\,\psi_0^0(r)+\psi_2^m(r)\,\psi_0^0(R)\right)\\
&\qquad m=-2,-1,0,1,2.\\
(\pm 2,0)_a &= \psi_1^{\pm 1}(R)\,\psi_1^{\pm 1}(r)\\
(\pm 1,0)_a &= \frac{1}{\sqrt{2}}\left(\psi_1^{\pm 1}(R)\,\psi_1^0(r)+\psi_1^{\pm 1}(r)\,\psi_1^0(R)\right)\\
(0,0)_a &= \frac{1}{\sqrt{2}}\left(\psi_1^1(R)\,\psi_1^{-1}(r)+\psi_1^1(r)\,\psi_1^{-1}(R)\right)
\end{aligned}\right\} \quad \text{A 4}
$$

dp.

Only the symmetric functions are listed, the antisymmetric functions are obtained from them by interchanging R and r.

$$
\left.\begin{aligned}
(\pm 2,\pm 1)_s &= \frac{\sqrt{3}}{2}\,\psi_3^{\pm 3}(R)\,\psi_0^0(r)-\frac{1}{2}\,\psi_1^{\pm 1}(R)\,\psi_2^{\pm 2}(r)\\
(\pm 2,0)_s &= \frac{1}{2}\,\psi_3^{\pm 2}(R)\,\psi_0^0(r)+\frac{1}{2}\,\psi_1^0(R)\,\psi_2^{\pm 2}(r)-\\
&\quad -\frac{1}{\sqrt{2}}\,\psi_1^{\pm 1}(R)\,\psi_2^{\pm 1}(r)\\
(\pm 1,\pm 1)_s &= \frac{1}{\sqrt{2}}\,\psi_3^{\pm 2}(R)\,\psi_0^0(r)-\frac{1}{\sqrt{2}}\,\psi_1^0(R)\,\psi_2^{\pm 2}(r)\\
(\pm 2,\mp 1)_s &= \frac{1}{2\sqrt{5}}\,\psi_3^{\pm 1}(R)\,\psi_0^0(r)-\frac{1}{\sqrt{3}}\,\psi_1^{\pm 1}(R)\,\psi_{10}^0(r)+\\
&\quad +\frac{1}{\sqrt{5}}\,\psi_{11}^{\pm 1}(R)\,\psi_0^0(r)-\frac{1}{\sqrt{6}}\,\psi_1^{\pm 1}(R)\,\psi_2^0(r)+\\
&\quad +\frac{1}{2}\,\psi_1^{\mp 1}(R)\,\psi_2^{\pm 2}(r)\\
(\pm 1,0)_s &= \sqrt{\frac{2}{5}}\,\psi_3^{\pm 1}(R)\,\psi_0^0(r)+\frac{1}{\sqrt{6}}\,\psi_1^{\pm 1}(R)\,\psi_{10}^0(r)-\\
&\quad -\frac{1}{\sqrt{10}}\,\psi_{11}^{\pm 1}(R)\,\psi_0^0(r)-\frac{1}{\sqrt{3}}\,\psi_1^{\pm 1}(R)\,\psi_2^0(r)\\
(0,\pm 1)_s &= \sqrt{\frac{3}{10}}\,\psi_3^{\pm 1}(R)\,\psi_0^0(r)-\frac{\sqrt{2}}{6}\,\psi_1^{\pm 1}(R)\,\psi_{10}^0(r)+\\
&\quad +\frac{1}{\sqrt{30}}\,\psi_{11}^{\pm 1}(R)\,\psi_0^0(r)+\frac{1}{3}\,\psi_1^{\pm 1}(R)\,\psi_2^0(r)-\\
&\quad -\frac{1}{\sqrt{6}}\,\psi_1^{\mp 1}(R)\,\psi_2^{\pm 2}(r)-\frac{1}{\sqrt{3}}\,\psi_1^0(R)\,\psi_2^{\pm 1}(r)
\end{aligned}\right\} \quad \text{A 5}
$$

$$
\begin{aligned}
(\pm 1, \mp 1)_s = {} & \frac{1}{2}\sqrt{\frac{3}{5}}\,\psi_3^0(R)\,\psi_0^0(r) - \frac{1}{\sqrt{6}}\,\psi_1^0(R)\,\psi_{10}^0(r) + \\
& + \frac{1}{\sqrt{10}}\,\psi_{11}^0(R)\,\psi_0^0(r) + \frac{1}{2}\,\psi_1^{-1}(R)\,\psi_2^1(r) - \\
& - \frac{1}{2\sqrt{3}}\,\psi_1^0(R)\,\psi_2^0(r) - \frac{1}{2}\,\psi_1^1(R)\,\psi_2^{-1}(r) \\
(0, 0)_s \quad = {} & \frac{3}{2\sqrt{5}}\,\psi_3^0(R)\,\psi_0^0(r) + \frac{\sqrt{2}}{3}\,\psi_1^0(R)\,\psi_{10}^0(r) - \\
& - \sqrt{\frac{2}{15}}\,\psi_{11}^0(R)\,\psi_0^0(r) - \frac{1}{2\sqrt{3}}\,\psi_1^{-1}(R)\,\psi_2^1(r) - \\
& - \frac{1}{6}\,\psi_1^0(R)\,\psi_2^0(r) - \frac{1}{2\sqrt{3}}\,\psi_1^1(R)\,\psi_2^{-1}(r)\,.
\end{aligned}
$$

References.

[1]) M. G. Mayer, Phys. Rev. **78**, 16 (1950).
[2]) M. G. Mayer, Phys. Rev. **78**, 22 (1950).
[3]) G. Racah, to be published.
[4]) D. Kurath, Phys. Rev. **80**, 98 (1950).
[5]) I. Talmi, Phys. Rev. **82**, 101 (1951).
[6]) K. M. Case and A. Pais, Phys. Rev. **80**, 138 (1950).
[7]) D. R. Inglis, Phys. Rev. **77**, 724 (1949).
[8]) D. R. Inglis, Phys. Rev. **82**, 181 (1951), where references are given.
[9]) Haxel, Jensen, and Suess, Z. Phys. **128**, 301 (1950).
[10]) A. de-Shalit et al., Helv. Phys. Acta, in press.
[11]) E. U. Condon and G. H. Shortley, Theory of Atomic Spectra (Cambridge University Press, Cambridge 1935).
[12]) G. Racah, Theory of Complex Spectra, Phys. Rev. **61**, 186 (1942); **62**, 438 (1942); **63**, 367 (1943); **76**, 1352 (1949).
[13]) J. C. Slater, Phys. Rev. **34**, 1293 (1929), see also reference [11]), p. 174.
[14]) H. H. Marvin, Phys. Rev. **71**, 102 (1947).
[15]) W. Heisenberg, Z. Phys. **96**, 473 (1935).
[16]) D. R. Inglis, Phys. Rev. **51**, 531 (1937).
[17]) W. H. Shaffer, Rev. mod. Phys. **16**, 245 (1944).
[18]) E. Feenberg, Phys. Rev. **76**, 1275 (1949).
[19]) G. Racah, Phys. Rev. **78**, 662 (1950).
[20]) D. R. Inglis, Phys. Rev. **38**, 862 (1931).
[21]) G. Racah, private communication.
[22]) M. Goldhaber and A. W. Sunyar, Phys. Rev. **83**, 906 (1951).
[23]) H. H. Hummel and D. R. Inglis, Phys. Rev. **81**, 910 (1951); **83**, 1078 (1951).
[24]) D. R. Inglis, Phys. Rev. **50**, 783 (1936).
[25]) Reference [11]), p. 123.
[26]) Gaunt, Trans. Roy. Soc. London [A] **228**, 151 (1929).
[27]) E. Feenberg and E. P. Wigner, Phys. Rev. **51**, 95 (1937).
[28]) E. Feenberg and M. Phillips, Phys. Rev. **51**, 597 (1937).
[29]) F. Hund, Z. Phys. **105** 202 (1937).

Beiträge zur Theorie der Richtungskorrelation.

Kurt Alder, ETH., Zürich.

13. XII. 51.

1. Einleitung.

Die verschiedenen Zustände eines Atomkerns können durch folgende Grössen charakterisiert werden: Energie, Lebensdauer, Spin, Parität, magnetisches Moment und elektrisches Quadrupolmoment. Im Grundzustand sind die mechanischen, magnetischen oder elektrischen Momente durch die bekannten Methoden (Ausmessung der Hyperfeinstruktur) bestimmbar. Die Gesamtenergie des Kerns ist aus der massenspektroskopisch oder anderweitig bekannten Bindungsenergie berechenbar.

Für angeregte, kurzlebige Kernzustände versagen die für den Grundzustand üblichen Methoden, und es müssen andere Wege benutzt werden. Die Messung der Energiedifferenz zum Grundzustand und teilweise auch die Messung der Lebensdauer ist direkten Methoden zugänglich. Besonders die Betaspektroskopie ist schon seit langer Zeit mit gutem Erfolg verwendet worden. Die Messung der Lebensdauer mit Hilfe verzögerter Koinzidenzen wurde dagegen erst in den letzten Jahren entwickelt. Die Bestimmung der Spinwerte bzw. der Paritätsänderungen kann bis heute dagegen nur auf indirektem Wege erfolgen. Zur Ermittlung der Spinwerte und der Paritätsänderungen bedient man sich mit gutem Erfolg der Theorie der γ-Strahlen. Multipolordnung und Charakter der Strahlung können aus den Konversionskoeffizienten, die jetzt genau berechnet vorliegen (Rose, Spinrad, Goertzel[1]), erhalten werden. Die Schlüsse, die aus der Anwendung der Betatheorie gezogen werden, sind dagegen meist nicht eindeutig. Sie gestatten aber oft gewisse Fälle auszuschliessen. In manchen günstigen Fällen, besonders bei leichten Kernen, können auch Kernreaktionen Angaben über Spin und Parität liefern.

Eine eindeutige Zuordnung von Spin- und Paritätswerten zu den gefundenen Kernzuständen ist jedoch in den wenigsten Fällen möglich. Jede zusätzliche Aussage ist deshalb wertvoll. Die Messung der Richtungskorrelation, die in den letzten Jahren zunehmende Be-

deutung erlangt hat, vermag oft solche Angaben zu liefern und zwischen verschiedenen Möglichkeiten eindeutig zu entscheiden. Wenn von einem angeregten Kern zwei Teilchen sukzessive ausgesandt werden, so hängt die Wahrscheinlichkeit für Emissionen von der Lage der beiden Richtungen der emittierten Teilchen und der Spin- und Multipolzuordnung ab.

Die erste Theorie der Richtungskorrelation stammt von HAMILTON[2]). Weitere Rechnungen sind von verschiedenen Autoren durchgeführt, so von YANG[3]) über allgemeine gruppentheoretische Eigenschaften, von FALKOFF und LING[4]) über Interferenzterme bei Mischungen von verschiedenen Multipolordnungen, von FALKOFF und UHLENBECK[5]) über Korrelation beliebiger Teilchen. Wenn von einem oder beiden γ-Quanten noch die Polarisationsrichtung gemessen werden kann, so spricht man von Polarisationskorrelation. HAMILTON, ZINNES u.a.[6]) haben auch diesen Fall behandelt.

Die Resultate der verschiedenen Autoren ergeben, dass die relative Wahrscheinlichkeit als Polynom in $\cos^2\Theta$

$$W(\Theta) = 1 + A_2 \cos^2\Theta + A_4 \cos^4\Theta + \cdots + A_{2k} \cos^{2k}\Theta$$

dargestellt werden kann. Θ ist dabei der Winkel zwischen den beiden Emissionsrichtungen. Für den höchsten Exponenten $2k$ gilt die Auswahlregel

$$k \leqslant l_1, l_2, I_B,$$

wenn l_1 und l_2 die Multipolordnungen der beiden Strahlungen und I_B den Spin des mittleren Niveaus bedeuten. Bei reinen Strahlungen hängen die Konstanten nicht von Kernmatrixelementen ab, sondern sind gruppentheoretisch durch Spin und Multipolzuordnung bestimmt. Der Vergleich der gemessenen und berechneten Korrelationsfunktion $W(\Theta)$ ergibt somit, wie bereits angedeutet, wertvolle Hinweise auf Spinwerte und Strahlungscharakter.

Obwohl die Idee der Messung sehr einfach ist und die Theorie der γ-γ-Korrelation schon seit 1940 durch HAMILTON[2]) bereitgestellt war, sind die ersten erfolgreichen und zuverlässigen Messungen doch erst nach der Entwicklung des Szintillationszählers in den Jahren 1947 und 1948 durchgeführt worden. Nach diesen ersten Messungen von BRADY und DEUTSCH[7]) wurde die Methode rasch bekannt, und heute bildet die γ-γ-Korrelation ein wertvolles Hilfsmittel für die Kernspektroskopie[8]). Dagegen sind Korrelationen, bei denen eines oder beide Teilchen Elektronen sind, experimentell viel schwieriger zu messen. Dieses Gebiet der Richtungskorrelation besitzt deshalb heute noch eine geringe Bedeutung, vermag aber im Prinzip z. B.

über den Wechselwirkungsansatz in der Fermischen Betatheorie zu entscheiden.

Die Annahme aller bisher zitierten theoretischen Arbeiten ist, dass die Lebensdauer des mittleren Niveaus so kurz ist, dass eine Störung des Zustandes nach Emission des ersten Quants nicht möglich ist. GOERTZEL[9]) hat diese Annahme fallengelassen und in sehr allgemeiner Weise den Einfluss der Elektronenhülle berücksichtigt. Anderseits sind in einer Reihe von Messungen merkliche Anisotropien der Korrelation festgestellt worden, obwohl die Lebensdauer des mittleren Niveaus so gross ist, dass äussere Einflüsse sich bemerkbar machen könnten. In diesen Fällen wird die beobachtete Korrelation im allgemeinen nicht mit der berechneten übereinstimmen, so dass ein Schluss auf die Spinwerte erschwert oder gar verunmöglicht wird. Dagegen ist bei anderweitig bekannten Spinwerten die Abweichung der experimentellen von der theoretischen Korrelation ein Mass für die Wechselwirkung des Kernes mit der Umgebung (Hyperfeinstruktur). Dieser Effekt, der einerseits für die Bestimmung der „wahren" Korrelation störend wirkt, kann umgekehrt zur Bestimmung weiterer Kerneigenschaften verwendet werden. Die Hyperfeinstruktur gestattet ja bekanntlich, die verschiedenen Momente zu bestimmen. Wichtig und der Rechnung bequem zugänglich ist vor allem die Schwächung der Korrelation durch ein äusseres magnetisches Feld. Daraus wird sich später die Möglichkeit ergeben, das magnetische Moment im kurzlebigen mittleren Zustand zu bestimmen.

Kehren wir zurück zur ungestörten Korrelation, die in der oben angedeuteten Form geschrieben werden kann. Die Berechnung der Koeffizienten A_{2k} führt dann auf ausgedehnte numerische Rechnungen. GARDNER, RACAH und LLOYD[10]) zeigten jedoch, dass diese Rechnungen sich stark vereinfachen, wenn die Korrelationsfunktion $W(\Theta)$ nach gruppentheoretisch einfachen und der Geometrie des Problems angepassten Funktionen entwickelt wird. Für ungestörte und unpolarisierte Korrelationen hat man z. B. $W(\Theta)$ nach Kugelfunktionen (Legendresche Polynome) zu entwickeln:

$$W(\Theta) = \sum_n a_n P_n(\cos \Theta).$$

Die a_n lassen sich dann durch geschlossene Formeln ausdrücken. Das Ziel der vorliegenden Arbeit ist es, allgemeine Formeln für die Korrelation beliebiger Teilchen aufzustellen (inklusive Polarisationskorrelation und beliebige Mischung), wobei der Zwischenzustand durch äussere Einflüsse gestört werden kann.

2. Theorie der Richtungskorrelation.

Nach FALKOFF und UHLENBECK[5]) schreiben wir für die relative Wahrscheinlichkeit der Emission der beiden Teilchen

$$W(\vec{k}_1 \vec{k}_2) = S_1 S_2 \sum_{l,p} |\sum_m (A_l |H_1(\vec{k}_1)| B_m)(B_m |H_2(k_2)| C_p)|^2, \quad (1)$$

wo A_l, B_m, C_p die Wellenfunktionen für die entarteten Energieniveaus des Anfangs-, Zwischen- und Endzustandes bedeuten. $H_1(\vec{k}_1)$ stellt den Energieoperator für die Emission des ersten Teilchens in die Richtung $\vec{k}_1$ dar. S_1, S_2 sind Mittelungen über nicht gemessene Spins, Polarisationen, Neutrinorichtungen.

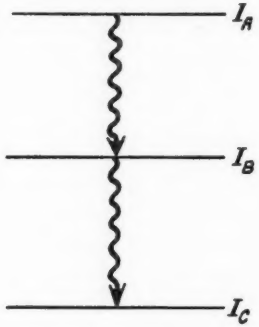

Wird die Entartung der Energieniveaus im Zwischenzustand durch eine äussere Wechselwirkung aufgehoben, so verändert dies die Korrelation. GOERTZEL[9]) hat diesen Fall behandelt und erhält für die relative Wahrscheinlichkeit

$$W(\vec{k}_1, \vec{k}_2) =$$

$$S_1 S_2 \sum_{l,m,m',p} \frac{(A_l |H_1(\vec{k})| B_m)(B_m |H_2(\vec{k})| C_p)(A_l |H_1(\vec{k}_1)| B_{m'})^* (B_{m'} |H_2(\vec{k})| C_p)^*}{1 - i\,\omega_{mm'}\tau}. \quad (2)$$

τ ist die Lebensdauer des mittleren Niveaus, $\omega_{mm'}$ die Energieaufspaltung zwischen den Zuständen B_m und $B_{m'}$ (dividiert durch $\hbar$).

Für die weiteren Überlegungen nehmen wir an, dass die Kernspins der drei Energiezustände I_A, I_B, I_C sind. Die dazugehörigen magnetischen Quantenzahlen seien M_A, M_B, M_C.

Wir betrachten Funktionen $Y_{LM}(A_i \cdots)$*), die von Grössen A_i (Polarisationsgrössen) abhängen sollen und sich bei einer Drehung des Koordinatensystems wie folgt transformieren:

$$Y_{LM}(D\,A_i \cdots) = \sum_m D^L_{mM}(\alpha\beta\gamma)\, Y_{Lm}(A_i \cdots). \tag{3}$$

D soll die Drehung charakterisieren, die durch die drei Eulerschen Winkel α, β, γ gegeben ist. $D^L_{mM}(\alpha, \beta, \gamma)$ ist der dazugehörige Darstellungskoeffizient.

Für die Wechselwirkung fordern wir aus physikalischen Gründen Drehinvarianz. Dies führt dann offenbar auf folgenden Ansatz für den Energieoperator

$$H = \sum_L a_L \sum_{M=-L}^{+L} Y_{LM}(X_i \cdots)\, Y^*_{LM}(A_i \cdots), \tag{4}$$

wo die X_i sich nur auf den Kern und die A_i nur auf die emittierten Teilchen beziehen sollen. Für das Matrixelement $(Jm\,|H|\,J'm')$ folgt damit der Ausdruck

$$(Jm\,|H|\,J'm') = \sum_L a_L \sum_{-L}^{+L} (Jm\,|Y_{LM}(X_i \cdots)|\,J'm')\, Y^*_{LM}(A_i \cdots). \tag{5}$$

$[Jm\,|Y_{LM}(X_i \cdots)|\,J'm']$ kann aus allgemeinen gruppentheoretischen Gründen in zwei Faktoren zerlegt werden:

$$(Jm\,|Y_{LM}(X_i \cdots)|\,J'm') = C^{J'm'}_{JmLM} f(J, J', L, X_i \cdots), \tag{6}$$

wo f von den magnetischen Quantenzahlen m, m', M unabhängig ist. Der erste Faktor ist ein Clebsch-Gordon-Koeffizient, der die Vektoraddition

$$\vec{J} + \vec{L} = \vec{J'} \qquad m + M = m'$$

vermittelt. Da dieser Koeffizient immer dann verschwindet, wenn obige Beziehungen nicht erfüllt sind, bleibt mit $a_L f = \alpha_L$

$$(Jm\,|H|\,J'm') = \sum \alpha_L C^{J'm'}_{JmLM}\, Y^*_{LM}(A_i \cdots)_{M=m'-m}. \tag{7}$$

Dieses Resultat in (2) eingesetzt, ergibt bei einer beliebigen Wahl der z-Achse für die Korrelationsfunktion

$$W(\vec{k}_1 \vec{k}_2) = \sum \alpha_{L_1} \alpha^*_{L_2} C^{I_A M_A}_{I_B M_B L_1 M_1} C^{I_A M_A}_{I_B M'_B L_2 M_2} F^{M_1 M_2}_{L_1 L_2}(\vec{k}_1)$$

$$\beta_{L_3} \beta^*_{L_4} C^{I_B M_B}_{I_C M_C L_3 M_3} C^{I_B M'_B}_{I_C M_C L_4 M_4} F^{M_3 M_4}_{L_3 L_4}(\vec{k}_2) \frac{1}{1 - i\omega_{BB'}\tau}, \tag{8}$$

*) Diese Funktionen sind eine Verallgemeinerung der polarisierten Kugelfunktionen von FALKOFF und UHLENBECK[5]).

wo abkürzungsweise gesetzt ist

$$F_{L_1 L_2}^{M_1 M_2}(\vec{k}) = S\{Y_{L_1 M_1}^{*}(A_i \cdots)\, Y_{L_2 M_2}(A_i \cdots)\}. \tag{9}$$

Die $F_{L_1 L_2}^{M_1 M_2}(\vec{k})$ lassen sich noch weiter vereinfachen. Wir führen eine Drehung des Koordinatensystems so aus, dass die Emissionsrichtung in die z-Achse fällt. Die drei Eulerschen Winkel sind dann:

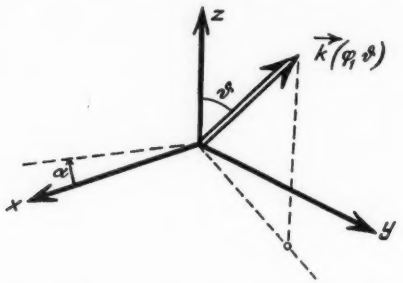

$\alpha = \varphi - \pi/2$, $\beta = \vartheta$, γ beliebig. Es kann $\gamma = 0$ gesetzt werden.

Wegen der Transformationseigenschaften der Y_{LM} ist

$$F_{L_1 L_2}^{M_1 M_2}(\vartheta, \varphi) = \sum_{m_1 m_2} D_{M_1 m_1}^{L_1 *}(\varphi - \frac{\pi}{2}, \vartheta, 0)\, D_{M_2 m_2}^{L_2}(\varphi - \frac{\pi}{2}, \vartheta, 0)\, C_{L_1 L_2}^{m_1 m_2} \tag{10}$$

mit

$$C_{L_1 L_2}^{m_1 m_2} = F_{L_1 L_2}^{m_1 m_2}(0) =$$

$$= S\{Y_{L_1 m_1}^{*}(A_i \cdots \vec{k} \equiv z, \gamma = 0)\, Y_{L_2 m_2}(A_i \cdots \vec{k} \equiv z, \gamma = 0)\}. \tag{11}$$

Die Formeln (8), (9), (10), (11) gestatten jede beliebige Korrelation (inklusive Polarisationen und Mischungen) zu berechnen. Die einzigen Unbekannten sind die modellabhängigen Kernmatrixelemente α_L, β_L, und die $F_{L_1 L_2}^{M_1 M_2}(0)$.

Wir wollen uns vorerst auf den Fall beschränken, dass keine der Polarisationsgrössen A_i gemessen werde. S bedeutet dann die Mittelung über alle A_i. Mitteln wir zunächst über alle möglichen Lagen,

---

Aus bekannten gruppentheoretischen Relationen der Darstellungskoeffizienten [Appendix A (8), (4)] leitet man die folgenden Eigenschaften der F her:

$$\int F_{L_1 L_2}^{M_1 M_2}\, d\Omega = \delta_{M_1 M_2}\, \delta_{L_1 L_2} \cdot \text{const};\ \text{const unabhängig von } M,$$

$$\sum_{-L}^{+L} F_{LL}^{MM}(\vartheta) \quad \text{unabhängig von } \vartheta.$$

Diese beiden Sätze sind in Falkoff und Uhlenbeck[5]) zitiert.

die aus einer speziellen Lage durch Drehung um $\vec{k}$ um den Winkel γ entstehen, so führt dies wegen der Transformationseigenschaften der Y_{LM} auf ein Integral

$$\int_0^{2\pi} e^{i(m_1-m_2)\gamma}\, d\gamma = 2\pi\, \delta_{m_1 m_2}, \tag{12}$$

d.h. es muss

$$F_{L_1 L_2}^{m_1 m_2}(0) = \delta_{m_1 m_2} F_{L_1 L_2}^{m_1 m_2}(0) \tag{13}$$

sein. (13) ist äquivalent mit der Bemerkung (HAMILTON[2]), GOERTZEL[9]), FALKOFF und UHLENBECK[5]), LLOYD[11]) und LIPPMANN[12])), dass sämtliche Interferenzterme verschwinden, wenn die z-Achse in die Richtung des einen Quantes gelegt wird. Aus der Herleitung geht hervor, dass dieser Satz nicht mehr richtig ist, wenn Polarisationen gemessen werden können.

(13) sagt weiter aus, dass $F_{L_1 L_2}^{M_1 M_2}$ nur von Min (L_1, L_2) willkürlichen Koeffizienten abhängt. Diese Bemerkung stammt ebenfalls von FALKOFF und UHLENBECK[5]).

Die Formeln (8), (9), (10), (11) für die Richtungskorrelation beliebiger Teilchen können noch vereinfacht werden. Die Summen über magnetische Quantenzahlen tragen ja im allgemeinen nur geometrischen Charakter und es muss daher möglich sein, diese explizit auszuwerten. Dies führt auf sogenannte Racah-Koeffizienten, deren Definitionen und Beziehungen mit anderen oft gebrauchten gruppentheoretischen Relationen im Appendix zusammengestellt sind.

Speziell ist nach Appendix A (3), (7)

$$F_{L_1 L_2}^{M_1 M_2}(\vartheta, \varphi)$$
$$= \sum_{m,\, k \text{ gerade}} C^{k\, M_2 - M_1}_{L_1 - M_1\, L_2 M_2} C^{k\, 0}_{L_1 - m\, L_2 m} D^{k}_{M_2 - M_1, 0}\left(\varphi - \frac{\pi}{2}, \vartheta, 0\right)(-1)^{m - M_1} F_{L_1 L_2}^{m m}(0). \tag{14}$$

(14) in (8) eingesetzt ergibt dann

$$W(\vec{k}_1 \vec{k}_2) = \sum_{\substack{k_1 k_2 \\ \mu}} a_\mu^{k_1 k_2} D^{k_1}_{\mu 0}\left(\varphi_1 - \frac{\pi}{2}, \vartheta_1, 0\right) D^{k_2 *}_{\mu 0}\left(\varphi_2 - \frac{\pi}{2}, \vartheta_2, 0\right), \tag{15}$$

*) Dass in (14) nur über die geraden k summiert zu werden braucht, folgt aus der Erhaltung der Parität. Es existieren nämlich zwei verschiedene Arten von $Y_{LM}(A_i \cdots)$: solche, die bei einer Spiegelung das Vorzeichen wechseln und solche, die invariant bleiben. Da man für die Wechselwirkung H ausser der Drehinvarianz auch Spiegelungsinvarianz fordern muss, folgt, dass Parität $Y_{LM}(X_i \cdots)$ = Parität $Y_{LM}(A_i \cdots) \neq$ Paritätsänderung des betrachteten Übergangs ist: Diese Grösse ist aber fest, so dass $F_{L_1 L_2}^{M_1 M_2}(\vec{k}) = S\left\{Y^*_{L_1 M_1}(A_i \cdots)\, Y_{L_2 M_2}(A_i \cdots)\right\}$ eine gerade Parität besitzt.

wo die $a_\mu^{k_1 k_2}$ sich wie folgt darstellen lassen:

$$a_\mu^{k_1 k_2} = \mathrm{I}^{k_1} \cdot \mathrm{II}^{k_2} \cdot \mathrm{III}_\mu^{k_1 k_2}. \tag{16}$$

Die drei Faktoren haben die folgende Bedeutung:

$$\left.\begin{aligned}
\mathrm{I}^{k_1} &= \sqrt{2k_1+1} \sum_{L_1 L_2} \alpha_{L_1} \alpha^*_{L_2} (-1)^{I_A - I_B + L_2} W(I_B I_A k_1 L_2 / L_1 I_B) \times \\
&\quad \times \left\{ \sum_m (-1)^{L_1 - m} C^{k\,0}_{L_1 m\, L_2 - m} F^{m\,m}_{L_1 L_2}(0) \right\}, \\
\mathrm{II}^{k_2} &= \sqrt{2k_2+1} \sum_{L_2 L_4} \beta_{L_2} \beta^*_{L_4} (-1)^{I_C - I_B + L_4} W(I_B I_C k_2 L_4 / L_3 I_B) \times \\
&\quad \times \left\{ \sum (-1)^{L_2 - m} C^{k\,0}_{L_2 m\, L_4 - m} F^{m\,m}_{L_2 L_4}(0) \right\}, \\
\mathrm{III}_\mu^{k_1 k_2} &= \sum_{M_B M_B'} C^{I_B M_B}_{I_B M_B' k_1 \mu} C^{I_B M_B}_{I_B M_B' k_2 \mu} \cdot \frac{1}{1 - i\omega_{BB'}\tau}. \\
&\qquad k_1, k_2 \text{ gerade}
\end{aligned}\right\} \tag{17}$$

3. Allgemeine Eigenschaften der Korrelationsfunktionen.

Die Formeln (15) sind Entwicklungen von $W(\vec{k}_1, \vec{k}_2)$ in natürlicher Weise nach Darstellungskoeffizienten. Die Auswahlregeln der Racah-Koeffizienten (Appendix B) verlangen

$$\left.\begin{aligned}
|I_A - I_B| \leqq L_{1,2} \leqq |I_A + I_B| \quad & |I_C - I_B| \leqq L_{3,4} \leqq I_C + I_B \\
0 \leqq 2k_1 \leqq 2I_B \quad & |L_1 - L_2| \leqq 2k_1 \leqq L_1 + L_2 \\
0 \leqq 2k_2 \leqq 2I_B \quad & |L_3 - L_4| \leqq 2k_2 \leqq L_3 + L_4
\end{aligned}\right\} \tag{18}$$

Die ersten beiden Ungleichungen sind nichts anderes als der Satz von der Erhaltung des Drehimpulses.

Ist $\omega_{BB'}\tau \ll 1$, d.h. die Störung des mittleren Niveaus klein, so ergibt sich eine weitere Vereinfachung.

Es ist nämlich

$$\mathrm{III}_\mu^{k_1 k_2} = \sum_{M_B M_B'} C^{I_B M_B}_{I_B M_B' k_1 \mu} C^{I_B M_B}_{I_B M_B' k_2 \mu} = \delta_{k_1 k_2} \frac{2I_B + 1}{2k+1} \tag{19}$$

also

$$\begin{aligned}
W(\vec{k}_1 \vec{k}_2) &= \sum_{k,\mu} \frac{1}{2k+1} \mathrm{I}^k \cdot \mathrm{II}^k D^k_{\mu 0}\left(\varphi_1 - \frac{\pi}{2}, \vartheta_1, 0\right) D^{k*}_{\mu 0}\left(\varphi_2 - \frac{\pi}{2}, \vartheta_2, 0\right) = \\
&= \sum_{k,\mu} \frac{1}{2k+1} \mathrm{I}^k \cdot \mathrm{II}^k D^k_{\mu 0}\left(\varphi_1 - \frac{\pi}{2}, \vartheta_1, 0\right) D^k_{0\mu}\left(0, \vartheta_2, \frac{\pi}{2} - \varphi_2\right).
\end{aligned} \tag{20}$$

Die Summe über μ kann aus der Gruppeneigenschaft der Raumdrehungen leicht bestimmt werden.

Es seien Φ, Θ, Ψ die Eulerschen Winkel der zusammengesetzten Drehung ST mit

$$T = \left\{\varphi_1 - \frac{\pi}{2}, \vartheta_1, 0\right\},$$

$$S = \left\{0, \vartheta_2, \frac{\pi}{2} - \varphi_2\right\}.$$

Die Bedeutung des Winkels Θ lässt sich durch eine kleine Rechnung leicht erhalten. Es ist $\Theta = < (\vec{k}_1, \vec{k}_2)$.

Aus

$$\sum_{\mu} D^k_{\mu_1 \mu}(S)\, D^k_{\mu \mu_2}(T) = D^k_{\mu_1 \mu_2}(S\,T) \tag{21}$$

ergibt sich also

$$\begin{aligned} W(k_1 k_2) &= \sum_{k \text{ gerade}} \frac{1}{2k+1} \mathrm{I}^k \cdot \mathrm{II}^k \cdot D^k_{00}(\Phi, \Theta, \Psi) = \\ &= \sum_{k \text{ gerade}} \frac{1}{2k+1} \mathrm{I}^k \cdot \mathrm{II}^k D^k_{00}(0, \Theta, 0) = \\ &= \sum_{k \text{ gerade}} \frac{1}{2k+1} \mathrm{I}^k \cdot \mathrm{II}^k P_k(\cos\Theta) = \sum_{k \text{ gerade}} a_k P_k(\cos\Theta). \end{aligned} \tag{22}$$

Die Korrelationsfunktion ist speziell von der Lage der z-Achse unabhängig. Sie ist eine Summe von Potenzen in $\cos^2\Theta$. Der höchste Exponent ist nach den Auswahlregeln (18) durch

$$\mathrm{Min}\,\{2I_B, \mathrm{Max}\,(L_1 + L_2), \mathrm{Max}\,(L_3 + L_4)\}$$

begrenzt. Ist dagegen die Störung $\omega\tau$ nicht mehr vernachlässigbar, so hat man mit den allgemeinen Formeln (17) zu rechnen. Diese können aber wie folgt interpretiert werden:

Wir entwickeln die ungestörte Korrelationsfunktion nach Kugelfunktionen

$$W(\vec{k}_1 \vec{k}_2) = \sum_{k,\mu} a_k \frac{1}{2k+1} Y^{\mu}_k(\vec{k}_1)\, Y^{-\mu}_k(\vec{k}_2). \tag{23}$$

Den Einfluss der Störung erhalten wir nun, indem jedes Glied (k, μ) mit einem Schwächungsfaktor G^{μ}_k („attenuation factor") multipliziert wird:

$$W(\vec{k}_1 \vec{k}_2) = \sum_{k,\mu} a_k G^{\mu}_k \frac{1}{2k+1} Y^{\mu}_k(\vec{k}_1)\, Y^{-\mu}_k(\vec{k}_2), \tag{24}$$

wo

$$G^{\mu}_k = (2k+1)\,\mathrm{III}^{kk}_{\mu} = (2k+1) \sum_{m,m'} \left| C^{I_B m}_{I_B m' k \mu} \right|^2 \frac{1}{1 - i\,\omega_{m m'} \tau}. \tag{25}$$

Dies bleibt offenbar nur solange richtig, als unser Ausdruck

$$\mathrm{III}_{\mu}^{k_1 k_2} = \delta_{k_1 k_2}\, \mathrm{III}_{\mu}^{k_1 k_2} \tag{26}$$

ist. Neben dem oben betrachteten Fall $\omega\tau \ll 1$ gilt (26) auch dann, wenn die Hyperfeinaufspaltung zwischen verschiedenen magnetischen Quantenzahlen gleich gross ist (z. B. Aufspaltung im schwachen Magnetfeld). Ist die Hyperfeinaufspaltung nicht äquidistant, so müssen noch Interferenzterme berücksichtigt werden, die durch den Schwächungsmechanismus erzeugt werden. Nach (17) ist

$$W(\vec{k}_1 \vec{k}_2) = \sum_{\substack{k_1 k_2 \\ \mu}} \mathrm{I}^{k_1} \mathrm{II}^{k_2} \mathrm{III}_{\mu}^{k_1 k_2} \frac{1}{\sqrt{2k_1+1}} Y_{k_1}^{\mu}(\vec{k}_1) \frac{1}{\sqrt{2k_2+1}} Y_{k_2}^{-\mu}(\vec{k}_2). \tag{27}$$

Wenn statt unpolarisierter Strahlung irgendwelche Grössen (Polarisationen) zusätzlich gemessen werden, so wird der obige Formalismus nur unwesentlich geändert.

In den Formeln (17) hat man einfach $\sum_{m}$ durch den Ausdruck

$$\left\{ \sum_{m_1 m_2} (-1)^{L_1 - m_1} C_{L_1 m_1 L_2 - m_2}^{k_1 - \mu_1} F_{L_1 L_2}^{m_1 m_2}(0) \right\}$$

und $D_{0\mu}^{k_1}$ durch $D_{\mu_1 \mu}^{k_1}$ zu ersetzen.

$$\left.\begin{aligned}
\mathrm{I}_{\mu_1}^{k_1} &= \sqrt{2k_1+1} \sum_{L_1 L_2} \alpha_{L_1} \alpha_{L_2}^{*} (-1)^{I_A - I_B + L_2} W(I_B I_A k_1 L_2 / L_1 I_B) \times \\
&\quad \times \left\{ \sum_{m_1 m_2} (-1)^{L_1 - m_1} C_{L_1 m_1 L_2 - m_2}^{k_1 - \mu_1} F_{L_1 L_2}^{m_1 m_2}(0) \right\} \\
\mathrm{II}_{\mu_2}^{k_2} &= \sqrt{2k_2+1} \sum_{L_3 L_4} \beta_{L_3} \beta_{L_4}^{*} (-1)^{I_C - I_B + L_4} W(I_B I_C k_2 L_4 / L_3 I_B) \times \\
&\quad \times \left\{ \sum_{m_3 m_4} (-1)^{L_3 - m_3} C_{L_3 m_3 L_4 - m_4}^{k_2 \mu_2} F_{L_3 L_4}^{m_3 m_4}(0) \right\} \\
\mathrm{III}_{\mu_1}^{k_1 k_2} &= \sum_{M_B M_B'} C_{I_B M_B' k_1 \mu}^{I_B M_B} C_{I_B M_B' k_2 \mu}^{I_B M_B} \frac{1}{1 - i\,\omega_{B B'} \tau}
\end{aligned}\right\} \tag{28}$$

$$a_{\mu_1 \mu_2 \mu}^{k_1 k_2} = \mathrm{I}_{\mu_1}^{k_1} \mathrm{II}_{\mu_2}^{k_2} \mathrm{III}_{\mu}^{k_1 k_2}$$

$$W(\vec{k}_1 \vec{k}_2) = \sum_{\mu_1 \mu_2 \mu} a_{\mu_1 \mu_2 \mu}^{k_1 k_2} D_{\mu \mu_1}^{k_1} \left(\varphi_1 - \frac{\pi}{2}, \vartheta_1 0\right) D_{\mu_2 \mu}^{k_2} \left(0, \vartheta_2 \frac{\pi}{2} - \varphi_2\right).$$

Die $F_{L_1 L_2}^{m_1 m_2}(0)$ hängen natürlich jetzt noch von den gemessenen Polarisationsgrössen $A_i \cdots$ ab.

Für verschwindende Schwächung $\omega\tau \ll 1$ lässt sich die Summe über μ wie vorhin auswerten und erhält

$$W(\vec{k}_1 \vec{k}_2) = \sum_{\mu_1 \mu_2} \frac{1}{2k+1} \mathrm{I}^k_{\mu_1} \mathrm{II}^k_{\mu_2} D^k_{\mu_1 \mu_2}(\Phi, \Theta, \Psi). \tag{29}$$

Die Eulerschen Winkel Φ und Ψ sind vom speziell gewählten Koordinatensystem abhängig. Dies ist nicht verwunderlich, da die Polarisationsgrössen $A_i \cdots$ ja auf dieses festgewählte System bezogen sind.

Wählen wir als Koordinatensystem dasjenige, das als z-Achse die Emissionsrichtung des einen Quants und als (z, y)-Ebene die Ebene der beiden Quanten besitzt, so ist $\Phi = 0$, $\Psi = 0$. Wir haben

$$W(\vec{k}_1 \vec{k}_2) = \sum_{k_1 \mu_1 \mu_2} \frac{1}{2k+1} \mathrm{I}^k_{\mu_1} \mathrm{II}^k_{\mu_2} D^k_{\mu_1 \mu_2}(0, \Theta, 0). \tag{30}$$

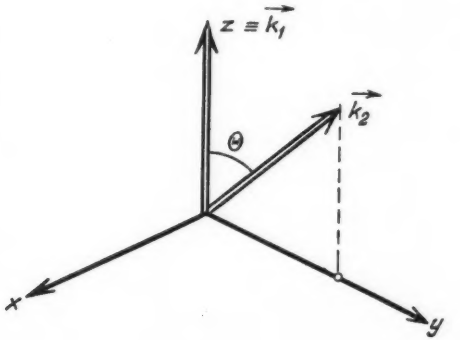

Schwächungen durch äussere Einflüsse können wie oben diskutiert werden.

4. Diskussion der Schwächungserscheinungen.

Die Korrelation kann durch irgendwelche äussere oder innere Felder gestört werden. Als inneres Feld wollen wir das Magnetfeld der Hülle am Ort des Kerns annehmen. Die Hülle werde durch den Drehimpuls J charakterisiert. Er setzt sich mit dem Kernspin I zu einem totalen Drehimpuls F zusammen. In den obigen Formeln hat man jetzt unter den A_l, B_m, C_p die Wellenfunktionen des gesamten Atoms (Kern und Hülle) zu verstehen. Dabei ist aber zu beachten, dass der Operator H nur auf die Kerneigenfunktionen wirkt.

Wegen der (I, J)-Kopplung können aber die Kernmatrixelemente der Form $(A_t\,|H_1|\,B_m)$ leicht auf gewöhnliche Kernmatrixelemente umtransformiert werden. Es gilt z. B.

$$(I_A\,J\,F_\alpha m_\alpha|H_1|I_B\,J\,F_\beta m_\beta) = \sum_{M_A\,M_B} C^{F_\alpha m_\alpha}_{I_A M_A J s}\,(I_A\,M_A|H_1|\,I_B\,M_B)\,C^{F_\beta m_\beta}_{I_B M_B J r} \tag{31}$$

Diese und analoge Formeln in (2) eingesetzt ergeben unter Berücksichtigung der Orthogonalitätsrelationen der Clebsch-Gordon-Koeffizienten für III

$$\mathrm{III}^{k_1 k_2}_{\mu} = \sum C^{I_B M_B}_{I_B M'_B k_1 \mu} C^{I_B M_B}_{I_B M'_B k_2 \mu} C^{F m}_{I_B M'_B J r} \times \\ \times C^{F m}_{I_B M_B J s} C^{F' m'}_{I_B M_B J s} C^{F' m'}_{I_B M'_B J r} \frac{1}{1 - i\,\omega_{F m;\,F' m'}}. \tag{32}$$

Diese Summe kann wieder durch Racah-Koeffizienten aufsummiert werden:

$$\mathrm{III}^{k_1 k_2}_{\mu} = \sum_{F F'} (2F+1)\,W(I_B J k_1 F/F' I_B)\,W(I_B J k_2 F/F' I_B) \times \\ \times \sum_{m m'} C^{F m}_{F' m' k_1 \mu} C^{F m}_{F' m' k_2 \mu} \frac{1}{1 - i\,\omega_{F m;\,F' m'}}. \tag{33}$$

Für äquidistante Hyperfeinaufspaltung ist $\mathrm{III}^{k_1 k_2}_{\mu}$ von der Form $\delta_{k_1 k_2}$. Also verschwinden die Interferenzterme und es bleibt

$$\mathrm{III}^{k}_{\mu} = \sum_{F, F'} (2F+1)\,|W(I_B J k F/F' I_B)|^2 \sum_{m m'} |C^{F m}_{F' m' k \mu}|^2 \frac{1}{1 - i\,\omega_{F m;\,F' m'}}.$$

Diese Formel ist nur solange richtig, als die äussere Wechselwirkung die (I, J)-Kopplung nicht zerstört.

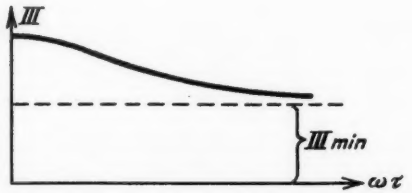

Für den Spezialfall $H = 0$ kann die Summe über m, m' noch ausgeführt werden. Es ist

$$\mathrm{III}^{k} = \frac{1}{2k+1} \sum_{F, F'} \frac{(2F+1)\,(2F'+1)\,|W(I_B J k F/F' I_B)|^2}{1 + (\omega_{F F'}\,\tau)^2} \tag{34}$$

$\omega_{FF'}\tau$ ist ein Mass für die Schwächung. III in Abhängigkeit von $\omega\tau$ ist eine monoton fallende Funktion.

Für $\omega\tau \ll 1$ kann jedoch III nicht verschwinden. Es bleibt

$$(\mathrm{III}^k)_{\min} = \frac{1}{2k+1} \sum_F (2F+1)^2 |W(I_B J k F/F I_B)|^2. \quad (35)$$

Die obigen Formeln erlauben wieder eine einfache Interpretation. Wenn die ungestörte Korrelationsfunktion in der Form

$$W(\Theta) = \sum_k a_k P_k(\cos\Theta)$$

vorliegt, so äussert sich der Einfluss der Hülle in einem Schwächungsfaktor

$$G_k = (2k+1)\,\mathrm{III}^k,$$

$$W(\Theta) = \sum_k a_k G_k P_k(\cos\Theta).$$

Die Diskussion von G_k bzw. $(G_k)_{\min}$ in Funktion der Grössen $\omega\tau$, I_B, k geschieht am besten für $J = 1/2$. In diesem Fall lassen sich die Racah-Koeffizienten leicht berechnen. Es ist

$$\left.\begin{aligned}
W\left(I_B \tfrac{1}{2} k\, I_B + \tfrac{1}{2} \middle/ I_B + \tfrac{1}{2} I_B\right) &= \frac{1}{2(I_B+1)(2I_B+1)} \\
&\quad \sqrt{(2I_B+1-k)(2I_B+k+2)} \\
W\left(I_B \tfrac{1}{2} k\, I_B + \tfrac{1}{2} \middle/ I_B - \tfrac{1}{2} I_B\right) &= -\frac{1}{2(2I_B+1)} \sqrt{\frac{k(k+1)}{I_B(I_B+1)}} \\
W\left(I_B \tfrac{1}{2} k\, I_B - \tfrac{1}{2} \middle/ I_B + \tfrac{1}{2} I_B\right) &= \frac{1}{2(2I_B+1)} \sqrt{\frac{k(k+1)}{I_B(I_B+1)}} \\
W\left(I_B \tfrac{1}{2} k\, I_B - \tfrac{1}{2} \middle/ I_B - \tfrac{1}{2} I_B\right) &= \frac{1}{2(I_B+1)(2I_B+1)} \\
&\quad \sqrt{(2I_B+1-k)(2I_B+k+2)} \\
G_k &= 1 - \frac{k(k+1)}{(2I_B+1)^2} T \\
T &= \frac{(\omega\tau)^2}{1+(\omega\tau)^2} \\
(G_k)_{\min} &= 1 - \frac{k(k+1)}{(2I_B+1)^2}.
\end{aligned}\right\} \quad (36)$$

$(G_k)_{\min}$ für verschiedene k und I_B ist in der folgenden Tabelle niedergelegt.

Aus der Tabelle ist ersichtlich, dass Glieder mit höheren $\cos^n\Theta$ empfindlicher geschwächt werden, als diejenigen mit niedrigen Po-

tenzen. Ferner ist die Schwächung kleiner, je grösser der Spin I_B im mittleren Zustand ist.

I_B \ k	2	4	6	8	10
1	0,33				
$^3/_2$	0,52				
2	0,76	0,20			
$^5/_2$	0,83	0,44			
3	0,88	0,59	0,15		
$^7/_2$	0,90	0,68	0,34		
4	0,93	0,75	0,48	0,11	
$^9/_2$	0,94	0,80	0,58	0,28	
5	0,95	0,84	0,65	0,40	0,09

Für ein äusseres Magnetfeld ohne Berücksichtigung eventueller Hülleneffekte kann der Schwächungsfaktor ebenfalls leicht berechnet werden. Es ist nämlich

$$\omega_{mm'} = r\,\omega = r\,\mu\,H/I\,\hbar = r\,g\,\mu_k\,H/\hbar \tag{37}$$

(μ, g magnetischer Moment und g-Faktor des mittleren Zustandes; μ_k Kernmagneton). Für G_k^r ergibt sich dann

$$G_k^r = \frac{1}{1 - i\,r\,\omega\,\tau}. \tag{38}$$

Wenn wir das äussere Magnetfeld H senkrecht zur Ebene der zwei Quanten anlegen, werden die Formeln besonders einfach

$$W(\vartheta, H) = \sum_r b_r \frac{1}{1 - i\,r\,\omega\,\tau}\, e^{i\,r\,\vartheta}, \tag{39}$$

wo ϑ der Winkel zwischen den beiden Quanten ist. Das magnetische Feld H induziert eine Schwächung und eine Phasenverschiebung. Für $\omega\tau \ll 1$ äussert sich dies in einer Rotation der Symmetrieachse um den klassischen Präzessionswinkel $\Phi = \omega\tau$.

Wenn die beiden Zähler die beiden Partikel nicht unterscheiden können, so wird der Schwächungsfaktor reell:

$$G_k^r = \frac{1}{2}\left\{\frac{1}{1 - i\,r\,\omega\,\tau} + \frac{1}{1 + i\,r\,\omega\,\tau}\right\} = \frac{1}{1 + (r\,\omega\,\tau)^2}. \tag{40}$$

Eine Messung von G_k^r mit gleich empfindlichen Zählern gibt somit nur die Grösse, nicht aber das Vorzeichen des gyromagnetischen Faktors des Kernes.

Berechnung der Konstanten $F_{L_1 L_2}^{m_1 m_2}(0)$ für einige Spezialfälle.

Aus physikalischen Gründen verschwindet $F_{L_1 L_2}^{m_1 m_2}(0)$, wenn es nicht gelingt, die z-Komponenten m_1 bzw. m_2 des Drehimpulses ohne Bahnimpuls (sondern nur durch Spin, Neutrinos usw.) wegzutragen. Es ist also speziell

für Spin-0-Teilchen $F_{l_1 l_2}^{m m}(0) = 0$, ausser $m = 0$;

für γ-Strahlen $F_{l_1 l_2}^{m_1 m_2}(0) = 0$, ausser $m_{1,2} = \pm 1$.

Spin-0-Teilchen.

Es ist
$$F_{l_1 l_2}^{00}(0) = \{Y_{l_1}^0(0)\, Y_{l_1}^0(0)\} = 1. \tag{41}$$

γ-Strahlen.

Es ist $Y_l^1 \sim \varepsilon_+$ für elektrische Strahlung

$Y_l^1 \sim -i\,\varepsilon_+$ für magnetische Strahlung $\varepsilon_+ = e_x + i e_y$.

Mit $Y_l^{-1} = -(Y_l^1)^*$ gewinnt man ohne weiteres:

	el-el	mg-mg	el-mg	mg-el
$F_{l_1 l_2}^{11}$	1	1	$-i$	i
$F_{l_1 l_2}^{-1-1}$	1	1	i	$-i$

Sämtliche von l abhängige Grössen sind dabei zum Matrixelement geschlagen. Daher sind die Matrixelemente von Falkoff und Ling von den unsrigen verschieden. Es gilt

$$\alpha_l = \sqrt{2l+1}\, i^{-l} (\alpha_l)_{\text{Falk-Ling}}.$$

Wenn Polarisationen gemessen werden, können die zugehörigen $F_{l_1 l_2}^{m_1 m_2}(0)$ ebenfalls leicht angegeben werden. Dabei wollen wir das Koordinationssystem, auf das die Polarisationsgrössen bezogen werden, wie oben wählen [z-Achse in Richtung des einen Quants, (z, y)-Ebene = Ebene der beiden Quanten].

φ bedeutet den Winkel, den der Polarisationsvektor mit der Ebene der beiden Quanten einschliesst.

	el-el	mg-mg	el-mg	mg-el
$F_{l_1 l_2}^{1-1}$	$e^{-i2\varphi}$	$-e^{-i2\varphi}$	$ie^{-i2\varphi}$	$ie^{-i2\varphi}$
$F_{l_1 l_2}^{-11}$	$e^{i2\varphi}$	$-e^{i2\varphi}$	$-ie^{i2\varphi}$	$-ie^{i2\varphi}$

γ-Konversion.

Für gewisse Fälle lassen sich auch hier die Konstanten F leicht angeben. Insbesondere ist die Konversion eines s-Elektrons leicht zu behandeln. Das durch Konversion ausgesandte Elektron bildet mit dem in der K-Schale verbleibenden aus Paritätsgründen

a) bei elektrischer Konversion einen Singulettzustand;

b) bei magnetischer Konversion einen Triplettzustand.

Bei elektrischer Konversion verhält sich das Teilchen offenbar wie ein Spin-0-Teilchen

$$F_{ll}^{00}(0) = 1 \qquad F_{ll}^{mm}(0) = 0 \qquad m \neq 0;$$

wird das Elektron magnetisch konvertiert, so wird es in einer $(l-1)$- oder $(l+1)$-Welle ausgesandt.

Erfolgt die Emission in einer $(l+1)$-Welle, so ist das F_{ll}^{mm} gegeben durch

$$F_{ll}^{mm}(0) = \Big|\sum_{\mu} C_{l-1\,\mu;\,1\,m-\mu}^{l\,m}\, Y_{l-1,\mu}(0)\, X_{1,m-\mu}\Big|^2,$$

wo X_1 die Triplettspineigenfunktion bedeutet. Dieser Ausdruck reduziert sich aber sofort auf

$$F_{ll}^{mm}(0) = \big|C_{l-1\,0;\,1\,m}^{l\,m}\big|^2. \tag{42}$$

Für die $(l+1)$-Welle ergibt die analoge Überlegung

$$F_{ll}^{mm}(0) = \big|C_{l+1\,0;\,1\,m}^{l\,m}\big|^2. \tag{43}$$

Speziell ist noch daraus ersichtlich, dass $F_{ll}^{mm}(0) = 0$ ist, für $m > 1$.

Es ergibt sich dann nach den Tabellen von Condon und Shertley für die Clebsch-Gordon-Koeffizienten:

	F_{ll}^{11}	F_{ll}^{00}	F_{ll}^{-1-1}
$l-1$	$\frac{l(l+1)}{2}$	l^2	$\frac{l(l+1)}{2}$
$l+1$	$\frac{l(l+1)}{2}$	$(l+1)^2$	$\frac{l(l+1)}{2}$

β-Strahlung.

In der $(Z = 0)$-Näherung sind von Falkoff und Uhlenbeck die $F_l^m(\vartheta)$ für erlaubte sowie verbotene Übergänge erster und zweiter Art berechnet worden. Wir bestimmen aus jener Arbeit die $F_l^m(0)$:

$$\begin{aligned} l &= 1, & l &= 2, \\ F_1^0(0) &= 1-\lambda, & F_2^0(0) &= 1+\mu_1+\mu_2, \\ F_1^{\pm 1}(0) &= 1+\lambda, & F_2^{\pm 1}(0) &= \frac{2}{3}+\mu_1+\frac{1}{3}\mu_2, \\ & & F_2^{\pm 2}(0) &= -\frac{1}{3}+\mu_1-\frac{1}{3}\mu_2. \end{aligned}$$

Für die Bedeutung der λ, μ_1, μ_2 siehe FALKOFF und UHLENBECK, wo diese Parameter auch für die verschiedenen Wechselwirkungsansätze berechnet sind.

Herrn Prof. Dr. W. PAULI und Herrn Prof. Dr. V. WEISSKOPF möchte ich für ihr Interesse, das sie an dieser Arbeit bekundet haben, meinen herzlichsten Dank aussprechen. Den Herren Dr. H. FRAUENFELDER, Dr. R. SCHAFROTH und meinem Freund E. HEER danke ich für viele anregende Diskussionen.

Literatur.

[1]) M. E. ROSE, G. GOERTZEL, B. SPINRAD, J. HARR und P. STRONG, Phys. Rev. **83**, 79 (1951).
[2]) D. R. HAMILTON, Phys. Rev. **58**, 122 (1940).
[3]) C. N. YANG, Phys. Rev. **74**, 764 (1948).
[4]) D. L. FALKOFF und D. S. LING, Phys. Rev. **76**, 1639 (1949).
[5]) D. L. FALKOFF und G. E. UHLENBECK, Phys. Rev. **79**, 323 (1950).
[6]) D. R. HAMILTON, Phys. Rev. **74**, 728 (1948); I. ZINNES, Phys. Rev. **80**, 363 (1950).
[7]) E. L. BRADY und H. DEUTSCH, Phys. Rev. **72**, 870 (1947).
[8]) H. DEUTSCH, Reports of Progress in Physics XIV, 196.
[9]) G. GOERTZEL, Phys. Rev. **62**, 763 (1946).
[10]) J. W. GARDNER, Proc. Phys. Soc. **62**, 763 (1949); S. P. LLOYD, Dissertation, unveröffentlicht; Phys. Rev. **83**, 716 (1951); G. RACAH, im Druck.
[11]) S. P. LLOYD, Phys. Rev. **80**, 118 (1950).
[12]) B. A. LIPPMANN, Phys. Rev. **81**, 162 (1951).

APPENDIX

A. *Einige oft gebrauchte gruppentheoretische Relationen.*

$$D^j_{\mu'\mu}(\alpha\beta\gamma) = \sum_{\varkappa}(-1)^{\varkappa}\frac{\sqrt{(j+\mu)!\,(j-\mu)!\,(j+\mu')!\,(j-\mu')!}}{(j-\mu'-\varkappa)!\,(j+\mu-\varkappa)!\,\varkappa!\,(\varkappa+\mu'-\mu)!}\times$$

$$\times\, e^{i\mu'\alpha}\cos^{2j+\mu-\mu'-2\varkappa}\left(\frac{1}{2}\beta\right)\cdot\sin^{2\varkappa+\mu'-\mu}\left(\frac{1}{2}\beta\right)e^{i\mu\gamma} \tag{1}$$

$$\sum_{\mu} D^j_{\mu'\mu}(S)\cdot D^j_{\mu\mu''}(T) = D^j_{\mu'\mu''}(ST) \tag{2}$$

$$D^j_{\mu'\mu}(\alpha\beta\gamma) = (-1)^{\mu-\mu'}D^j_{-\mu'-\mu}(\alpha\beta\gamma)^* \tag{3}$$

$D^j_{\mu'\mu}$ bildet eine unitäre Matrix (4)

$$D^L_{\mu 0}(\alpha\beta\gamma) = \sqrt{\frac{4\pi}{2L+1}}\,Y^M_L(\beta,\alpha) \tag{5}$$

Y auf 1 normierte Kugelfunktion

$$D^j_{\mu'\mu}(0,0,0) = \delta_{\mu'\mu} \tag{6}$$

$$D^J_{MN}\cdot D^j_{mn} = \sum_{k=|J-j|}^{J+j} C^{k\,M+m}_{J\,M\,j\,m}\cdot D^k_{M+m,N+n}\cdot C^{k\,N+n}_{J\,N\,j\,n} \tag{7}$$

$$\int D^J_{MN} \cdot D^j_{mn}\, d\Omega = \delta_{Jj} \cdot \delta_{Mm}\, \delta_{Nn} \frac{4\pi}{2J+1} \tag{8}$$

$$C^{L\mu+\nu}_{l\mu\tilde{l}\nu} = \frac{\sqrt{(L+l-\tilde{l})!\,(L-l+\tilde{l})!\,(l+\tilde{l}-L)!\,(L+\mu+\nu)!\,(L-\mu-\nu)!}}{\sqrt{(L+l+\tilde{l}+1)!\,(l-\mu)!\,(l+\mu)!\,(\tilde{l}-\nu)!\,(l+\nu)!}} \times$$

$$\times \sum_{\varkappa} (-1)^{\varkappa+\tilde{l}+\nu} \sqrt{2L+1} \frac{(L+\tilde{l}+\mu-\varkappa)!\,(l-\mu+\varkappa)!}{(L-l+\tilde{l}-\varkappa)!\,(L+\mu+\nu-\varkappa)!\,\varkappa!\,(\varkappa+l-\tilde{l}-\mu-\nu)!} \tag{9}$$

$$\sum_{\alpha,\gamma} C^{c\gamma}_{a\alpha b\beta} \cdot C^{c\gamma}_{a\alpha b'\beta} = \delta_{bb'} \frac{2c+1}{2b+1} \quad \beta \text{ fest} \tag{10}$$

$$\left.\begin{aligned} C^{c\gamma}_{a\alpha b\beta} &= (-1)^{a+b-c} \cdot C^{c-\gamma}_{a-\alpha\, b-\beta} \\ C^{c\gamma}_{a\alpha b\beta} &= (-1)^{a+b-c} \cdot C^{c\gamma}_{b\beta a\alpha} \\ C^{c\gamma}_{a\alpha b\beta} &= (-1)^{a-\alpha} \sqrt{\frac{2c+1}{2b+1}}\, C^{b\beta}_{c\gamma\, a-\alpha} \\ C^{c\gamma}_{a\alpha b\beta} &= (-1)^{b+\beta} \sqrt{\frac{2c+1}{2a+1}}\, C^{a\alpha}_{b-\beta\, c\gamma} \end{aligned}\right\} \tag{11}$$

$$\sum_{\alpha\beta\delta} C^{c\gamma}_{a\alpha b\beta} \cdot C^{e\varepsilon}_{d\delta b\beta} \cdot C^{d\delta}_{a\alpha f\Phi} = \sqrt{2c+1}\sqrt{2d+1}\, W(cbfd/ae)\, C^{e\varepsilon}_{c\gamma f\Phi} \tag{12}$$

wo $W(abcd/ef)$ der sogenannte Racah-Koeffizient ist, der von sechs ganz- oder halbzahligen positiven Quantenzahlen abhängt. Dieser Koeffizient kann aus folgender Formel berechnet werden.

$$\omega(abcd/ef) =$$

$$= \sum_z (-1)^z \frac{(a+b+c+d+1-z)!}{(a+b-e-z)!\,(c+d-e-z)!\,(a+c-f-z)!\,(b+d-f-z)! \times} = \\ \times (b+d-f-z)!\,z!\,(e+f-a-d+z)!\,(e+f-b-c+z)!$$

$$W(abcd/ef) =$$

$$= \left[\frac{(a+b-e)!\,(a+e-b)!\,(b+e-a)!\,(c+d-e)!\,(c+e-d)!\,(d+e-d)! \times}{\times (a+c-f)!\,(a+f-c)!\,(c+f-a)!\,(b+d-f)!\,(b+f-d)!\,(d+f-b)!} \right]^{1/2} \times \\ (a+b+e+1)!\,(c+d+e+1)!\,(a+c+f+1)!\,b+d+f+1)! \times$$

$$\times \omega(abcd/ef). \tag{13}$$

Es gelten die folgenden Beziehungen:

$$W(abcd/ef) = W(badc/ef) = W(cdab/ef) = W(acbd/fe)$$
$$= (-1)^{e+f-a-d} \cdot W(ebcf/ad) = (-1)^{e+f-b-c} \cdot W(aefd/bc).$$

Die Racah-Koeffizienten verschwinden nur dann nicht, wenn die vier Triaden

$$(abe) \quad (cde) \quad (acf) \quad (bdf)$$

alle trigonometrische Ungleichungen der Form $|a-b| \leqslant c \leqslant a+b$ erfüllen.

B. *Allgemeine Formeln für oft gebrauchte Racah-Koeffizienten.*

Alle benötigten Racah-Koeffizienten sind von der Form

$$W(I_B I_A k, l_1/l_2 I_B).$$

Meistens ist jedoch in praktischen Anwendungen

$$l_1 = l_2 \text{ oder } l_1 = l_2 \pm 1 \qquad |I_A - I_B| = l_1 \text{ oder } l_1 - 1,$$

so dass man nur wenige Koeffizienten zu berechnen hat. Es ist

$$W(I, I-l, k, l/l\, I) = \left\{\frac{2l!\,2l!\,(2I+k+1)!\,(2I-k)!}{(2I+1)!\,(2I+1)!\,(2l+k+1)!\,(2l-k)!}\right\}^{1/2}$$

$$W(I, I+l, k, l/l\, I) = (-1)^k \left\{\frac{2I!\,2I!\,2l!\,2l!}{(2I-k)!\,(2l-k)!\,(2l+k+1)!\,(2I+k+1)!}\right\}^{1/2}$$

$$W(I, I-l+1, k, l/l\, I) = 2\,[2l\,(I+1) - k\,(k+1)\,(I-l+1)] \times$$
$$\times \left\{\frac{(2l-1)!\,(2l-1)!\,(2I-k)!\,(2I+k+1)!}{(2I+2)!\,(2I+2)!\,(2l+k+1)!\,(2l-k)!}\right\}^{1/2}$$

$$W(I, I+l-1, k, l/l\, I) = 2\,(-1)^k\,[2l\,I - k\,(k+1)\,(I+l)] \times$$
$$\times \left\{\frac{(2l-1)!\,(2l-1)!\,(2I-1)!\,(2I-1)!}{(2I+k+1)!\,(2l+k+1)!\,(2l-k)!\,(2I-k)!}\right\}^{1/2}$$

$$W(I, I-l, k, l/l+1, I) =$$
$$= \left\{2k\,(k+1)\,(I-l)\,\frac{2l!\,(2l+1)!\,(2I-k)!\,(2I+k+1)!}{(2l-k+1)!\,(2l+k+2)!\,(2I+1)!\,(2I+2)!}\right\}^{1/2}$$

$$W(I, I+l, k\, l/l+1, I) = (-1)^{k-1} \times$$
$$\times \left\{2k\,(k+1)\,(I+l+1)\,\frac{2l!\,(2l+1)!\,2I!\,(2I-1)!}{(2I-k)!\,(2I+k+1)!\,(2l-k+1)!\,(2l+k+2)!}\right\}^{1/2}$$

$$W(I\,J\,0F/F\,I) = \left\{\frac{1}{(2F+1)\,(2I+1)}\right\}^{1/2}$$

$$W(I\,J\,2F/F\,I) = \left\{\frac{(2F-2)!\,(2I-2)!}{(2F+3)!\,(2I+3)!}\right\}^{1/2} [3C(C+1) - 4I(I+1)F(F+1)$$
$$C = J(J+1) - F(F+1) - I(I+1).$$

C. *Allgemeine Formeln für Clebsch-Gordon-Koeffizienten.*

$$l_1 + l_2 + k = 2g$$
$$C^{k0}_{l_1 0 l_2 0} = (-1)^{g-k}\sqrt{2k+1}\,\frac{g!}{(g-l_1)!\,(g-l_2)!\,(g-k)!} \times$$
$$\times \sqrt{\frac{(l_1+l_2-k)!\,(l_1+k-l_2)!\,(l_2+k-l_1)!}{(l_1+l_2+k+1)!}}$$

$$C^{k0}_{l_1 1 l_2 - 1} = \frac{1}{2}\,\frac{k(k+1) - l_2(l_2+1) - l_1(l_1+1)}{\sqrt{l_1(l_1+1)\,l_2(l_2+1)}}\,C^{k0}_{l_1 0 l_2 0}$$

$$C^{k0}_{l_1 0 l_2 0} = 0 \qquad l_1 + l_2 + k = 2g+1.$$

Tabellen von Racah-Koeffizienten.

Allgemein

$$W(J, J', 0, L/L, J) = \left\{\frac{1}{(2L+1)(2J+1)}\right\}^{1/2}$$

Dipolstrahlung.

J'	$W(J, J', 2, 1/1, J)$
$J-1$	$\left\{\frac{1}{30}\cdot\frac{(J+1)(2J+3)}{J(2J-1)(2J+1)}\right\}^{1/2}$
J	$\left\{\frac{1}{30}\cdot\frac{(2J-1)(2J+3)}{J(J+1)(2J+1)}\right\}^{1/2}$
$J+1$	$\left\{\frac{1}{30}\cdot\frac{J(2J-1)}{(J+1)(2J+1)(2J+3)}\right\}^{1/2}$

Quadrupolstrahlung.

J'	$W(J, J', 2, 2/2, J)$
$J-2$	$\left\{\frac{2}{35}\cdot\frac{(J+1)(2J+3)}{J(2J-1)(2J+1)}\right\}^{1/2}$
$J-1$	$-(J-5)\left\{\frac{1}{70}\cdot\frac{(2J+3)}{J(J+1)(2J-1)(2J+1)}\right\}^{1/2}$
J	$-(2J-3)(2J+5)\left\{\frac{1}{70}\cdot\frac{1}{J(J+1)(2J-1)(2J+1)(2J+3)}\right\}^{1/2}$
$J+1$	$-(J+6)\cdot\left\{\frac{1}{70}\cdot\frac{2J-1}{J(J+1)(2J+1)(2J+3)}\right\}^{1/2}$
$J+2$	$\left\{\frac{2}{35}\cdot\frac{J(2J-1)}{(J+1)(2J+1)(2J+3)}\right\}^{1/2}$

J'	$W(J, J', 4, 2/2, J$
$J-2$	$\left\{\frac{1}{630}\cdot\frac{(J+1)(J+2)(2J+3)(2J+5)}{(J-1)J(2J-3)(2J-1)(2J+1)}\right\}^{1/2}$
$J-1$	$-\left\{\frac{2}{315}\cdot\frac{(J+2)(2J-3)(2J+3)(2J+5)}{(J-1)J(J+1)(2J-1)(2J+1)}\right\}^{1/2}$
J	$\left\{\frac{2}{35}\cdot\frac{(J-1)(J+2)(2J-3)(2J+5)}{J(J+1)(2J-1)(2J+1)(2J+3)}\right\}^{1/2}$
$J+1$	$-\left\{\frac{2}{315}\cdot\frac{(J-1)(2J-3)(2J-1)(2J+5)}{J(J+1)(J+2)(2J+1)(2J+3)}\right\}^{1/2}$
$J+2$	$\left\{\frac{(J-1)J(2J-3)(2J-1)}{630(J+1)(J+2)(2J+1)(2J+3)(2J+5)}\right\}^{1/2}$

Oktopolstrahlung.

J'	$W(J, J', 2, 3/3\,J)$
$J-3$	$\frac{1}{2}\left\{\frac{5}{21}\cdot\frac{J+1}{J}\cdot\frac{(2J+3)}{(2J-1)(2J+1)}\right\}^{1/2}$
$J-2$	$\frac{3}{2}\left\{\frac{5}{21}\cdot\frac{1}{J(J+1)}\cdot\frac{(2J+3)}{(2J-1)(2J+1)}\right\}^{1/2}$
$J+2$	$-\frac{3}{2}\left\{\frac{5}{21}\cdot\frac{1}{J(J+1)}\cdot\frac{(2J-1)}{(2J+1)(2J+3)}\right\}^{1/2}$
$J+3$	$\frac{1}{2}\left\{\frac{5}{21}\cdot\frac{J}{J+1}\cdot\frac{2J-1}{(2J+1)(2J+3)}\right\}^{1/2}$

J'	$W(J, J', 4, 3/3\,J)$
$J-3$	$\left\{\frac{1}{154}\cdot\frac{(J+1)(J+2)}{(J-1)J}\cdot\frac{(2J+3)(2J+5)}{(2J-3)(2J-1)(2J+1)}\right\}^{1/2}$
$J-2$	$\frac{1}{3}(23-7J)\left\{\frac{1}{154}\cdot\frac{(J+2)}{(J-1)J(J+1)}\cdot\frac{(2J+3)(2J+5)}{(2J-3)(2J-1)(2J+1)}\right\}^{1/2}$
$J+2$	$-\frac{1}{3}(30+7J)\left\{\frac{1}{154}\cdot\frac{J-1}{J(J+1)(J+2)}\cdot\frac{(2J-3)(2J-1)}{(2J+1)(2J+3)(2J+5)}\right\}^{1/2}$
$J+3$	$\left\{\frac{1}{154}\cdot\frac{J(J-1)}{(J+2)(J+1)}\cdot\frac{(2J-1)(2J-3)}{(2J+5)(2J+3)(2J+1)}\right\}^{1/2}$

J'	$W(J, J', 6, 3/3\,J)$
$J-3$	$\frac{1}{2}\left\{\frac{1}{3\cdot7\cdot11\cdot13}\cdot\frac{(J+1)(J+2)(J+3)}{J(J-1)(J-2)}\cdot\frac{(2J+3)(2J+5)(2J+7)}{(2J+1)(2J-1)(2J-3)(2J-5)}\right\}^{1/2}$
$J-2$	$\frac{3}{2}(5-2J)\times$
	$\times\left\{\frac{1}{3\cdot7\cdot11\cdot13}\cdot\frac{(J+2)(J+3)}{(J+1)J(J-1)(J-2)}\cdot\frac{(2J+3)(2J+5)(2J+7)}{(2J+1)(2J-1)(2J-3)(2J-5)}\right\}^{1/2}$
$J+2$	$-\frac{2}{3}(2J+7)\times$
	$\times\left\{\frac{1}{3\cdot7\cdot11\cdot13}\cdot\frac{(J-1)(J-2)}{J(J+1)(J+2)(J+3)}\cdot\frac{(2J-1)(2J-3)(2J-5)}{(2J+1)(2J+3)(2J+5)(2J+7)}\right\}^{1/2}$
$J+3$	$\frac{1}{2}\left\{\frac{1}{3\cdot7\cdot11\cdot13}\cdot\frac{J(J-1)(J-2)}{(J+1)(J+2)(J+3)}\cdot\frac{(2J-1)(2J-3)(2J-5)}{(2J+1)(2J+3)(2J+5)(2J+7)}\right\}^{1/2}$

2^4-Pol-Strahlung.

J'	$W(J, J', 2, 4/4\,J)$
$J-4$	$\frac{2}{3}\left\{\frac{7}{55}\cdot\frac{J+1}{J}\cdot\frac{2J+3}{(2J-1)(2J+1)}\right\}^{1/2}$
$J-3$	$\frac{1}{6}(J+13)\left\{\frac{7}{55}\cdot\frac{1}{J(J+1)}\cdot\frac{2J+3}{(2J-1)(2J+1)}\right\}^{1/2}$
$J+3$	$\frac{1}{6}(J-12)\left\{\frac{7}{55}\cdot\frac{1}{J(J+1)}\cdot\frac{2J-1}{(2J+1)(2J+3)}\right\}^{1/2}$
$J+4$	$\frac{2}{3}\left\{\frac{7}{55}\cdot\frac{J}{J+1}\cdot\frac{2J-1}{(2J+1)(2J+3)}\right\}^{1/2}$

J'	$W(J, J', 4, 4/4\,J)$
$J-4$	$\frac{1}{3}\left\{\frac{14}{143}\cdot\frac{(J+1)(J+2)}{(J-1)J}\cdot\frac{(2J+3)(2J+5)}{(2J-3)(2J-1)(2J+1)}\right\}^{1/2}$
$J-3$	$\frac{1}{6}(17-3J)\left\{\frac{14}{143}\cdot\frac{(J+2)}{(J-1)J(J+1)}\cdot\frac{(2J+3)(2J+5)}{(2J-3)(2J-1)(2J+1)}\right\}^{1/2}$
$J+3$	$-\frac{1}{6}(20+3J)\left\{\frac{14}{143}\cdot\frac{(J-1)}{J(J+1)(J+2)}\cdot\frac{(2J-3)(2J-1)}{(2J+1)(2J+3)(2J+5)}\right\}^{1/2}$
$J+4$	$\frac{1}{3}\left\{\frac{14}{143}\cdot\frac{J(J-1)}{(J+1)(J+2)}\cdot\frac{(2J-1)(2J-3)}{(2J+1)(2J+3)(2J+5)}\right\}^{1/2}$

J'	$W(J, J', 6, 4/4\,J)$
$J-4$	$\frac{2}{3}\left\{\frac{1}{5\cdot11\cdot13}\cdot\frac{(J+1)(J+2)(J+3)}{J(J-1)(J-2)}\cdot\frac{(2J+3)(2J+5)(2J+7)}{(2J+1)(2J-1)(2J-3)(2J-5)}\right\}^{1/2}$
$J-3$	$\frac{1}{6}(67-17J)\times$ $\times\left\{\frac{1}{5\cdot11\cdot13}\cdot\frac{(J+2)(J+3)}{(J+1)J(J-1)(J-2)}\cdot\frac{(2J+3)(2J+5)(2J+7)}{(2J+1)(2J-1)(2J-3)(2J-5)}\right\}^{1/2}$
$J+3$	$-\frac{1}{6}(84+17J)\times$ $\times\left\{\frac{1}{5\cdot11\cdot13}\cdot\frac{(J-2)(J-1)}{J(J+1)(J+2)(J+3)}\cdot\frac{(2J-1)(2J-3)(2J-5)}{(2J+1)(2J+3)(2J+5)(2J+7)}\right\}^{1/2}$
$J+4$	$\frac{2}{3}\left\{\frac{1}{5\cdot11\cdot13}\cdot\frac{J(J-1)(J-2)}{(J+1)(J+2)(J+3)}\cdot\frac{(2J-1)(2J-3)(2J-5)}{(2J+1)(2J+3)(2J+5)(2J+7)}\right\}^{1/2}$

Interferenzkoeffizienten.

Dipol-Quadrupol-Strahlung.

J'	$W(J, J', 2, 1/2, J)$
$J-1$	$\left\{\frac{1}{10}\cdot\frac{(J-1)(2J+3)}{J(2J-1)(2J+1)}\right\}^{1/2}$
J	$\left\{\frac{3}{10}\cdot\frac{1}{J(J+1)(2J+1)}\right\}^{1/2}$
$J+1$	$-\left\{\frac{1}{10}\cdot\frac{(J+2)(2J-1)}{(J+1)(2J+1)(2J+3)}\right\}^{1/2}$

Quadrupol-Oktopol-Strahlung.

J'	$W(J, J', 2, 2/3, J)$
$J-2$	$\left\{\frac{1}{14}\cdot\frac{J-2}{J}\cdot\frac{2J+3}{(2J-1)(2J+1)}\right\}^{1/2}$
$J+2$	$-\left\{\frac{1}{14}\cdot\frac{J+3}{J-1}\cdot\frac{2J-1}{(2J+1)(2J+3)}\right\}^{1/2}$
J'	$W(J, J', 4, 2/3, J)$
$J-2$	$\frac{1}{3}\left\{\frac{1}{7}\cdot\frac{(J-2)(J+2)}{(J-1)J}\cdot\frac{(2J+3)(2J+5)}{(2J-3)(2J-1)(2J+1)}\right\}^{1/2}$
$J+2$	$-\frac{1}{3}\left\{\frac{1}{7}\cdot\frac{(J+3)(J-1)}{(J+2)(J+1)}\cdot\frac{(2J-3)(2J-1)}{(2J+5)(2J+3)(2J+1)}\right\}^{1/2}$

$(2^3 - 2^4)$-*Polstrahlung.*

J'	$W(J, J', 2, 3/4, J)$
$J-3$	$\frac{1}{2}\left\{\frac{1}{5}\cdot\frac{J-3}{J}\cdot\frac{2J+3}{(2J-1)(2J+1)}\right\}^{1/2}$
$J+3$	$-\frac{1}{2}\left\{\frac{1}{5}\cdot\frac{J+4}{J-1}\cdot\frac{2J-1}{(2J+1)(2J+3)}\right\}^{1/2}$
J'	$W(J, J', 4, 3/4, J)$
$J-3$	$\frac{1}{6}\left\{\frac{10}{11}\cdot\frac{(J-3)(J+2)}{J(J-1)}\cdot\frac{(2J+3)(2J+5)}{(2J-3)(2J-1)(2J+1)}\right\}^{1/2}$
$J+3$	$-\frac{1}{6}\left\{\frac{10}{11}\cdot\frac{(J+4)(J-1)}{(J+2)(J+1)}\cdot\frac{(2J-3)(2J-1)}{(2J+5)(2J+3)(2J+1)}\right\}^{1/2}$

Clebsch-Gordon-Koeffizienten.

$$C^{00}_{10\,10} = -\sqrt{\frac{1}{3}} \qquad C^{00}_{11\,1-1} = \sqrt{\frac{1}{3}}$$

$$C^{20}_{10\,10} = \sqrt{\frac{2}{3}} \qquad C^{20}_{11\,1-1} = \sqrt{\frac{1}{6}}$$

$$C^{00}_{20\,20} = \sqrt{\frac{1}{5}} \qquad C^{00}_{21\,2-1} = -\sqrt{\frac{1}{5}} \qquad C^{00}_{22\,2-2} = \sqrt{\frac{1}{5}}$$

$$C^{20}_{20\,20} = -\sqrt{\frac{2}{7}} \qquad C^{20}_{21\,2-1} = \sqrt{\frac{1}{14}} \qquad C^{20}_{22\,2-2} = \sqrt{\frac{2}{7}}$$

$$C^{40}_{20\,20} = \sqrt{\frac{18}{35}} \qquad C^{40}_{21\,2-1} = \sqrt{\frac{8}{35}} \qquad C^{40}_{22\,2-2} = \sqrt{\frac{1}{70}}$$

$$C^{00}_{30\,30} = -\sqrt{\frac{1}{7}} \qquad C^{00}_{31\,3-1} = \sqrt{\frac{1}{7}}$$

$$C^{20}_{30\,30} = 2\sqrt{\frac{1}{21}} \qquad C^{20}_{31\,3-1} = -\frac{1}{2}\sqrt{\frac{3}{7}}$$

$$C^{40}_{30\,30} = -3\sqrt{\frac{2}{77}} \qquad C^{40}_{31\,3-1} = \frac{1}{2}\sqrt{\frac{2}{77}}$$

$$C^{60}_{30\,30} = 10\sqrt{\frac{1}{3\cdot 7\cdot 11}} \qquad C^{60}_{31\,3-1} = \frac{5}{2}\sqrt{\frac{3}{77}}$$

$$C^{00}_{40\,40} = \frac{1}{3} \qquad C^{00}_{41\,4-1} = -\frac{1}{3}$$

$$C^{20}_{40\,40} = -\frac{10}{3}\sqrt{\frac{1}{77}} \qquad C^{20}_{41\,4-1} = \frac{17}{6}\sqrt{\frac{1}{77}}$$

$$C^{40}_{40\,40} = 9\sqrt{\frac{2}{7\cdot 11\cdot 13}} \qquad C^{40}_{41\,4-1} = -\frac{9}{2}\sqrt{\frac{2}{7\cdot 11\cdot 13}}$$

$$C^{60}_{40\,40} = -\frac{2}{3}\sqrt{\frac{5}{11}} \qquad C^{60}_{41\,4-1} = -\frac{1}{30}\sqrt{\frac{5}{11}}$$

Elektronenspektren zwischen 1 und 10 KeV

von **H. Schneider, O. Huber, F. Humbel, A. de Shalit***) und **W. Zünti**
ETH., Zürich.

(23. I. 1952.)

Summary. The spectrum of low energy (1–10 KeV) electrons has been measured for the cases of Ag^{107}, Ag^{109}, Tc^{99}, Hg^{197}, Au^{195}, Au^{199}, and Au^{198} using a coincidence technique, in which the electrons are accelerated in a lens spectrometer. The apparatus is described, and the results are compared with the predictions of the single particle shell model.

Einleitung.

Dem Schalenmodell von M. G. MAYER gelingt es durch Einführung der Spinbahnkopplung die meisten Grundzustände der Atomkerne zu beschreiben, und auch das Auftreten von Isomeren in Gruppen am Ende abgeschlossener Schalen zu erklären. Die meisten bekannten „ug"-Isomere haben nach diesem Modell ihren Platz am Ende abgeschlossener Schalen, weil dort hohe Spindifferenzen auftreten. Die vorausgesagten Zustände, zwischen denen ein isomerer Übergang stattfinden kann, sind: $g_{9/2} - p_{1/2}$ in der 50er Schale, $h_{11/2} - d_{3/2}$ in der 82er Schale, sowie $i_{13/2} - f_{5/2}$ in der 126er Schale. Ein solcher Übergang würde also eine Drehimpulsänderung von 4 und Paritätswechsel erforderlich machen; man spricht deshalb von M4-Isomeren. Etwa 36 Isomere in diesem Gebiet zeigen nun tatsächlich M4-Strahlung[1]) und lassen sich gut in das System des Schalenmodells einordnen.

Es gibt aber auch Ausnahmen unter den Isomeren am Ende abgeschlossener Schalen, deren Strahlung mit Sicherheit nicht als M4 interpretiert werden kann. Bei diesen schliesst die Lebensdauer-Energie-Beziehung von V. WEISSKOPF[2]) den M4-Charakter aus und die phänomenologische Klassifikation von GOLDHABER[1]) lässt auf E3- resp. M3-Strahlung schliessen. Diese Isomere könnten also mit dem Einteilchenmodell nicht mehr erklärt werden, falls die Sicherheit besteht, dass der Übergang nicht in Kaskade erfolgt. Besonders deutlich wird das Versagen des reinen Einteilchenmodells bei den Silberisomeren Ag^{107} und Ag^{109}. Beide haben im Grundzustand den Spin 1/2. Die beobachtete Drehimpulsänderung[1]) von 3 führt ein-

*) From The Hebrew University, Jerusalem.

deutig auf einen Zustand mit dem Spin 7/2. In der 50er Schale hat aber das betreffende Niveau modellmässig den Spin 9/2.

Es steht damit zur Diskussion, ob für diese Anregung mehrere Nukleonen verantwortlich sind, oder ob vielleicht doch Kaskadenübergänge vorliegen, die infolge sehr kleiner Energie der ausgesandten Strahlung allen bisherigen Beobachtungen entgangen sind. Daher erschien es uns angezeigt, die experimentellen Daten erneut zu prüfen im Hinblick auf das Gebiet kleiner Energien, die sich im β-Spektrometer infolge der Absorption im Zählrohrfenster jeder Beobachtung entzogen haben. So wäre zum Beispiel ein Niveau von 2 KeV, wie es beim Tc^{99} mit Koinzidenzmessungen und Proportionalzähler[3]) entdeckt wurde, bisher sicher allen Messungen im Spektrometer entgangen, und gerade solche Niveaux würden auf die Diskussion um das Einteilchenmodell entscheidenden Einfluss ausüben. Wir haben deshalb eine Messtechnik entwickelt, die es ermöglicht, durch Nachbeschleunigung der Elektronen im Linsenspektrometer das Spektrum bis zur Energie 1 KeV hinunter zu untersuchen. Nach Energien unterhalb 1 KeV zu suchen ist unnötig, weil diese auf zu grosse Lebensdauern führen würden, die mit der Erfahrung nicht in Einklang zu bringen sind. Bei diesen kleinen Energien findet man zahlreiche Augerlinien und die richtige Interpretation des Spektrums wird erst mit Hilfe gleichzeitiger Koinzidenzmessung[4]) möglich. Mit diesem Nachbeschleunigungsverfahren konnten wir 3 der erwähnten ug-Isomere (Ag^{107}, Ag^{109}, Au^{197}) untersuchen, von denen die 2 Silberisomere mit Sicherheit zu den Ausnahmen zu rechnen sind. Den hypothetischen Übergang kleiner Energie ($1 \leqslant E \leqslant 10$ KeV) konnten wir mit Sicherheit ausschliessen. Ebenso haben wir mit dieser Technik die Spektren des Au^{195} und des Au^{199} aufgenommen. Diese 2 Zerfallsschemata, die in einer späteren Arbeit[19]) mitgeteilt werden, sind in guter Übereinstimmung mit dem Einteilchenmodell.

Beim Tc^{99} konnten wir auch im Spektrometer die 2-KeV-Linie finden. Ihre Existenz wurde durch Koinzidenzmessung im Spektrometer nachgewiesen, und ihre Energie mit Hilfe der M- und N-Konversionslinien bestimmt.

Beschleunigung der Elektronen im Spektrometer.

Will man die Messungen von β-Spektren auf sehr kleine Energien ausdehnen, so setzt zunächst die Absorption des Zählrohrfensters eine Grenze, weil selbst bei Verwendung der dünnsten noch brauchbaren Folien ($\sim 0{,}1$ mg/cm^2) Elektronen mit einer Energie unterhalb 6 KeV nicht mehr gezählt werden können. Die Verwendbar-

keit des Zählrohres im Spektrometer ist deshalb begrenzt. Da die Entwicklung von Detektoren grosser Ausbeute in diesem Gebiet kleiner Energien grosse Schwierigkeiten mit sich bringt, besteht wohl die einfachste Lösung des Problems darin, die Elektronen künstlich durch Anlegen eines elektrischen Feldes zu beschleunigen.

Man wird folglich entweder die radioaktive Quelle, deren β-Emission im Spektrometer untersucht werden soll, auf ein negatives oder das Zählrohr auf ein positives Potential bringen. Die Aufladung des Zählrohres ist von BUTT[5]) benutzt worden, um die Augerlinien des Thoriums zu untersuchen. In unserer Anordnung befindet sich die Quelle auf negativem Potential, so dass die Elektronen eine Beschleunigung erfahren, bevor sie das Magnetfeld des Spektrometers passieren. Der wesentliche Vorteil dieser Konstruktion besteht darin, dass das Zählrohr von der Beschleunigungsanlage räumlich durch das Spektrometer getrennt ist. Deshalb kann der „Untergrund",

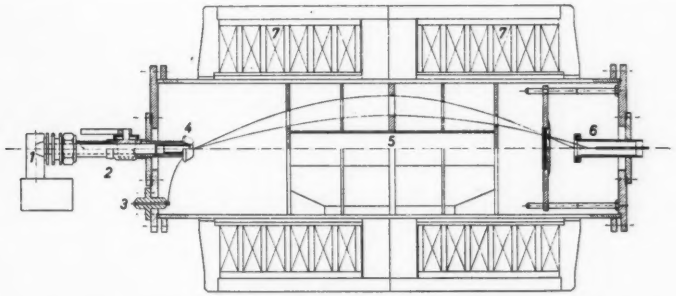

Fig. 1.
Messanordnung im Schnitt. 1. Photomultiplier. 2. Lichtleiter. 3. Anschluss für die Beschleunigungsspannung. 4. Torusförmige Elektrode mit Präparat und Anthracenkristall. 5. Bleikörper. 6. Geiger-Müller-Zähler. 7. Magnetwicklung.

der von der Feldemission herrührt, nur bei einem $H\varrho$-Wert auftreten. An dieser Stelle im Spektrum entsteht die „Nullinie", die für die Eichung der Anlage sehr nützlich ist. Natürlich muss von der gemessenen Energie die Beschleunigungsenergie in Abzug gebracht werden, was durch das Auftreten der Nullinie erleichtert wird. Die Position dieser Linie gibt uns die Elektronen mit der Energie Null im Spektrum.

Da ferner die Intensität und die Energie der Linien im Bereich kleiner Energie wegen Selbstabsorption und Rückstreuung im Präparat oft stark verfälscht sind, erschien es uns stets notwendig, die Interpretation der Linien mit Koinzidenzmessungen zu stützen. Zu

diesem Zwecke befindet sich hinter dem Präparat ein Anthracenkristall (ebenfalls auf Hochspannung), dessen Lichtblitze durch einen isolierenden Lichtleiter aus Plexiglas aus dem Spektrometer heraus und einem Photomultiplier zugeführt werden, der somit auf Erdpotential stehen kann. Ein Schema dieser Anordnung zeigt Fig. 1.

Da sich Präparat und Anthracenkristall auf gleichem Potential befinden, bleibt die Ansprechwahrscheinlichkeit (ε_{Sc}) des Scintillationszählers unverändert. Sie wurde nach der bei O. Huber, F. Humbel, H. Schneider und W. Zünti[6]) beschriebenen Methode bestimmt.

Der Raumwinkel zwischen Präparat und Kristall beträgt $\omega_{Sc} = 0{,}135$. Das Auflösungsvermögen der Koinzidenzschaltung wurde zu $\tau = 2{,}3 \cdot 10^{-7}$ sec bestimmt.

Definieren wir:

$$\text{Koinzidenzrate} = \frac{\text{Koinzidenzen}}{\text{Einzelstösse im ZR.}},$$

so ist leicht einzusehen, dass die Koinzidenzrate einer Linie abhängt von der Anzahl der Partner, deren Ansprechwahrscheinlichkeit im Scintillationszähler, und bei einem γ-Übergang noch von der Konversion. Einzelheiten dieser Koinzidenztechnik sind in einer früheren Arbeit[4]) diskutiert worden.

Zur Theorie des Linsenspektrometers mit Beschleunigung der Elektronen.

Offenbar wird die Theorie des Linsenspektrometers, wie sie von Persiko[7]), Du Mond[8]) u. a. entwickelt wurde, bei Anwendung eines elektrischen Beschleunigungsfeldes eine Modifikation erfahren. Die numerische Lösung der allgemeinen elektronenoptischen Bahngleichungen[9]) für gemischte Felder ist meist nicht durchführbar, weil das elektrische Feld vor allem in der Nähe des Präparates unbekannt ist. Der Versuch, durch z. B. kugelförmige Gestaltung des Präparates das Feld zu definieren, kollidiert mit den Forderungen nach extrem dünnen Quellen und bringt somit erhebliche konstruktive Schwierigkeiten.

Nimmt man ein kugelsymmetrisches elektrisches Feld an, so zeigt die numerische Rechnung in erster Näherung keine Abweichung der Elektronenbahn gegenüber der Rechnung ohne elektrisches Feld. Ein ebenes Feld hingegen, dessen Kraftlinien parallel zur Spektrometerachse gerichtet sind, lässt die Bahnen mit genügend kleiner Anfangsenergie sehr bald entlang den Kraftlinien verlaufen, so dass die Elektronen mit normalem Startwinkel die Blenden nicht mehr erreichen. Dann wird der elektronenoptische Raumwinkel nicht

mehr mit dem geometrischen übereinstimmen. — Dieser Effekt ist tatsächlich vorhanden und er konnte durch einfache Experimente untersucht werden, die im nächsten Kapitel beschrieben werden. — Von grösserem Interesse ist es, zunächst die Auflösung zu berechnen, um ein Bild von der zu erwartenden Abweichung zu erhalten.

Die Theorie des Linsenspektrometers mit rein magnetischem Feld ergibt für das relative Auflösungsvermögen:

$$\frac{d\varepsilon}{\varepsilon} = \frac{(\varepsilon+2)}{(\varepsilon+1)} \cdot \frac{dJ}{J}$$

wobei

ε = kinetische Energie in mc^2
J = Strom in Amp

bedeutet. Um die entsprechende Formel für das Spektrometer mit Beschleunigung zu erhalten, gehen wir aus von der Energie in relativistischer Schreibweise:

$$\frac{E}{c} = \pm \sqrt{m_0^2 c^2 + p^2}$$

mit der oben eingeführten Bezeichnung:

$$(1+\varepsilon)^2 = 1 + \frac{p^2}{m_0^2 c^2}.$$

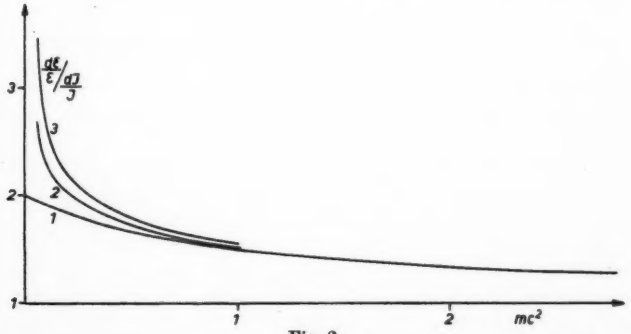

Fig. 2.

Zum Auflösungsvermögen. Kurve 1: $V = 0$. Kurve 2: $V = 10$ kV. Kurve 3: $V = 20$ kV.

Teilen wir die kinetische Energie in die ursprüngliche und die zusätzliche auf, indem wir die Beschleunigungsenergie $U = eV$ in mc^2 addieren, so erhalten wir:

$$(1+\varepsilon+U)^2 = 1 + \frac{p^2}{m_0^2 c^2}.$$

Benutzen wir ferner die Proportionalität zwischen dem Impuls der Elektronen und dem Strom im Spektrometer, so erhält man:

$$(1 + \varepsilon + U)^2 = 1 + aJ^2,$$

womit a als Apparatekonstante eingeführt ist.

Daraus ergibt sich durch Differentiation:

$$\frac{d\varepsilon}{\varepsilon} = \frac{(1+\varepsilon+U)^2-1}{(1+\varepsilon+U)\cdot\varepsilon} \cdot \frac{dJ}{J}.$$

Für den Fall $U = 0$ geht die Formel über in die normale. Man sieht, dass für $U \neq 0$ aber $\varepsilon = 0$ die Funktion $(d\varepsilon/\varepsilon)/(dJ/J)$ gegen ∞ streben muss. Fig. 2 zeigt dieses Verhalten bei verschiedenen Beschleunigungen als Parameter.

Das bedeutet, dass bei der Stosszahlkorrektur nicht mehr durch $H\varrho$ zu dividieren ist, sondern durch $H\varrho \cdot F(U, \varepsilon)$. Diese Funktion ist in ähnlicher Weise leicht zu berechnen. Sie soll hier nicht angegeben werden, da die Korrektur in unserem Messbereich sehr klein bleibt. Sie beträgt bei $\varepsilon = 1$ KeV und Beschleunigungsspannung $V = 20$ kV nur etwa 4%.

Das Auflösungsvermögen verschlechtert sich also mit der Beschleunigung. Man wird diese deshalb nur gerade so gross wählen, dass die Absorption der Zählrohrfolie ausgeglichen wird.

Absorption in der Zählrohrfolie und Raumwinkel.

Da eine elektronenoptische Berechnung der Bahnen ohne Kenntnis des elektrischen Feldes nicht durchführbar ist, musste experimentell die Variation des Raumwinkels mit der Beschleunigung ermittelt werden. — Durch Vergleich zweier Messungen mit und ohne Nachbeschleunigung erhält man das relative Produkt aus Raumwinkel und Durchlässigkeit. — Fig. 3 zeigt die Linien des Cd^{107} bei verschiedenen Beschleunigungsspannungen. Die Verschiebung der Linien entspricht innerhalb der Messgenauigkeit der angelegten Spannung. Die L-Augergruppe gewinnt dabei schnell an Intensität und dieses Anwachsen rührt von der Variation des Raumwinkels und der Durchlässigkeit her.

Um die beiden Effekte getrennt zu ermitteln, haben wir zunächst die Durchlässigkeit der verwendeten Folien bestimmt. Zu diesem Zwecke wurden die Konversionslinien des langlebigen Au^{195} als Funktion der Foliendicke gemessen. Auf diese Weise erhält man für die verschiedenen Energien die relative Durchlässigkeit als Funktion der Foliendicke. In erster Näherung kann die absolute Durchlässigkeit durch lineare Extrapolation der Stosszahlen auf die Foliendicke

0 gewonnen werden. Die Methode hat den Vorteil, dass die Absorption im Spektrometer selber bei unveränderter Geometrie gemessen werden kann. Absolutmessungen, die ausserhalb des Spektrometers mit monochromatischen Elektronen vorgenommen wurden[10] [11],

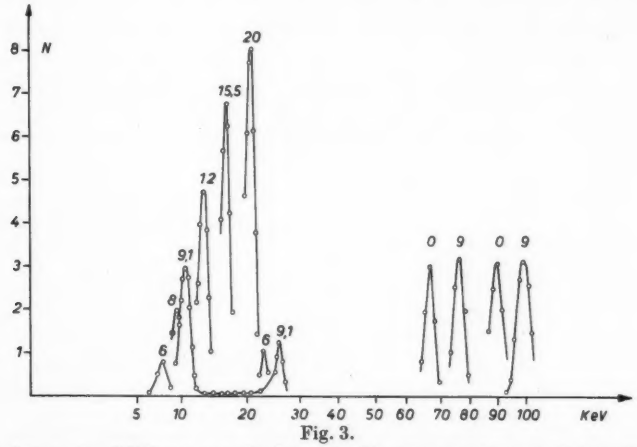

Fig. 3.

Spektrum des Cd^{107} mit verschiedener Beschleunigungsspannung. *L*-Augerlinien mit 6 kV, 8 kV, 9,1 kV, 12 kV, 15,5 kV und 20 kV. *K*-Augerlinien mit 6 und 9,1 kV K_{93}-Konversion mit 0 und 9 kV. L_{93}-Konversion mit 0 und 9 kV.

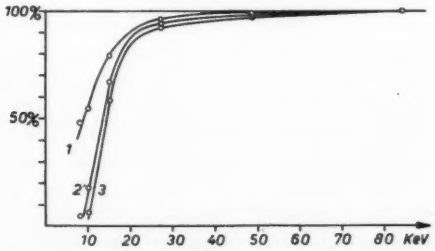

Fig. 4.

Durchlässigkeit der verwendeten Formvarfolien. Kurve 1: 0,086 mg/cm². Kurve 2: 0,156 mg/cm². Kurve 3: 0,186 mg/cm².

zeigen, dass die Kurven bei extrem schwacher Absorption flacher verlaufen, als es der linearen Extrapolation entspricht. Für die vorliegenden Messungen bedeutet das aber nur eine Korrektur, d.h. die Näherung durch lineare Extrapolation kann als gut angesehen werden. Fig. 4 zeigt die Durchlässigkeit der verwendeten Folien.

Da die Absorption nun bekannt ist, lässt sich der Raumwinkel ermitteln. Das Verhalten dieses elektronenoptischen Raumwinkels bei 6 und 10 kV Beschleunigung zeigt Fig. 5. Hier ist der Faktor, mit dem der geometrische Raumwinkel zu multiplizieren ist, in Abhängigkeit von der Energie der gemessenen Elektronen, aufgetragen.

Qualitativ entspricht die Kurve durchaus den Erwartungen. Bei grossen Energien ist der Faktor nahezu 1, denn die Spannung hat keinen grossen Einfluss. Wird die Energie der Elektronen vergleichbar mit der Beschleunigungsenergie oder kleiner, so wächst der Einfluss mehr und mehr, und zwar zunächst in positivem Sinne. Bei

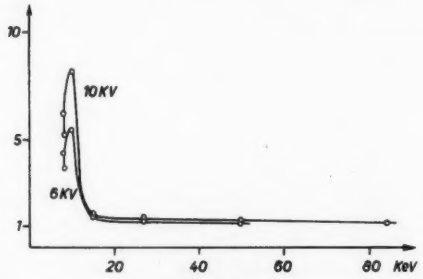

Fig. 5.

Variation des elektronenoptischen Raumwinkels mit der Energie der Elektronen. Beschleunigungsspannung als Parameter.

sehr kleinen Energien jedoch nimmt der Raumwinkel wieder ab, weil das elektrische Feld in der Nähe der radioaktiven Quelle parallel zur Spektrometerachse gerichtet ist. Das Maximum der Vergrösserung beträgt für 6 kV Beschleunigung ca. 5,5 und die Raumwinkelkorrekturen sind für Intensitätsbestimmungen zudem stark energieabhängig. Da sich jedoch die Interpretation der Linien in diesem Bereich auf die Koinzidenzen stützt, so spielt die Intensität der gemessenen Linien keine entscheidende Rolle mehr. Die Intensität ist ohnehin wegen der Selbstabsorption im Präparat unsicher.

Das Isomer Tc^{99}.

Tc^{99} entsteht durch β-Zerfall aus Mo^{99}, dessen Halbwertszeit 67 h beträgt. Von dieser Aktivität lässt sich chemisch das 6-stündige Tc-Isomer abtrennen[12]). Die 6-stündige Halbwertszeit des Isomers wurde einem Übergang von 1,8 KeV zugeschrieben[3]), die demjenigen von 141 KeV vorangeht.

Die „Crossover"-Linie von 143 KeV[13]) ergibt für die Energie des isomeren Überganges 2 KeV. — Die beschriebene Anordnung sollte nun erlauben, die M- und N-Konversion dieser Tc-Linie im Spektrometer zu messen. — MoO_3 wurde mit langsamen Neutronen in der Harwell-Pile bestrahlt. Nach einer von JACOBI[14]) beschriebenen Methode konnte das Tc als Oxychinolat getrennt und trägerfrei auf eine Metallfolie von 0,4 mg/cm² elektrolysiert werden. Die drei hier interessierenden Gebiete des Spektrums zeigt Fig. 6.

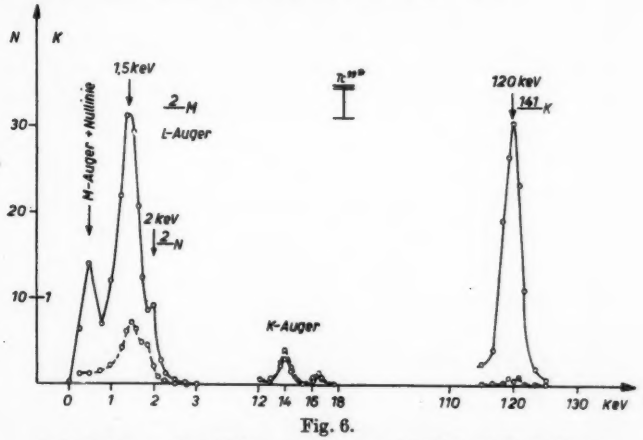

Fig. 6.

Ausschnitte aus dem Elektronenspektrum des Tc^{99} mit Koinzidenzen.

Die Konversionslinien bei 1,5 und 2 KeV überlappen mit den L-Augerelektronen und können im Spektrum der Einzelstösse nicht von diesen unterschieden werden. Aber an Hand der Koinzidenzrate können sie eindeutig identifiziert werden. Die K-Augerelektronen zeigen eine Koinzidenzrate von 11% entsprechend der Geometrie der Anordnung und der Ansprechwahrscheinlichkeit der Koinzidenzpartner im Scintillationszähler. Jedes Augerelektron der K-Gruppe ist in Koinzidenz mit einem K-Konversionselektron des 141-KeV-Überganges, das mit einer Ansprechwahrscheinlichkeit von 83% im Scintillationszähler registriert wird. Die Koinzidenzrate sollte also $\omega_{Sc} \cdot \varepsilon_{Sc} = 0{,}13 \cdot 0{,}83 = 0{,}11$ betragen, in Übereinstimmung mit dem Versuch. Im Bereich der L-Gruppe findet man dagegen eine Koinzidenzrate von nur etwa 2,2%. Das bedeutet, dass etwa 4/5 aller Elektronen in dieser Gruppe Konversionselektronen sind, und nur 1/5 als Augerelektronen in Frage kommen. Denn ein Augerelektron der L-Gruppe hat mindestens so viele Koinzidenz-

partner wie ein K-Augerelektron. Diese Konversionselektronen können also nur zu einer Linie gehören, die in Kaskade mit einer schwach konvertierten Strahlung liegt. Und das ist die 141-KeV-Linie, die zu 10% konvertiert ist. Wir interpretieren die zwei Spitzen in der Gruppe bei 1,5 und 2 KeV als M- und N-Konversion, und daraus ergibt sich die γ-Energie des isomeren Überganges zu 2 KeV in guter Übereinstimmung mit der Messung des Crossovers und jener im Proportionalzähler.

Die Isomere Ag^{107} und Ag^{109}.

Beide Kerne entstehen aus ihren Isobaren im Cadmium und wurden durch (p, n)-Reaktion im Cyclotron des Institutes durch Bestrahlen von Silber hergestellt. Wir haben in einem evakuierten Pyrexrohr das Cadmium verdampft, und die Aktivität schlägt sich dabei trägerfrei auf eine im Rohr vorhandene Goldfolie von 0,4 mg/cm² und 0,6 cm Durchmesser nieder.

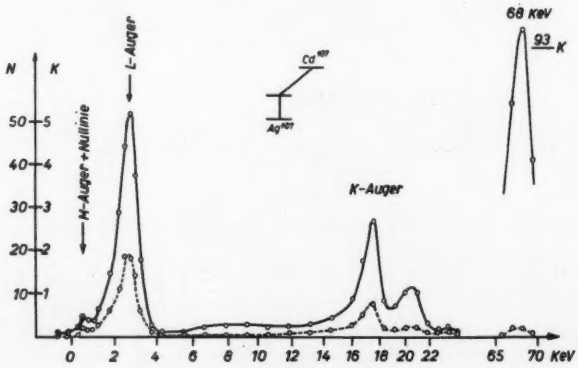

Fig. 7.

Elektronenspektrum des Cd^{107} zwischen 0 und 22 KeV mit Koinzidenzen. Im gleichen Maßstab die 93_K-Konversionslinie.

Fig. 7 und 8 zeigen das Spektrum der Elektronen zwischen 0 und 20 KeV mit den zugehörigen Koinzidenzen.

Die Elektronen, die vom K-Einfang herrühren, haben wegen der nachfolgenden Halbwertszeit des Isomers keine Koinzidenzpartner. Deshalb wird die Koinzidenzrate der Augerelektronen viel kleiner als im Falle des Technetiums, denn dort liegt ja kein K-Einfang vor. Sie beträgt für die K-Gruppe $(2{,}9 \pm 0{,}1)$% und für die L-Gruppe $(3{,}1 \pm 0{,}1)$%. Der Unterschied entspricht gerade den Erwartungen, da die L-Konversionslinie eine grössere Ansprechwahrscheinlichkeit

im Anthracenzähler besitzt. Eine Konversionslinie würde, wenn sie wie beim Tc^{99} in die L-Augergruppe fällt, die Koinzidenzrate auf mindestens 10% erhöhen, denn diese müsste mit der hochkonvertierten 87- resp. 93-KeV-Linie in Kaskade liegen. Ein solcher Übergang kann hier mit Sicherheit ausgeschlossen werden.

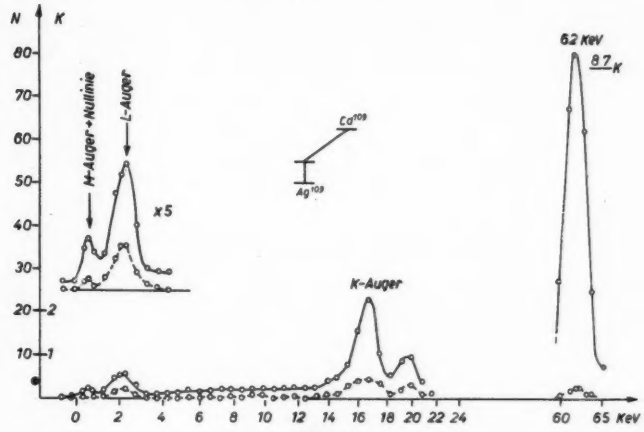

Fig. 8.

Elektronenspektrum des Cd^{109} zwischen 0 und 22 KeV mit Koinzidenzen. Im gleichen Maßstab die 87_K-Konversionslinie.

Das Isomer Au^{197}.

Über den Zerfall des Hg^{197} sind von verschiedenen Autoren Untersuchungen angestellt worden (siehe Zusammenfassung in [15]).

Nach dem in früheren Arbeiten angegebenen Zerfallsschema folgen dem isomeren Zustand von 7 sec Halbwertszeit im Au^{197} drei γ-Linien von 275, 191 und 77 KeV. Spin und Parität des Grundzustandes sind aus Messungen der Hyperfeinstruktur sowie des Kernmomentes bekannt. Sie lassen eindeutig auf einen $d_{3/2}$-Zustand schliessen. Die Drehimpulsänderung zwischen dem isomeren- und dem Grundzustand wurde aus der Anregung mit Neutronen ermittelt[16]). Aus der Anregungskurve wurde auf ein $\Delta I = 4$ und auf Paritätswechsel geschlossen. Damit erhält das Isomer den Drehimpuls 11/2 — (wahrscheinlich $h_{11/2}$). Diese Zuordnung wird dadurch erhärtet, dass man dem 25-h-Isomer im Hg^{197} den Drehimpuls 13/2 zuschreibt, was auf Grund der experimentellen Daten der γ-Kaskade im Hg^{197} sehr wahrscheinlich ist. Grundzustand und isomerer

Zustand des Au^{197} würden damit gut in die Termfolge des Schalenmodells passen. Der isomere Zustand führt also über zwei Zwischenniveaux in den Grundzustand. Auf Grund der Messungen können diesen Niveaux Drehimpuls und Parität nicht eindeutig zugeordnet werden. Weil nur 2% aller Zerfälle des Hg^{197} 23 h über das $h_{11/2}$-Niveau führen und zudem diese Linien teilweise durch die Konversionslinien des Hg^{197} verdeckt werden, sind die Messungen sehr erschwert. Trotzdem lässt sich sagen, dass die Ergebnisse nicht in Übereinstimmung mit allen theoretischen Forderungen gebracht werden können, nämlich: Konversion, Lebensdauer-Energie-Beziehung und K/L-Verhältnis. Um daher mehr über den Zerfall des Au^{197} zu erfahren, haben wir das Spektrum bis zur Energie 1 KeV gemessen und den Zerfall des Pt^{197} zum Au^{197} untersucht.

Der 18-h-Übergang Pt^{197}–Au^{197}.

In der Harwell-Pile wurde spektralreiner Platinschwamm während 3 Tagen mit langsamen Neutronen bestrahlt. Der (n,γ)-Prozess liefert aus den 6 stabilen Pt-Isotopen nur 3 gut messbare Aktivi-

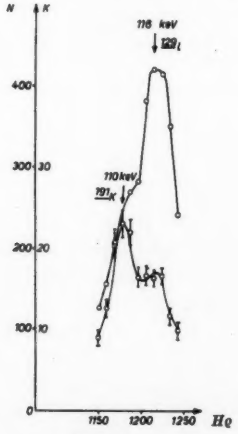

Fig. 9.

Ausschnitt aus dem Elektronenspektrum des Pt^{197} mit Koinzidenzen, zum Nachweis der 191_K-Konversionslinie im Au^{197}.

täten. Pt^{199} zerfällt mit einer Halbwertszeit von 28 min zu Au^{199}, und dieses aktive Gold kann chemisch abgetrennt werden. Somit bleibt noch der angeregte Zustand des Pt^{195} [19]) und der gesuchte β-

Übergang des Pt^{197}. Im Pt^{195} findet man nur Konversionslinien, deren höchste Energie 115 KeV beträgt. Das 18-h-Spektrum konnte somit auch in Gegenwart dieser Linien gemessen werden. In diesem Spektrum haben wir nun ausser den Linien des Pt^{195}, die mit 3,8 *d* Halbwertszeit abklingen, zwei Konversionslinien bei 62 und 73 KeV gefunden, welche eine Halbwertszeit von 18 h aufweisen. Die Energie dieser Linien und ihr Intensitätsverhältnis (3,6) stimmt genau mit der Energie und dem L/M-Verhältnis der bekannten 77-KeV-Linie im Au^{197} überein. Es kann daher kein Zweifel bestehen, dass es sich hier um den gleichen γ-Übergang handelt. Wir haben daher

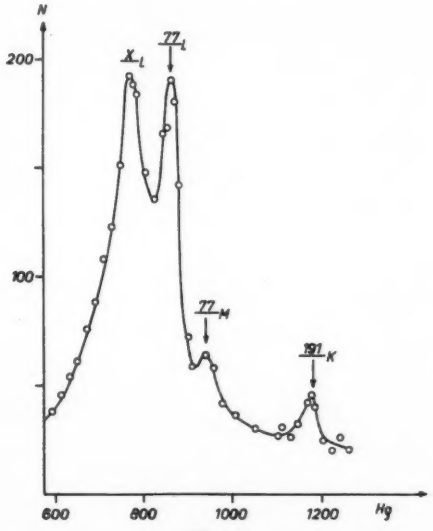

Fig. 10.

Photoelektronenspektrum der Platinfraktion zum Nachweis 77_L, 77_M und der 191_K-Linie. Konverter 2,6 mg/cm^{-2} Au.

auch nach der 191-K-Konversion gesucht, welche bei 121 KeV zu erwarten ist. Diese Linie erscheint tatsächlich im Spektrometer. Sie ist aber etwa 50mal schwächer und wird überdies fast verdeckt von der sehr intensiven 129-L-Linie des Pt^{195}. Mit Hilfe von Koinzidenzen konnte sie aber einwandfrei identifiziert werden. Fig. 9 zeigt einen Ausschnitt aus dem Elektronenspektrum.

Beide γ-Übergänge sind ausserdem im Spektrum der Photoelektronen nachzuweisen (Fig. 10).

Somit ist der β-Übergang durch 3 Experimente sichergestellt: 1. β-Spektrum, 2. Konversionslinien 77 L, 77 M und 191 K und 3. Photoelektronenspektrum der Platinfraktion. Aus der Intensität der Photolinien folgt unter Berücksichtigung der energieabhängigen Photoausbeute, dass 1,5% aller Übergänge auf das 268-KeV-Niveau

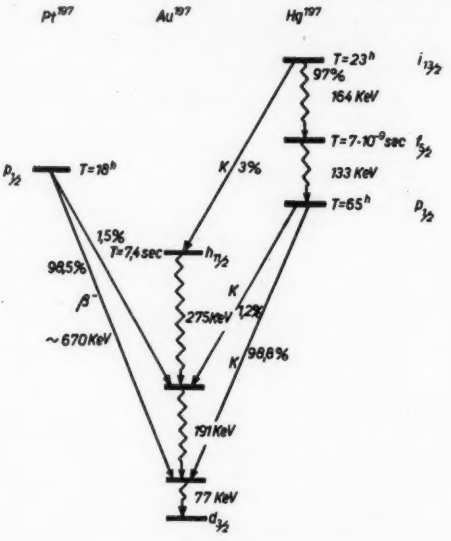

Fig. 11.

Zerfallsschema des Pt^{197} kombiniert mit dem schon bekannten Schema des Hg^{197} und Au^{197}.

im Au^{197} führen. Für das β-Spektrum ergibt sich durch Auswertung des FK.-Diagramms eine Grenzenergie von 670 KeV. Die Energie des Partialspektrums beträgt demnach 479 KeV (670—191). Das Zerfallsschema des Pt^{197} zeigt Fig. 11.

Das Elektronenspektrum des Hg^{197} und Au^{197} zwischen 1 und 10 KeV.

Die Aktivität wurde im Cyklotron des Institutes durch die Reaktion Au (p, n) Hg hergestellt, und konnte durch Verdampfen im Vakuum trägerfrei auf eine Goldfolie von 0,4 mg/cm² niedergeschlagen werden. Diese Folie konnte direkt als Quelle im Spektrometer Verwendung finden. Fig. 12 zeigt das Spektrum, das mit einer Be-

schleunigung von 6 kV aufgenommen wurde. Das Zählrohrfenster war 0,1 mg/cm² Formvarfolie.

Dass eine Kern-γ-Strahlung im Gebiet zwischen 1 und 10 KeV dieser Messung nicht hätte entgehen können, zeigt folgende Überlegung: Diese Strahlung wäre vollständig konvertiert. Die Wahrscheinlichkeit dafür, dass ein Elektron dieser Linie pro Zerfall des Hg^{197} 23 h emittiert wird, wäre demnach 0,03, denn nur dieser

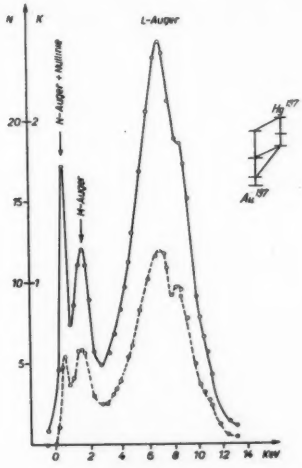

Fig. 12.

Elektronenspektrum des Hg^{197} + Au^{197} zwischen 0 und 12 KeV mit Koinzidenzen.

Bruchteil führt über das fragliche Niveau. Als Konkurrenzprozess stehen dem die L-Augerelektronen gegenüber. Eine Schätzung der L-Augerausbeute auf Grund von Messungen der L- und K-Augergruppe im Spektrum des Au^{195} ergibt etwa 25%. Addiert man alle Möglichkeiten für L-Augerprozesse im Zerfallsschema des Au^{197} + Hg^{197}, so erhält man damit eine Wahrscheinlichkeit von 0,5 pro Zerfall des Hg^{197} 23 h. Die fragliche Linie müsste also eine Intensität von ca. 6% aller L-Augerelektronen haben. Man kann berechnen, dass eine Konversionslinie von dieser Intensität die Koinzidenzrate etwa um den Faktor 2 vergrössern müsste. Da die gemessene Koinzidenzrate aber über den ganzen Bereich der L-Augergruppe innerhalb von 10% konstant ist, kann eine Konversionslinie selbst von dieser kleinen Intensität ausgeschlossen werden.

Au^{195}.

Spektralreines Platin wurde im Cyklotron des kernphysikalischen Institutes in Amsterdam mit Deuteronen bestrahlt*). Trennt man das Gold elektrolytisch vom Platin, so findet man noch folgende Halbwertszeiten: 39 h (Au^{194}), 3,2 d (Au^{199}), 5,6 d (Au^{196}) und 185 d (Au^{195}). Nachdem alle kürzeren Perioden abgeklungen waren, wurde das Au^{195} trägerfrei auf eine dünne Goldfolie elektrolysiert. Fig. 13 zeigt das Spektrum mit 6 kV Beschleunigung.

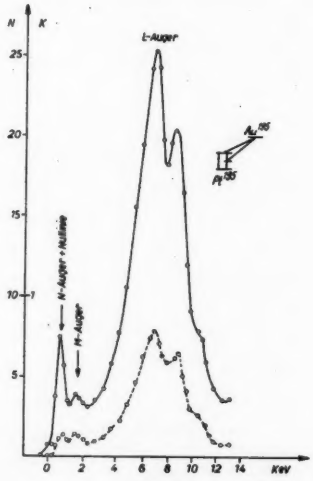

Fig. 13.

Elektronenspektrum des Au^{195} zwischen 0 und 12 KeV mit Koinzidenzen.

Beim Vergleich dieser Messung mit jener vom $Au^{197} + Hg^{197}$ fällt auf, dass die *N*-Augergruppe relativ zur *L*-Gruppe und zur Nullinie weniger intensiv ist. Um das verständlich zu machen, muss einiges über die Präparate gesagt werden: Es hat sich gezeigt, dass die Goldfolie, auf der die Aktivität niedergeschlagen oder elektrolysiert ist, auf der Formvarfolie, die als mechanischer Träger dient, nur haftet, solange kein elektrisches Feld angelegt ist. Um zu verhindern, dass die elektrostatischen Kräfte des Feldes die Goldfolie

*) Herrn Professor Bakker sind wir für die Bestrahlung, die in seinem Institut durchgeführt wurde, sehr zu Dank verpflichtet.

zerstören, haben wir das Präparat mit einer darübergespannten Formvarhaut von 0,01 mg/cm² fixiert. Diese ist natürlich bei jedem Präparat etwas verschieden und wirkt als Absorber. Ausserdem diffundieren mit der Zeit die aktiven Atome etwas in die Goldfolie hinein, was wahrscheinlich gerade beim Au^{195} mitspielt. Diese Selbstabsorption hat aber keinen Einfluss auf die Koinzidenzrate und auf diese stützt sich ja die Interpretation der Messung.

Au^{199}.

Das bei der Bestrahlung mit langsamen Neutronen im Platin entstehende Pt^{199} zerfällt mit einer Halbwertszeit von 28 min unter β-Emission zu Au^{199}. Die Halbwertszeit des Au^{199} beträgt 3,2 d.

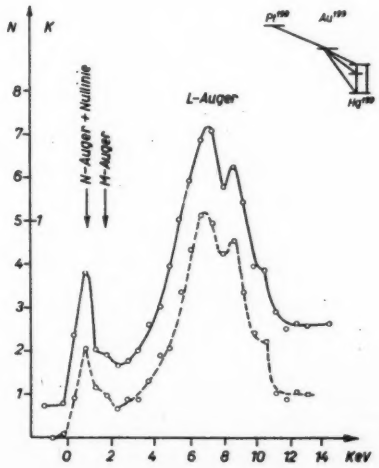

Fig. 14.
Elektronenspektrum des Au^{199} zwischen 0 und 12 KeV mit Koinzidenzen.

Man kann diese Aktivität als Gold chemisch abtrennen und trägerfrei elektrolysieren. Der β-Zerfall des Au^{199} führt zum stabilen Hg^{199}. Fig. 14 zeigt das Spektrum. Die Nullinie erscheint hier intensiver, weil das Präparat relativ schwach war.

Au^{198}.

Bestrahlt man Gold mit langsamen Neutronen, so entsteht durch (n,γ)-Prozess Au^{198}, das mit 2,6 d Halbwertszeit zu Hg^{198} zerfällt. Durch Elektrolyse kann man also kein trägerfreies Präparat herstellen. Immerhin ist die spezifische Aktivität des käuflichen Isotopes so gross, dass das Spektrum gemessen werden kann. Fig. 15 zeigt das Spektrum des Au^{198}.

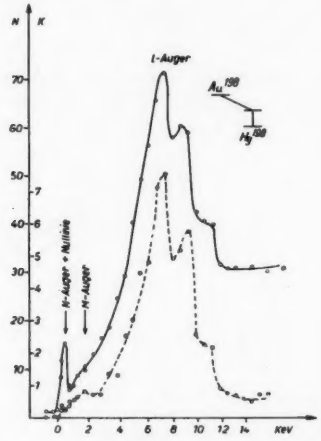

Fig. 15.

Elektronenspektrum des Au^{198} zwischen 0 und 12 KeV mit Koinzidenzen.

Diskussion.

Die Messungen an den drei Isomeren Ag^{107}, Ag^{109} und Au^{197} zeigen, dass ausser den schon bekannten Kern-γ-Strahlungen keine weiteren Emissionen in dem untersuchten Energiegebiet vorkommen. Ein isomerer Übergang kleiner Energie konnte in allen drei Fällen ausgeschlossen werden.

Bei den zwei Silberisomeren besteht damit eine Diskrepanz zwischen der aus der Lebensdauer-Energiebeziehung und dem gemessenen K/L-Verhältnis hergeleiteten Drehimpulsdifferenz von 3 und der Forderung des strengen Einteilchenmodells. Mit dem Schalenmodell in seiner Fassung als Einteilchenmodell können die Niveaux dieser Isomere also nicht mehr erklärt werden. Beim Au^{197} kann

diese Entscheidung noch nicht getroffen werden, weil der Multipolcharakter der γ-Kaskade noch nicht hinreichend genau bekannt ist.

Die Untersuchungen an den Kernen Au^{195} und Au^{199} stehen in engem Zusammenhang mit den Zerfallsschemen, die in der folgenden Arbeit[19]) beschrieben werden. Sie beweisen, dass hier die Übereinstimmung mit dem Einteilchenmodell vollkommen ist, und dass keine weiteren Niveaux existieren. Für die in jener Arbeit aufgezeigte Systematik bezüglich der Energie entsprechender Zustände bei ug-Kernen, die sich um je 2 Nukleonen unterscheiden, war es nämlich von fundamentaler Bedeutung, das Gebiet kleiner Energien zu untersuchen. Die Existenz eines Niveaus kleiner Energie in einem der Kerne Au^{195}, Hg^{197} oder Au^{199} hätte bezüglich der Zuordnung gemäss dem Schalenmodell zu grossen Schwierigkeiten geführt.

Von allen hier untersuchten Kernen ist Hg^{198} der einzige gg-Typ, und dieser verdient noch in anderem Zusammenhang Interesse. Von verschiedenen Autoren[17]) wurden hier verzögerte Koinzidenzen gefunden, die einem Niveau von sehr kleiner Energie zugeschrieben wurden. Dieser Übergang sollte zeitlich dem Übergang von 411 KeV folgen. Ein solches Niveau im Au^{198} wäre aber eine interessante Ausnahme, denn nimmt man der j-j-Kopplung entsprechend an, dass die angeregten Zustände in einem gg-Kern durch Aufbrechen eines Paares von zwei Nukleonen entstehen, so sollte dazu eine relativ grosse Energie gehören Dieses Verhalten ist auch durch die Erfahrung bestätigt[18]). Unsere Messungen können aber diesen Übergang bis 1 KeV ausschliessen.

Unserem verehrten Lehrer, Herrn Professor Dr. P. Scherrer, sind wir für sein förderndes Interesse an dieser Arbeit zu Dank verpflichtet.

Literatur.

[1]) M. Goldhaber und A. W. Sunyar, Phys. Rev. **83**, 96 (1951).
[2]) V. F. Weisskopf, private Mitteilung und Phys. Rev. **81**, 470 (1951).
[3]) H. Medicus, D. Maeder und H. Schneider, Helv. Phys. Acta **24**, 72 (1951).
[4]) O. Huber, F. Humbel, H. Schneider und A. de Shalit, Helv. Phys. Acta **25**, 1 (1952).
[5]) D. K. Butt, Proc. Phys. Soc. [A] **63**, 9, 986 (1950).
[6]) O. Huber, F. Humbel, H. Schneider und W. Zünti, Helv. Phys. Acta **23**, 855 (1951).
[7]) E. Persico, Rev. Sci. Instr. **20**, Nr. 3, 191 (1949).
[8]) Du Mond, Rev. Sci. Instr. **20**, Nr. 3, 160 (1949).

[9]) Zworykin, Morton, Ramberg, Hiller und Vance, „Electron Optics and the Electron Microscope", John Wiley a. S., New York.
[10]) Handbuch der Physik (Geiger und Scheel) **22**, 1 (1933).
[11]) C. Burckhardt, Diplomarbeit ETH. Zürich (1952).
[12]) G. T. Seaborg und Segrè, Phys. Rev. **55**, 808 (1939).
[13]) I. W. Mihelich, M. Goldhaber und E. Wilson, Phys. Rev. [A] **83**, 216 (1951).
[14]) E. Jacobi, Helv. Chim. Acta [A] **31**, 2118 (1948).
[15]) O. Huber, F. Humbel, H. Schneider, A. de Shalit und W. Zünti, Helv. Phys. Acta **24**, 127 (1950).
[16]) Ebel und V. F. Weisskopf, private Mitteilung.
[17]) K. P. Meyer, E. Baldinger und P. Huber, Helv. Phys. Acta **23**, 517 (1950).
[18]) P. Stähelin und P. Preiswerk, Helv. Phys. Acta (im Druck).
[19]) A. de Shalit, O. Huber und H. Schneider, Helv. Phys. Acta **25**, 279 (1952).

On the decay of some odd isotopes of Pt, Au and Hg

by **A. de-Shalit***), **O. Huber**, and **H. Schneider**, Phys. Inst. der ETH., Zurich.

(4. XII. 51.)

Zusammenfassung: Der Zerfall der Kerne Pt^{195*}, Au^{195} und Au^{199} wurde untersucht. Für die Messungen wurde eine Koinzidenzanordnung im β-Spektrometer benützt. Zerfallsschemen sowie Konversionskoeffizienten werden angegeben. Die Resultate werden diskutiert unter dem Aspekt des Schalenmodells und es wird nachgewiesen, dass alle angeregten Zustände in diesen drei Kernen, sowie auch im Hg^{197}, mit den Forderungen eines Einteilchenmodells nach MAYER verträglich sind.

Introduction.

The existence of a shell structure in nuclei has recently been determined in many different ways[1-3]). One usually notices that a certain property of nuclei, when plotted against the number of protons or neutrons in the nucleus, has a breakdown at certain "magic-numbers" which is interpreted as an indication for the beginning of a new shell.

Since the recognition of these magic-numbers, the first aim of a nuclear model has been to explain the closing of the shells at these numbers. This could be achieved by different models[4-8]), and the further choice among them is dictated by the behaviour of each of them all along the shell.

The model of MAYER, which is usually considered to be the most successful one, is, at least for the ground states, a single particle model. The natural question is whether this single particle model can be extended to include also excited states, and to what an extent.

In order to calculate nuclear energy levels one may proceed in the following way:

An effective potential-well is postulated and the eigenstates in it are derived. One then considers the different configurations obtained

*) Now at the Palmer Phys. Lab. Princeton N. J., U. S. A.

by distributing those nucleons which are not in closed shells or sub-shells among the empty states. Each such configuration, which in the j-j-coupling scheme will be characterized by giving the occupation numbers n_i of the different sub-shells $(j_1^{n_1}, j_2^{n_2}, \ldots)$, has generally a number of terms arising from different relative orientations of the angular momenta of each nucleon.

In Mayer's model the lowest configurations are those in which there is exactly one odd occupation number (for odd A nuclei), and further, the lowest term in each configuration has the spin and parity of that state to which the odd particle belongs. That is: the lowest state of a configuration is a single-nucleon state.

A priori there are no serious objections to a situation in which the energy differences between the lowest terms of some different configurations will be smaller than the difference between the lowest term and the next one in the same configuration. That is: a single particle model could, in principle, exist for the first few excited states of odd nuclei. It could be realized, for instance, among particles moving in an oscillator potential-well slightly deformed. As is well known the energy levels of the (three dimensional) oscillator are degenerate with respect to the orbital angular momentum, and thus a slight deformation of this potential could give rise to a situation in which the "single particle levels" are lower than the excited terms of the lowest configuration.

As in Mayer's model the effective potential is a slightly deformed oscillator well, it might be well expected that the lowest excited states will in fact be single-particle ones.

This assumption is further strengthened by comparing the energy levels of odd-even nuclei with those of the neighbouring even-even ones. In general the first excited state of an even-even nucleus is higher than the first few levels in its odd-even neighbours. Even-even nuclei show a tendency of having more or less equi-distant levels of the same parity and whose spins differ by two units: $0 - 2 - 4$. This situation is characteristic for the terms formed by the excited states of a configuration of equivalent particles. Thus, if we really interpret these levels as such, the interpretation of the first excited states of odd-even nuclei as single particle ones would get further support. It should be noted that a big energy difference between the terms of a configuration of an even number of nucleons does not necessarily imply the same distance between the terms of a configuration of an odd number of nucleons. It serves merely to give an idea of the energy needed to "break" the pairing between the nucleons.

Another check on the validity of the single particle model for the first excited states of odd nuclei arises from the following simple considerations:

If the separation of the levels in a configuration is smaller than the separation between the lowest states of different configurations, one would expect to find similar decay schemes for two nuclei of which the one has n particles in the outmost shell and the other has n holes; the decay schemes of successive odd nuclei should be in principle different. If, however, the single particle model predominates, one should find, for odd A nuclei, exactly the same decay schemes all along the shell. That is:

> all odd A nuclei having their odd particle in the same sub-shell should have the same "set" of levels, the relative positions of which should vary continuously from one nucleus to the other[9]).

This work was undertaken in order to check if this result holds or not, and we chose for this purpose some odd A isotopes of Pt, Au, and Hg. The previous decay schemes of the isotopes we were about to examine would have definitely contradicted the above conclusion, as they were substantially different from each other. It therefore seemed worth while to check them with refined technique.

For this purpose we used a magnetic lens spectrometer supplemented by a coincidence arrangement which enables the measuring of the number of coincidences of each conversion line with all its "partners". This was technically done by placing a scintillation counter just behind the sample and taking coincidences between all the electrons measured in this scintillation counter and electrons of definite energy arriving at the Geiger counter on the other side of the spectrometer. This arrangement and its applications are described elsewhere[10,11]).

As for the samples, it was found most useful to prepare them by electrolysis. We could get very nice results by using as cathodes thin ($\sim 0{,}4$ mg/cm^2) gold foils which were floating on the solution to be electrolysed; we were thus sure that the active material was deposited on one side of the backing only, and the backing effects could be minimized.

In Chapter I we give experimental results on some odd N nuclei, and in Chapter II we shall discuss their decay schemes and others from the standpoint of Mayer's shell model.

CHAPTER I.

Spectroscopic measurements.

A. The Pt n-γ-products.

Spectroscopically pure Pt was irradiated by neutrons in the pile of HARWELL. Except for possible isotopes of short half-lives the periods found were of 18^h, $3{,}16^d$, $3{,}8^d$ and $\sim 70^d$.

The 18^h activity is known to be due to Pt^{197} decaying to the 77 keV and 268 keV levels in Au^{197} [12]). The $3{,}16^d$ activity is due to the β-decay of Au^{199} to Hg^{199} [13]); the Au^{199} is produced from the 29^m Pt^{199}. As will be shown later the $3{,}8^d$ activity arises from an isomeric transition in Pt^{195}. The 70^d activity, which was of a very low intensity, is probably due to some impurities of Ir which has a very high cross-section for the n-γ-reaction.

§ 1. *Au^{199}; experimental results.*

The electron spectrum of Au^{199} is shown in Fig. 1 together with the coincidence spectrum. The interpretation of these graphs is given in Table I.

Table I.

Energy of conv. line in keV	Interpretation	Relative intensity*)	Coincidence rate**)
1	*M* Auger		
7			
8,5	*L* Auger		
10,2			
36	50,6 *L*	5,83	12,2%
47	50,6 *M*	1,77	
50	*K* Auger		
74,6	157,5 *K*	22,7	8,6%
125,2	208,1 *K*	11,3	7,5%
145	157,5 *L*	33,7	8,1%
155	157,5 *M*	11,7	8,0%
194	208,1 *L*	2,0	7,1%
205	208,1 *M*	0,8	

*) These values were taken from another measurement with a better resolving power (1,5%).

**) Simple considerations show that the coincidence rate (number of coincidences per electron counted on the conversion line) at different points of the same line should be equal (indeed, deviations from this constancy were used to establish an overlaping of two different lines). The coincidence rates listed in the Table are averages of 4—5 points on each line; the fluctuations do not exceed 5% in any case and are less than 2% in most of them.

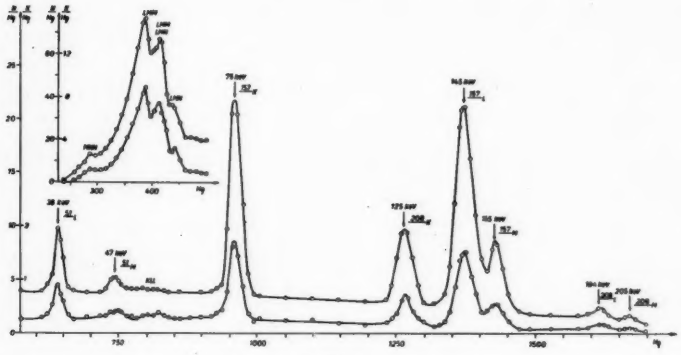

Fig. 1.

Electron spectrum of Au^{199}.

Upper curve – single counts; lower curve – coincidences.

"a" was taken with an acceleration of 6 KeV.

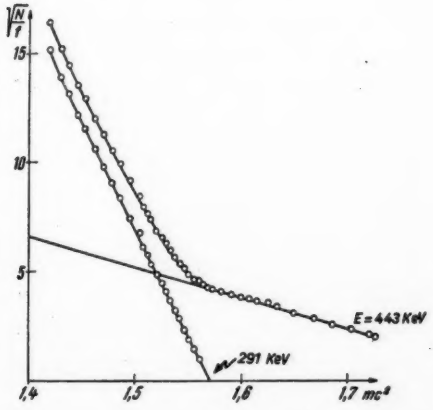

Fig. 2.

Kurie plot of β-spectrum of Au^{199}.

Fig. 2 shows a Kurie plot of the β-spectrum of Au^{199} which demonstrates the definite existence of two spectra of maximum energies 291 $\pm$ 5 keV and 443 $\pm$ 7 keV. Some 93% of the β-transi-

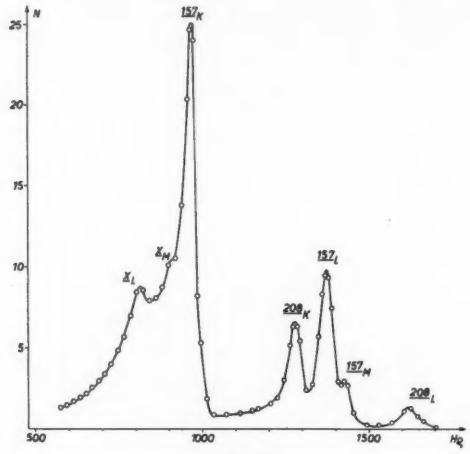

Fig. 3.
Photo-electrons of Au^{199}

Table II.

Energy of photo line	Interpretation	Relative intensity
55 keV	X-rays *L*	
64 keV	X-rays *M*	
76 keV	157 *K*	25
127 keV	208 *K*	5,2
145 keV	157 *L*	9,5
155 keV	157 *M*	
196 keV	208 *L*	1,4

tions go to the excited states in Hg^{199}, whereas 7% decay directly to the ground state.

Fig. 3 shows the photo-electron spectrum of Au^{199} taken with an Au radiator of 2,6 mg/cm^2 thickness. The interpretation of this graph is given in Table II.

An attempt to find angular correlation between the K conversion electrons of the 208 keV γ-ray and the rest of the spectrum, as well as between the K conversion electrons of the 157 keV γ-ray and the rest of the spectrum, gave negative results[14]).

Discussion of experimental results; decay scheme.

From the $K - L$ differences it is seen that the 208 and the 157 keV γ-rays are most probably converted in Hg. The 51 keV γ-ray has an appreciable amount of coincidences so that this γ-ray, too, should be converted in the same nucleus, for otherwise it will have no partner to be in coincidence with.

These results agree with those of HILL[15]). No indication could be found for the lines of 24 keV, 70 keV, and 230 keV reported by BEACH et al.[13]).

The difference in energy between the two main β-spectra (Fig. 2) indicates that they are leading to the initial and final levels of the 157 keV γ-transition. The fact that the 50,6 keV γ-ray and the 157 keV γ-ray sum up to give 208 keV, suggests that the first two are in cascade with each other and in parallel with the last one.

The absence of photo-electrons of the 51 keV γ-ray (Fig. 3) puts an upper limit of 10% for the ratio of the non-converted 51 keV γ-ray intensity to that of the X-rays. That is: if we denote by $\varkappa^{51}$ the total conversion coefficient of the 51 keV γ-ray ($\varkappa = N_e/N$, $\varkappa = \varkappa_K + \varkappa_L + \varkappa_M$), and if μ_{51} is the number of transitions via the 51 keV γ-ray per disintegration of Au^{199}, etc., we have:

$$\mu_{51}(1-\varkappa^{51}) \leqslant 0{,}1[\mu_{157}\varkappa_K^{157} + \mu_{208}\varkappa_K^{208}]. \tag{1}$$

It is clear that:

$$\mu_{51}\varkappa^{51} : \mu_{157}\varkappa_K^{157} : \mu_{208}\varkappa_K^{208} = Z^{51} : Z_K^{157} : Z_K^{208} \tag{2}$$

so that by introducing (2) into (1) one gets:

$$\left(\frac{1}{\varkappa^{51}} - 1\right) \leqslant 0{,}1\frac{Z_K^{157} + Z_K^{208}}{Z^{51}}. \tag{3}$$

Inserting the values given in Table I for the relative intensities of the conversion lines one gets from (3):

$$\varkappa^{51} > 0{,}70. \tag{4}$$

To determine now whether the 51 keV γ-ray follows the 157 keV one or preceeds it, we note that in the first case the number of the 51 keV transitions is at least as big as that of the 157 keV ones, so that:

$$\frac{Z^{51}}{\varkappa^{51}} \geqslant \frac{Z^{157}}{\varkappa^{157}} \geqslant Z^{157}.$$

Therefore, assuming that the 51 keV γ-ray follows the 157 keV one, would lead to the relation

$$Z^{51} \geqslant 0{,}7\, Z^{157}$$

which is seen not to be the case (Table I). Thus, if they are at all in cascade, the 51 keV γ-ray preceeds the 157 keV one. This is also

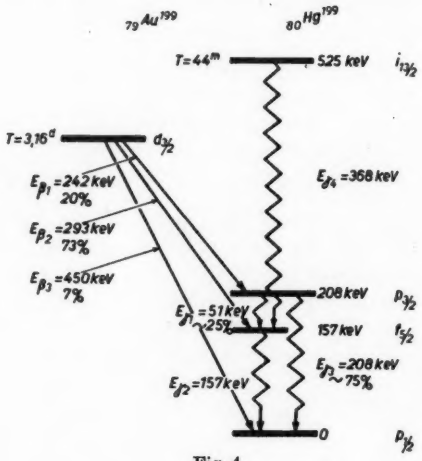

Fig. 4.
Decay scheme of Au^{199}.

confirmed by the decay of the 44^m isomeric state in Hg^{199}, since there is no indication of either a 51 keV or a 208 keV γ-ray, the only ones found being a 368 keV and the 157 keV γ-rays.

It is thus suggested that the decay scheme of Au^{199}-Hg^{199} is as shown in Fig. 4.

Our experimental data enable now a further check on this decay scheme, as well as the determination of the conversion coefficients and the different branching ratios.

We use the following symbols:

N = number of disintegrations per unit time,
Z = number of conversion electrons counted per unit time,
K = number of coincidences per unit time of a conversion line with all its partners,
ω_{Sc} = solid angle of the scintillation counter,
ω_{Sp} = solid angle of the spectrometer,
λ_i = branching ratios for the spectra,
μ = branching of the 208 keV level via the 51 keV transition,
$\varepsilon(p)$ = efficiency of scintillation counter for electrons of momentum p,
$f(p)$ = "shape" function of the spectrum $[\int f(p)\,dp = 1]$,
β = coincidence rate on a conversion line.

The following relations are easily proved:

$$\left.\begin{aligned} Z^{51}_{L,M} &= N\,\lambda_1 \cdot \mu\,\omega_{Sp}\,\varkappa^{51}_{L,M} \\ Z^{157}_{K,L,M} &= N\,(\lambda_2 + \lambda_1 \cdot \mu)\,\omega_{Sp}\,\varkappa^{157}_{K,L,M} \\ Z^{208}_{K,L,M} &= N\,\lambda_1\,(1-\mu)\,\omega_{Sp}\,\varkappa^{208}_{K,L,M} \end{aligned}\right\} \tag{5}$$

$$\left.\begin{aligned} K^{51}_{L,M} &= Z^{51}_{L,M}\,\omega_{Sc}\left[\int f_1(p)\,\varepsilon(p)\,dp + \sum_{i=K,L,M} \varepsilon_i^{157}\,\varkappa_i^{157}\right] \\ K^{157}_{K,L,M} &= Z^{157}_{K,L,M}\,\omega_{Sc}\left[\frac{\lambda_2}{\lambda_2+\lambda_1\cdot\mu}\int f_2(p)\,\varepsilon(p)\,dp + \frac{\lambda_1\mu}{\lambda_2+\lambda_1\cdot\mu}\times\right. \\ &\qquad \left.\times\left(f_1(p)\,\varepsilon(p)\,dp + \sum_{i=L,M}\varepsilon_i^{51}\,\varkappa_i^{51}\right)\right] \\ K^{208}_{K,L,M} &= Z^{208}_{K,L,M}\,\omega_{Sc}\int f_1(p)\,\varepsilon(p)\,dp \end{aligned}\right\} \tag{6}$$

Combining (5) and (6) one gets:

$$\beta_{51} - \beta_{208} = \omega_{Sc}\sum_{i=K,L,M}\varepsilon_i^{157}\,\varkappa_i^{157} = \omega_{Sc}\,\varkappa^{157}\sum\varepsilon_i^{157}\,\frac{Z_i^{157}}{Z^{157}}$$

Hence:

$$\varkappa^{157} = \frac{(\beta_{51}-\beta_{208})\,Z^{157}}{\omega_{Sc}\sum\varepsilon_i^{157}\cdot Z_i^{157}}. \tag{7}$$

From the experimental values of β (Table I) we see that the coincidence rates for the K conversion lines are bigger than the ones for the corresponding L and M lines. This different coincidence rate for the K conversion lines is due to additional coincidences with the K Auger electrons. The efficiency of these electrons in the scintil-

lation counter arrangement is 50%[16]). Taking the Auger coefficient in Hg to be 0,06[17]) one finds, with $\omega_{Sc} = 0{,}13$, that the Auger contribution to the coincidence rate for a K conversion line in Hg is 0,4%. This just explains the above difference. (That the difference in β is really due to coincidences with the K Auger electrons can be nicely shown by picking up from the crystal, with the help of an attenuator, only the big kicks caused by high energy electrons; in this case the K Auger electrons efficiency is very low in relation to the efficiency of the other electrons present[16]) and the coincidence rate is then exactly the same for all conversion lines of the same γ-ray.)

Subtracting the above 0,4% from the coincidence rates on the K conversion lines given in Table I, we get the following average values for the coincidence rates on the three lines:

$$\beta_{51} = 12{,}2\% \qquad \beta_{157} = 8{,}1\% \qquad \beta_{208} = 7{,}1\% \tag{8}$$

Substituting these values in (7) we get:

$$\varkappa^{157} = 0{,}50 \pm 0{,}02. \tag{9}$$

To determine the conversion coefficient of the 208 keV γ-ray we use the photo-electron measurements. The efficiency of the Au radiator for 157 keV and 208 keV γ-rays was determined by interpolation from experimental calibrated points. The calibration was done with the 172 keV and 247 keV γ-rays of In^{111}. As is easily seen one has, for any decay scheme:

$$\frac{N_\gamma^{208}}{Z^{208}} : \frac{N_\gamma^{157}}{Z^{157}} = \frac{1-\varkappa^{208}}{\varkappa^{208}} : \frac{1-\varkappa^{157}}{\varkappa^{157}}$$

and we find experimentally

$$\frac{1-\varkappa^{208}}{\varkappa^{208}} : \frac{1-\varkappa^{157}}{\varkappa^{157}} = 0{,}83\,. \tag{10}$$

Combining (9) and (10) we get:

$$\varkappa^{208} = 0{,}55 \pm 0{,}05\,. \tag{11}$$

It should be noted that correcting factors which were neglected in evaluating (11), such as absorption of the γ's in the sample and its container, tend to increase this value. It is estimated that they could raise this value by 5—10%.

The relation (10), which is independant of the decay scheme, excludes the possibility that the 208 keV γ-ray will follow the 157 keV

one; for this value means that the conversion coefficients of both γ-rays are roughly equal, and thus if the 208 keV γ-ray would follow the 157 keV, its conversion electrons should be at least as numerous as those of the 157 keV γ-ray, and this is easily seen not to be the case (Table I).

Taking in addition into account the relatively high coincidence rate of the 51 keV γ-ray, which shows that it must be in coincidence with at least two lines or a line and a spectrum, one can see that only the given decay scheme is consistent with all the experimental data.

The small difference in the coincidence rate for the 157 keV γ-ray and for the 208 keV γ-ray is partially due to the 157 keV being in cascade with the 51 keV transition, and mainly to the fact that the spectrum leading to the 157 keV level is of a higher energy than the one leading to the 208 keV level, and thus has a bigger efficiency in the crystal. This was proved by noticing that this difference grew relatively bigger when only the higher kicks from the crystal were allowed to contribute to the measured coincidences.

By means of the conversion coefficients it is now easy to determine the branching ratios. We get:

$$0{,}22 \leqslant \mu \leqslant 0{,}30 \quad 0{,}20 \leqslant \lambda_1/(\lambda_1+\lambda_2) \leqslant 0{,}23. \tag{12}$$

Table III.

The transitions in Hg^{199}.

γ	$\varkappa\,(=N_e/N)$				$\alpha\,(=N_e/N_\gamma)$				K/L
	K	L	M	Tot	K	L	M	Tot	
51		>0,54	>0,16	>0,70	—	>1,8	>0,5	>2,3	—
157	0,17	0,25	0,08	0,50	0,33	0,50	0,17	1,0	0,67
208	0,44	0,08	0,03	0,55	0,98	0,17	0,07	1,22	5,65

§ 2. *Pt^{195}; experimental results.*

The Pt fraction of the neutron irradiated Pt decayed with two of the periods referred to above, namely: 18^h and $3{,}8^d$.

Fig. 5 shows the electron and the coincidence spectra of the Pt fraction. The interpretation of these measurements is given in Table IV.

The information one can get from these measurements is mainly qualitative rather than quantitative due to the fact that some of

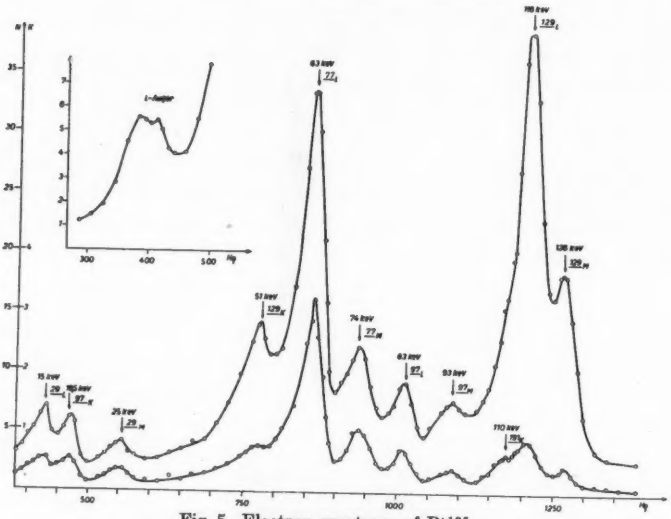

Fig. 5. Electron spectrum of Pt^{195}.
Upper curve – single counts; lower curve – coincidences
"a" was taken with an acceleration of 6 KeV.

Table IV.

Energy of conv. line keV	Half life	Conv. in	Inter-pretation	Relat. int.*)	Coinc. rate**)
6,5	3,8^d	Pt	L Auger		
8,5	3,8^d	Pt			
15	3,8^d	Pt	29 L		14 %
18,5	3,8^d	Pt	97 K		11,5%
25	3,8^d	Pt	29 $M+N$		14,4%
51	3,8^d	Pt	129 K	1,0	7,3%
63	18^h	Au	77 L		
74	18^h	Au	77 M		
83	3,8^d	Pt	97 L	0,75	12 %
93	3,8^d	Pt	97 M	0,2	
110	18^h	Au	191 K		
116	3,8^d	Pt	129 L	3,8	3,2%
126	3,8^d	Pt	129 M	1,8	3,0%

*) The relative intensities were measured after the short period (18 h) had decayed; those not given could not be evaluated because of the absorption in the sample.

**) The coincidence rate measurements in the spectrometer were carried out after the 18 h activity had decayed, both in the neutron irradiated Pt and in a deuteron-irradiated Pt, which was also found to contain the 3,8 d activity in its Pt fraction.

the important lines are of such a low energy that the absorption of the electrons in the rather thick sample prevents any evaluation of their intensity. We therefore measured in addition the photo-electrons emitted from a 2,6 mg/cm² Au radiator. These are shown in Fig. 6.

Discussion of experimental results; decay scheme.

Our sample was not carrier-free and indeed absorbed considerably the low conversion lines. Nevertheless it is believed that the measured $K - L$ differences do represent their real values. The L Auger-electron group, which retains its form in our sample, supports this assumption. We thus conclude that the 97 keV and the 129 keV γ-rays are converted in Pt or Au; Ir is excluded. We can further

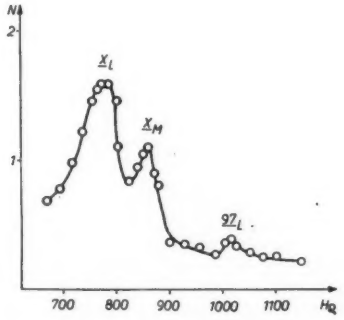

Fig. 6.

Photo-electrons of Pt^{195}.

exclude their conversion in Au from the absence of a β-spectrum. Thus an isomeric state in Pt is established.

The fact that all three lines: 29 keV, 97 keV, and 129 keV, have the same half-life suggests that they might be in cascade, if they all belong to the same nucleus.

The 129 keV and the 97 keV γ-rays are both converted in Pt; as the 29 keV γ-ray has coincidences and as the only electrons of the same period of $3{,}8^d$ are the conversion electrons of the 129 keV and 97 keV γ-rays, we conclude that the 29 keV γ-ray is also converted in Pt. For reasons to be given later we fix the order of the three γ-rays as shown in Fig. 7.

From the coincidence rate on the 97 keV conversion lines one concludes immediately that the 129 keV γ-ray is totally converted. (The 29 keV γ-ray contributes next to nothing to this coincidence rate because of the very low efficiency of the scintillation counter for its conversion electrons.)

The relative intensity of the 97 keV conversion electrons, compared to this of the 129 keV lines, could serve only as a rough lower limit to its conversion coefficient because of the uncertainties in the

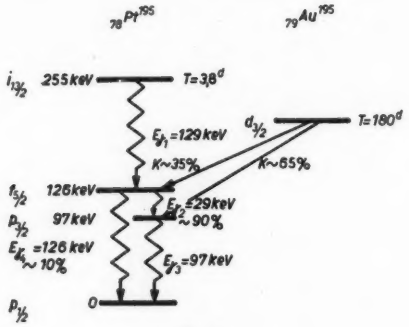

Fig. 7.

Decay scheme of $Au^{195}-Pt^{195}$.

absorption in the sample. We can therefore get a better value from the intensity of its photo-electrons as compared to the intensity of the X-rays photo-electrons (Fig. 6). For this we only need the relative efficiency of our radiator for L photo-electrons of the Pt X-rays and the 97 keV γ-ray. The L photo-electrons efficiency for Hg X-rays, 157 keV and 208 keV γ-rays could be easily determined from the photo-electron measurements in Au^{199} (Fig. 3), and from this we determined, by interpolation, our data. The resulting value for $\varkappa^{97}$ is:

$$\varkappa^{97} = 0{,}90 \pm 0{,}05. \tag{13}$$

To determine the true K/L ratio of the 97 keV conversion electrons we proceed in the following way: assuming $\varkappa^{129} = 1$ we see from Table IV that $\varkappa_L^{97} = 0{,}12$; combined with equation (13), we get:

$$(K/L)_{97} = 5{,}7. \tag{14}$$

Concerning the 29 keV γ-ray one can say that $\varkappa_L^{29} \geqslant \varkappa_K^{97}$, since the absorption of the 29 L line is bigger than that of the 97 K, and the experimental peaks are roughly equal (Fig. 5). Thus:

$$\varkappa_L^{29} \geqslant 0{,}75. \tag{15}$$

It is difficult to draw any quantitative results from the measurements of the coincidence rates for each of the lines. Most of the conversion lines with which we have to do in this case are of such a low energy that they fall on the steep part of the efficiency curve of the crystal. Thus relatively small variations in the energy due to scattering of the electrons in the sample and in the backing affect strongly the efficiency, which cannot therefore be controlled.

The most outstanding feature of these coincidence measurements is the big difference in β between the K conversion line of the 129 keV γ-ray and its L and M conversion lines. This was checked in a number of samples, and always gave the same result. A satisfactory explanation for it, which will be much supported later, is the existence of another γ-ray, of energy nearly equal to 129 keV, with a higher coincidence rate and bigger K/L ratio than those of the 129 keV γ-ray. One notices immediately that the cross-over transition 29 + 97 could fulfill these requirements if it were of low enough intensity to "hide" itself in the tails of the 129 keV conversion lines, and if it had a big enough K/L ratio. Its high coincidence rate will be explained by its being in cascade with the 129 keV γ-ray.

As the number of transitions via a 126 keV γ-ray (the cross-over transitions) is at any rate small, the 129 keV γ-ray is effectively in coincidence only with the 97 keV γ-ray in our coincidence arrangement (since the 29 keV conversion lines have zero efficiency at the crystal). Similarly the 97 keV γ-ray is effectively in coincidence only with the 129 keV γ-ray, whereas the 29 keV γ-ray is effectively in coincidence with both the 97 keV and the 129 keV γ-rays. Thus we should have:

$$\beta_{29} \sim \beta_{97} + \beta_{129}. \tag{16}$$

Inspection of Table IV shows that this is very nicely fulfilled if we take for β_{129} the value measured on the 129 L or 129 M lines, giving one further support to our decay scheme.

B. The Pt d-x.n products.

Pt was irradiated with deuterons in the cyclotron of the Instituut voor Kernphysisch Onderzoek in Amsterdam*). The Au fraction was separated electrolytically; it showed the known half-lives of: 39^h (Au 194), 180^d (Au 195), 5,6^d (Au 196), and 3,2^d (Au 199)[13]). In the Pt fraction the 3,8^d activity was found, and its spectrum agreed in all details with the 3,8^d activity from the neutron-irradiated Pt. No activity of intensity comparable to the 3,8^d one and with a longer half life was found in the Pt fraction.

§ 3. *Au^{195}; experimental results.*

The electron spectrum of the long lived Au^{195} is shown in Fig. 8, along with its coincidence spectrum. Although the decay of each line was not followed long enough to find small differences in their half-lives, it is believed they all have the same period since their ratios did not show any systematic increase or decrease. The interpretation of the spectrum is given in Table V together with the coincidence rate on some of the lines.

Table V.

Energy of conv. line in keV	Interpretation	Relat. inten.	Coinc. rate
8, 10, 12	*L* Auger		3,0%
15	29 *L*	9,0	2,9%
18,5	97 *K*	29,2	1,0%
24	29 *M*	3,1	2,5%
26,5	29 *N*	0,9	2,4%
49	126 *K*+*KLL* Auger		
51, 59, 62	*K* Auger		
83	97 *L*	9,2	0,6%
93	97 *M*+*N*	2,4	0,4%
113	126 *L*	0,55	0,4%
124	126 *M*	0,2	

*) We are deeply indebted to Prof. Bakker for carrying out this irradiation in his institute.

The interpretation of the Auger lines as such is based on energy considerations as well as on the fact that they were the only ones to follow a "compound" half-life composed of all the initial half-lives present in the Au fraction.

Discussion of experimental results; decay scheme.

The most striking feature of these measurements is the reappearence of the 29 keV and 97 keV γ-rays previously found in the neutron-irradiated Pt. Unfortunately the Pt sample was much thicker than this carrier free Au sample, so that no comparison of the K/L ratios can be done. However, the facts that the $(L/M)_{97}$ ratio is the same in both cases and that the γ-rays agree so well in energy favour very much their being the same lines.

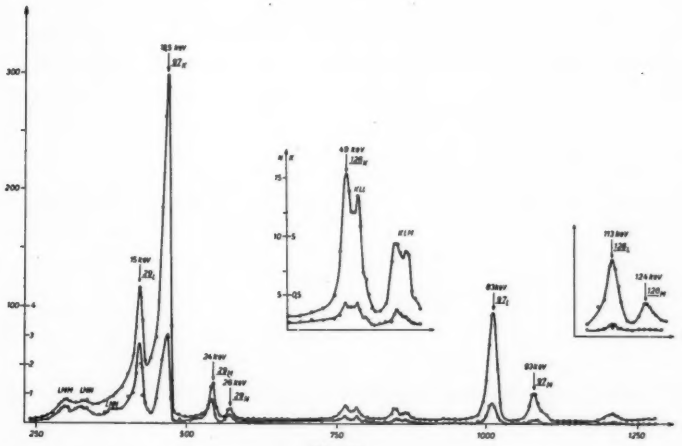

Fig. 8.

Electron spectrum of Au^{195}.
Upper curve – single counts; lower curve – coincidences.

Thus we justify, à posteriori, the assignment of mass number 195 to the $3{,}8^{d}$ isomeric state in Pt.

We further notice that although the Au sample is thinner than the Pt one, the 29 keV γ-ray is more intense in the second one. As the lines in the Au sample are formed through a K capture, this is only possible if the 29 keV γ-ray is above the 97 keV one.

A γ-ray of 126 keV and low intensity is seen to exist in the Au sample (Fig. 8). It was of great importance to clarify whether this

is the same one as the 129 keV γ-ray found in the Pt sample or not. If it were the same, then from intensity considerations one would conclude that the 129 keV γ-ray is above the others, and is thus responsible for the existence of the isomeric state in Pt. This would mean that the 129 keV γ-ray probably starts from a level of a high spin. As it is very improbable that a single level in Au will decay by K-capture to three levels in Pt which differ much in their spins, the identity of the "126" keV γ-ray and that of the 129 keV would imply the existence of an isomeric state in Au^{195} which decays to the isomeric state in Pt^{195} with roughly the same half-life of 180^d.

To clear this point it was not enough to measure the energies of the conversion lines, because the K conversion line of the 126 keV γ-ray overlaps partially the KLL Auger lines and the exact position of the maximum is not to be determined with the resolving power at our disposal. For the same reason it is impossible to draw any conclusions from the K/L ratio. The position of the L conversion lines will not settle the problem either, as variations in the relative intensity of the L_{I}, L_{II}, and L_{III} conversions may account for the coincidence of the "L" conversion lines of two slightly different γ-rays.

However, if the two lines are the same then the coincidence rates on both of them should be equal as can be seen by very simple considerations. Anyhow, any deviations from equality, caused by absorption in the sample and other by-effects, could only be in such a direction as to reduce the coincidence rate in our Pt sample. Comparison of Tables IV and V proves definitely that these two lines are different. The most natural assumption will now be that the 126 keV γ-ray is the cross-over transition (29 + 97), which is thus fed from the same level in Au as are the 29 keV and 97 keV γ-rays, and whose existence is also needed to explain the different coincidence rates on the 129 K and 129 L lines in the Pt sample. The decay scheme of Au^{195} would thus be as shown in Fig. 7.

A further check on this decay scheme is provided by considering the coincidence rates on the different lines; one should only remember in this connection that every line which is in coincidence with K Auger electrons (as is the case for all K conversion lines and for every conversion line which follows a K-capture) has, in Pt, a coincidence rate of 0,4% (see the discussion following Formula 7). We then see that the coincidence rates on the 126 keV conversion lines, as well as on those of the 97 keV γ-ray can be attributed to this effect. (The 97 K line is twice in coincidence with K Auger electrons: with those arising from the K-capture and with those

resulting from the filling of the holes in the K shell produced by the K conversion.) The additional coincidence rate on the 29 keV conversion lines arises from coincidences with the 97 keV conversion electrons; this rate fits with the coincidence rate on the 129 keV conversion lines in the 3,8^d Pt^{195}, which are also in coincidence with the same 97 keV γ-ray.

Using previously determined absorption curves of the counter foils we used[12]), and neglecting the absorption in the carrier free Au sample, we get, using the data of Table V:

$$(K/L)_{97} = 5{,}8 \pm 0{,}3 \quad (L/M)_{29} = 4{,}6 \pm 0{,}4 \tag{17}$$

in good agreement with (14) obtained in the Pt sample.

Using the values $\varkappa^{97} = 0{,}9$, $\varkappa_L^{29} = 0{,}76$ we get that 35% of the K-captures go to the 126 keV level and 65% go to the 97 keV level.

The total conversion coefficient of the 126 keV γ-ray could not be determined, but if one takes α_K from the tables of Rose et al.[18]), together with the K/L ratios from the experimental graphs for this ratio[19]), one finds that its conversion is not less than about 70% (for E 2; E 1 is very improbable), and thus that no more than 10% of the decays from the 126 keV level in Pt^{195} are going via the cross-over transition.

Table VI summarizes the results obtained for the different γ-rays appearing in the decay of Au^{195}-Pt^{195}.

Table VI.

γ	$\varkappa$				α				K/L
	K	L	M	Tot	K	L	M	Tot	
29		>0,75	>0,13	>0,88		>6,0	>1,3	>7,3	
97	0,74	0,13	0,03	0,90	7,4	1,3	0,3	9,0	5,8
126									<1,8
129	0,15	0,58	0,27	1	very big				0,26

CHAPTER II

Spin assignments.

§ 1. *Theoretical predictions.*

We shall now try to assign the spins and parities to the different states of the nuclei considered in the previous chapter as well as of other ones, and see to what extent can the shell-model be applied to these states and whether the rule referred to at the introduction holds or not. That is: we shall try to see whether successive odd nuclei which have their odd particle in the same sub-shell have or have not similar decay-schemes.

Let $E(j)$ be the energy of one nucleon in the state j, and let $E^*(j)$ be the energy of a pair of equivalent nucleons in the state j. That is:

$$E^*(j) = 2E(j) - P(j) \tag{1}$$

where $P(j)$ is the pairing energy in the state j.

For the sake of simplicity we shall talk of the "multiplet" of all the terms arising from a certain configuration of nucleons coupled according to the j-j coupling scheme. This should not be confused with the spin multiplets in the L-S coupling scheme. The "ground state" of a certain configuration would be the lowest term in its multiplet. We shall measure all energies from the bottom of the potential well, so that all energies are positive, and a bigger energy means a less bound state.

Let us consider two states — j_1 and j_2 — of which the first is the lower; that is:

$$E(j_1) < E(j_2). \tag{2}$$

Let us further assume that j_1 is also a lower state for pairs of nucleons, i.e.:

$$E^*(j_1) < E^*(j_2). \tag{3}$$

In spite of these relations it is sometimes possible that the ground state of the configuration $j_1^{n-1} j_2^2$ will be lower than any other configuration of $n+1$ nucleons, especially the configuration $j_1^n j_2^1$, if n is the number of particles in the closed shell j_1 ($n = 2j_1 + 1$).

To see what are the conditions for such a situation to be realized we note that the energy of the configuration $j_1^{n-1} j_2^2$ is:

$$E(n-1,2) = (n-2)/2\, E^*(j_1) + E(j_1) + E^*(j_2), \tag{4}$$

and similarly:

$$E(n,1) = (n/2)\, E^*(j_1) + E(j_2) \tag{5}$$

so that:

$$E(n-1,2) - E(n,1) = [E^*(j_2) - E^*(j_1)] - [E(j_2) - E(j_1)]. \tag{6}$$

Therefore: the ground state of the configuration $j_1^{n-1} j_2^2$ will be lower than the ground state of any other configuration provided the following inequality holds:

$$[E^*(j_2) - E^*(j_1)] < [E(j_2) - E(j_1)] \tag{7}$$

and provided $n = 2\, j_1 + 1$ (otherwise j_1^{n+1} is lower). From (1) and (2) we now get that a necessary condition for the existence of (7) is:

$$P(j_2) - P(j_1) > E(j_2) - E(j_1) > 0. \tag{8}$$

It will be recalled that in Mayer's model[8]) the pairing energy of nucleons in some states is assumed to bring these "paired" states so much lower that $[E^*(j_2) - E^*(j_1)] < 0$. This is easily seen to be an extreme case of our considerations.

For the sake of brevity we should like to call the above effect as that of "delayed closing" of sub-shells.

Pt^{195}, Hg^{197}, and Hg^{199} are all odd-neutron nuclei which have their odd neutron in the (82 — 126) shell. The shell model predicts for neutrons in this shell the following states:

$$h_{9/2}, f_{7/2}, p_{3/2}, p_{1/2}, f_{5/2}, i_{13/2}.$$

The energy of the states probably increases in this order. As the pairing energy is bigger for states of higher spin, we could expect a delayed closing of sub-shells only when the higher sub-shell has a higher spin too. Thus in the (82—126) neutron shell, the $p_{1/2}$ could remain unfilled while the upper sub-shells $f_{5/2}$ and $i_{13/2}$ are being filled.

Table VII contains the occupation numbers of the different levels for an odd nucleus which has 117 neutrons (such as Pt^{195}), as would be predicted by the shell model for the first few excited configura-

Table

Config.	$h_{9/2}$	$f_{7/2}$	$p_{3/2}$	$p_{1/2}$	$f_{5/}$
G	10	8	4	1	6
A	10	8	4	0	6
B	10	8	4	2	5
C	10	8	3	2	6
D	10	8	4	2	6
E	10	8	4	2	3

Table

Element	Energy of γ-ray	Exp. α_K	Calculated α_K							
			E 1	E 2	E 3	E 4	M 1	M 2	M 3	M
Pt^{195}	129	big				2,8	3,6	17,5	73	2
Pt^{195}	97	$7,4+8,2$ $-2,8$		0,95	1,7	3,9	7,6	38	>160	
Hg^{197}	164	>4,6				1,8			27	
Hg^{197}	133	0,5	0,17	0,47	0,97		3,4			
Hg^{199}	157	0,33	0,12	0,32	0,67		2,3			
Hg^{199}	208	0,98		0,16	0,32		0,94	8,0		
Hg^{199}	368	>6,8				0,29				4

able VII.

$f_{5/2}$	$i_{13/2}$	Energy difference
6	6	0
6	7	$E(13/2) - E(1/2)$
5	6	$[E^*(1/2) - E^*(5/2)] - [E(1/2) - E(5/2)]$
6	6	$[E^*(1/2) - E^*(3/2)] - [E(1/2) - E(3/2)]$
6	5	$[E^*(1/2) - E^*(13/2)] - [E(1/2) - E(13/2)]$
3	8	$[E^*(1/2) - E(1/2)] - [E^*(5/2) - E(5/2)] + [E^*(13/2) - E^*(5/2)]$

able VIII.

		Exp. K/L	Expected K/L								Ref.
I 3	M 4		E 1	E 2	E 3	E 4	M 1	M 2	M 3	M 4	
3	200	0,26		0,41	0,17				1,3	0,32	Present Work
160		5,8		<0,2			7,4	3,9			Present Work
7	86	0,45		0,42					1,7	0,52	[10])
		0,42		0,41	0,17				1,3	0,32	[10])
		0,67		0,40					1,65	0,30	Present Work
		5,65		1,0			7,8	6,0	2,4		Present Work
	4,4	1,6		2,45	1,63	0,56			4,4	1,62	[13])

tions, together with the energy difference between the lowest state of each configuration and the ground state G.

With the assumption of the single particle model the ground states of the configurations G, A, B, C, D, E are respectively: $p_{1/2}$, $i_{13/2}$, $f_{5/2}$, $p_{3/2}$, $i_{13/2}$, and $f_{5/2}$, and thus these should be the first few excited states in nuclei having 117 neutrons. It is easily seen that the same excited states should also occur in nuclei having any

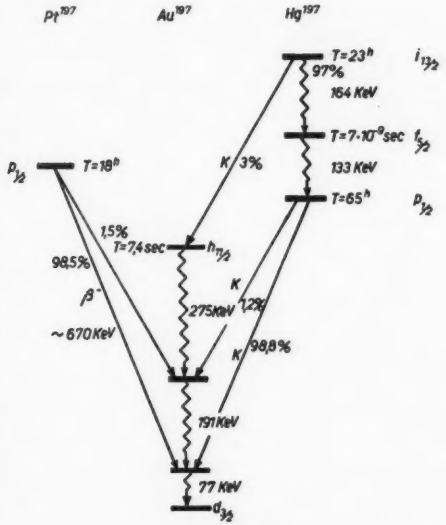

Fig. 9.
Decay scheme of Hg^{197}.

number of odd neutrons between 111 and 125, except the states A and D which do not appear at $N = 125$ and $N = 111$ respectively. States like E have little chances to be excited in usual cases since a transition to them usually involves a double nucleon transition and this is forbidden in a strict single particle model. Usually they are quite high too.

§ 2. *Comparison with experiment.*

Table VIII gives the experimental conversion coefficients and K/L ratios of some transitions in Pt and Hg, together with the calculated[18]) values of α_K and the expected K/L ratios[19]) for different multipole orders. For energies lower than 150 keV the values of α_K

were obtained by extrapolation. The expected K/L ratios were obtained by interpolation from the experimental graphs of K/L vs. Z^2/E; they are intended to give a rough estimate rather than an accurate value of the K/L ratio.

Pt^{195}.

The spin of Pt^{195} in the ground state is measured to be 1/2, and the magnetic moment suggests it is a $p_{1/2}$ state. The α_K of the 97 keV γ-ray could not be measured accurately because of its high value, but even with the relatively big error one sees from Table VIII that it could fit either with an E 4 or an M 1. However, the high K/L ratio of the 97 keV γ-ray and its short half-life ($< 10^{-6}$ sec as can be ascertained from our coincidence measurements) favour the M1 assignment rather than the E 4. Taking into account the spin of the ground state this shows that the 97 keV level is $p_{3/2}$.

The ground state of Au^{195} is probably $d_{3/2}$ (as are the ground states of Ir^{193} and Au^{197}, where both the spins and the magnetic moments are known). As the two K-captures from this state do not differ much in energy (29 keV) and are of the same order of intensity, we conclude that the 126 keV level could be $p_{1/2}$, $p_{3/2}$ or $f_{5/2}$ (opposite parity to that of $d_{3/2}$ and with $\Delta I = 0$ or 1). If it were $p_{1/2}$ or $p_{3/2}$ the 29 keV γ-ray and the 126 keV would both be M 1. This would not fit the experimental results which show that the 126 keV transition is less probable than the 29 keV one. We therefore conclude that the level at 126 keV is $f_{5/2}$.

As for the isomeric transition, its high conversion suggests it is a magnetic multipole, and its K/L ratio fixes it as an M 4. Thus the level at 255 keV is $i_{13/2}$.

Hg^{197}.

The spin of the ground state is probably 1/2 and the state is a $p_{1/2}$ (the same as in Hg^{199}). The 133 keV transition fits very well with an E 2 (Table VIII) and fixes the intermediate state as $f_{5/2}$. The half-life of the intermediate state also fits with the assignment of this multipole order for the 133 keV γ-ray[19]. The isomeric transition fits nicely the predicted values for α_K and K/L ratio of an M 4 transition. Thus the highest level is $i_{13/2}$.

A further evidence for the assignment of the spin 5/2 to the intermediate state is the $(e^- - e^-)$-angular correlation[20], which was shown to contain a $\cos^4\vartheta$ term, thus proving that the intermediate state has a spin of at least 5/2 units.

Hg^{199}.

The measured spin and magnetic moments of the ground state suggest it is a $p_{1/2}$ one. The 157 keV γ-ray fits best with an E 2 transition, thus fixing the 157 keV level as $f_{5/2}$. The branching of the level at 208 keV suggests that the 51 keV γ-ray and the 208 keV one are of the same multipole order. The conversion of the 208 keV γ-ray fixes it as an M 1 transition, thus suggesting that the level at 208 keV is $p_{3/2}$. The isomeric transition is again M 4, and the isomeric state — $i_{13/2}$. The absence of angular correlation between the β-spectrum from Au^{199} and any of the following γ-rays supports this spin assignment for the different levels in Hg^{199}.

§ 3. *Conclusion.*

It is seen that all the single particle states predicted by the shell model appear in these nuclei and no other levels are found. (The $p_{3/2}$ is not found experimentally in Hg^{197}; this could be wholly attributed to the mode of exciting the levels in this nucleus. If the $p_{3/2}$ state is above the $f_{5/2}$ or below and very near to it one cannot expect its being excited via a transition from the isomeric state or from the $f_{5/2}$ state. This is clearly seen in Hg^{199}.)

The relative positions of the different levels change continuously by adding two protons or two neutrons: the energy of the isomeric transition increases with a resulting decrease in the half-life. The energy of the E 2 transition which follows the isomeric state increases too with A, though less rapidly. The $p_{3/2}$ level moves upwards in relation to the $f_{5/2}$ level as one adds pairs of protons or neutrons.

It is perhaps instructive to compare this behavior of the energy levels with the behavior of the corresponding levels at the end of the (50—82) shell as exhibited by different isotopes of Te, Xe, and Ba. There, too, the isomeric transition ($h_{11/2} - d_{3/2}$) increases in energy as one adds pairs of equivalent nucleons, and in the same time the $s_{1/2}$ level moves upwards in relation to the $d_{3/2}$ one, and indeed crosses it, very much the same as the $p_{3/2}$ crosses the $f_{5/2}$ level in the (82—126) shell.

It is hoped that further study of other odd A isotopes of Hg, Pt, Os, etc. will show whether the excellent accord of the hitherto measured isotopes with the single particle model is accidental or real.

We wish to thank Prof. P. Scherrer for his kind interest in this work and Dr. Igal Talmi for many helpful discussions.

Referenees.

[1]) W. Elsasser, J. de phys. et rad. **5**, 625 (1934).
[2]) M. G. Mayer, Phys. Rev. **74**, 235 (1948).
[3]) H. E. Suess, Phys. Rev. **81**, 1071 (1951).
[4]) Haxel, Jensen, and Suess, Phys. Rev. **75**, 1766 (1949).
[5]) E. Feenberg and K. C. Hammack, Phys. Rev. **75**, 1877 (1949).
[6]) L. W. Nordheim, Phys. Rev. **75**, 1894 (1949).
[7]) M. G. Mayer, Phys. Rev. **75**, 1969 (1949).
[8]) M. G. Mayer, Phys. Rev. **78**, 16 (1950).
[9]) A. de-Shalit, to be published.
[10]) O. Huber, F. Humbel, H. Schneider, A. de-Shalit, and W. Zünti, Helv. Phys. Acta **24**, 127 (1951).
[11]) O. Huber, F. Humbel, H. Schneider and A. de-Shalit, Helv. Phys. Acta **25**, 3 (1952).
[12]) H. Schneider, O. Huber, and A. de-Shalit, Helv.Phys. Acta **25**, 259 (1952).
[13]) K. Way, L. Fano, M. Scott, and K. Thew, Nuclear Data, Circular of the N.B.S. No. 499.
[14]) We are indebted to Mr. H. Huber for performing this experiment.
[15]) R. D. Hill, Phys. Rev. **79**, 413 (1950); P. M. Sherk and R. D. Hill, Phys. Rev. **83**, 1097 (1951).
[16]) O Huber, F. Humbel, H. Schneider, and W. Zünti, Helv. Phys. Acta **23**, 855 (1950).
[17]) H. S. W. Massey and E. H. S. Burhop, Proc. Roy. Soc., A, **153**, 661 (1936).
[18]) Rose, Spinard, Goertzel, Haar, and Strong (privately circulated report).
[19]) M. Goldhaber and A. W. Sunyar, Phys. Rev.
[20]) H. Frauenfelder, M. Walter, and W. Zünti, Phys. Rev. **77**, 557 (1950).

Remarks Concerning a Paper by Wilker[1])

by **Richard W. Iskraut**
University of Maryland, College Park, Maryland, U.S.A.

(20. XII. 1951.)

WILKER states that, $W(1)$[2],

$$\frac{dr}{dt} = \frac{\partial r}{\partial t} + [r, H] \tag{1}$$

is invariant with respect to a homogeneous canonical transformation only for the trivial case of a free particle.

WILKER deduces this result by using the homogeneous canonical formalism, $W(2)$, $W(3)$,

$$q_i' = \frac{\partial \mathfrak{H}}{\partial p_i}, \quad P_i' = -\frac{\partial \mathfrak{H}}{\partial q_i}; \quad \mathfrak{H}(q_i, p_i) = 0 \tag{2}$$

$$[i = 1, \cdots f+1]$$

$$r' = \{r, \mathfrak{H}\} \tag{3}$$

$$\mathfrak{H} \equiv t'(\tau)(H + p_t) \tag{4}$$

WILKER shows, $W(4)$, that, if $r = r(q_i, t, p_i, p_t)$

$$\frac{dr}{dt} = \frac{\partial r}{\partial t} + [r, H] - \frac{\partial H}{\partial t}\frac{\partial r}{\partial p_t} \tag{5}$$

WILKER now concludes that (1) follows from (5) only if $\partial H/\partial t = 0$.

Now (1) is usually understood to apply in the formalism that can be LORENTZ invariant, but that is not LORENTZ invariant in appearance. In this formalism r is expressed as a function of q_i, p_i, t. If r is a function of H as well (or any other quantity, e.g. angular momentum),

$$\frac{dr}{dt} = \frac{\partial r}{\partial t} + [r, H] + \frac{\partial r}{\partial H}\frac{\partial H}{\partial t} \tag{6}$$

where $dH/dt = \partial H/\partial t$.

(6) is equivalent to WILKER's $W(4)$, (5) above, because $\mathfrak{H} = 0$, and $p_t = -H$. However, the third term on the right side of (6) will

---

[1]) P. WILKER, Helv. Phys. Acta, 319, **24**, 1951.

[2]) $W(1)$ etc. refers to WILKER's paper.

not appear if H is expressed as a function of q_i, p_i, t. (6) therefore reduces to (1) by arranging that $\partial r/\partial H = 0$, and not by using WILKER's stronger condition $\partial H/\partial t = 0$.

If $r = r(q_i, p_i, t)$ in one inertial system, and we carry out a LORENTZ transformation, the Hamiltonian will appear in the function. For a scalar r

$$r(q_i, p_i, t) = \bar{r}(\bar{q}_i, \bar{p}_i, \bar{H}, \bar{t}) \tag{7}$$

where the bar quantities refer to the new inertial system. $\bar{H}$, however, can be expressed as a function of $\bar{q}_i$, $\bar{p}_i$, $\bar{t}$, and, if we substitute $\bar{H}$ expressed as a function of $\bar{q}_i$, $\bar{p}_i$, $\bar{t}$ in $\bar{r}$, the expression (1) will also hold in the new inertial system, because $\partial \bar{r}/\partial \bar{H} = 0$.

It may also be remarked here that the homogeneous canonical formalism can be developed very simply by relating the formulation that is non-covariant in appearance

$$\delta \int L\left(x_i, \frac{dx_i}{dt}, t\right) dt = 0$$

with the covariant formulation

$$\delta \int \mathfrak{L}\left(x_\mu, \frac{dx_\mu}{d\tau}\right) d\tau = 0$$

in the following way:

$$L\left(x_i, \frac{dx_i}{dt}, t\right) dt = \mathfrak{L}\left(x_\mu, \frac{dx_\mu}{d\tau}\right) d\tau. \tag{8}$$

Lehrbücher und Monographien aus dem Gebiete der exakten Wissenschaften

MATHEMATIK

ZWINGGI, E.: Versicherungsmathematik	31.20
FUETER, R.: Analytische Geometrie der Ebene und des Raumes	24.95
LINDER, A.: Statistische Methoden für Naturwissenschafter, Mediziner und Ingenieure, 2. Auflage 1951	31.20
OSTROWSKI, A.: Vorlesungen über Differential- und Integralrechnung, Band 1, Funktionen einer Variablen	56.15
OSTROWSKI, A.: Vorlesungen über Differential- und Integralrechnung, Band 2, Funktionen mehrerer Variablen	69.70
STIEFEL, A.: Lehrbuch der darstellenden Geometrie	29.65
CARATHEODORY, C.: Funktionentheorie, Band 1	39.50
CARATHEODORY, C.: Funktionentheorie, Band 2	27.05
BIEBERBACH, L.: Theorie der geometrischen Konstruktionen	*
HERRMANN, H.: Übungen zur projektiven Geometrie	*

PHYSIK

GOMBAS, P.: Theorie- und Lösungsmethoden des Mehrteilchenproblems der Wellenmechanik	33.30
REICHENBACH, H.: Philosophische Grundlagen der Quantenmechanik	26.–

CHEMIE

NIGGLI, P.: Grundlagen der Stereochemie	37.45
BRANDENBERGER, E.: Röntgenographisch-analytische Chemie	31.20
KARRER, P., und JUCKER, E.: Carotinoide	47.85
NOWACKI, W.: Fouriersynthese von Kristallen	34.30

EXPERIMENTELLE BIOLOGIE

GÄUMANN, E.: Pflanzliche Infektionslehre, 2. Auflage 1951	46.30
LEHMANN, F. E.: Einführung in die physiologische Embryologie	39.50
MURALT, A. VON: Die Signalübermittlung im Nerven	43.70
GÄUMANN, E.: Die Pilze, Grundzüge ihrer Entwicklungsgeschichte und Morphologie	39.50

ASTRONOMIE

PAHLEN, E. VON DER: Einführung in die Dynamik von Sternsystemen	39.50
NIETHAMMER, TH.: Die genauen Methoden der astronomisch-geographischen Ortsbestimmung	36.40
WALDMEIER, M.: Einführung in die Astrophysik	49.40
WALDMEIER, M.: Die Sonnenkorona I	29.75

Lehr- und Handbücher der Ingenieurwissenschaften

STÜSSI, F.: Vorlesungen über Baustatik	40.05
MEISSNER, E., und ZIEGLER, H.: Mechanik, Band 1, Statik, 2. Aufl.	37.45
MEISSNER, E., und ZIEGLER, H.: Mechanik, Band 2, Dynamik	33.80
JAEGER, CH.: Technische Hydraulik	52.–
KUHLMANN, K.: Theoretische Elektrotechnik, Band 1	*
KUHLMANN, K.: Theoretische Elektrotechnik, Band 2	27.55
KUHLMANN, K.: Theoretische Elektrotechnik, Band 3	74.90
RUSTERHOLZ, A.: Elektronenoptik, Band 1	31.20
GOLDSTEIN, J.: Die Messwandler	*
VIDMAR, M.: Die Gestalt der elektrischen Freileitung	19.75

Wissenschaft und Kultur

SPEISER, A.: Die mathematische Denkweise	15.10
FIERZ-DAVID, H. E.: Die Entwicklungsgeschichte der Chemie	**
GAMOW, G.: Geburt und Tod der Sonne	25.50
STRAUB, H.: Die Geschichte der Bauingenieurkunst	23.40
NIGGLI, P.: Probleme der Naturwissenschaften	19.25
SPEISER, A.: Elemente der Philosophie und Mathematik	11.45

Technik

COHEN, A.: Rationelle Metallanalyse	47.85
RICHTER, R.: Elektrische Maschinen, Band 1	49.40
STÄGER, H.: Allgemeine Werkstoffkunde	49.40
BODEA, E.: Giorgis rationales MKS-Maßsystem mit Dimensionskohärenz	28.10
FIERZ-DAVID, H. E., und MERIAN, E.: Abriß der chemischen Technologie der Textilfasern	37.95
DISERENS, L.: Die neuesten Fortschritte in der Anwendung der Farbstoffe, Band 1, 3. Auflage 1951	122.70
DISERENS, L.: Die neuesten Fortschritte in der Anwendung der Farbstoffe, Band 2	81.10
DISERENS, L.: Die neuesten Fortschritte in der Anwendung der Farbstoffe, Band 3	78.—
DISERENS, L.: Neue Verfahren in der Technik der chemischen Veredlung der Textilfasern, Band 1	91.—
DISERENS, L.: Neue Verfahren in der Technik der chemischen Veredlung der Textilfasern, Band 2	*
DISERENS, L.: Neue Verfahren in der Technik der chemischen Veredlung der Textilfasern, Band 3	*

Einzelwerke

LOCHER-ERNST, L.: Differential- und Integralrechnung im Hinblick auf ihre Anwendung	49.90
HURWITZ, A.: Mathematische Werke, Band 1: Funktionentheorie	54.10
idem Band 2: Zahlentheorie, Algebra, Geometrie	54.10
SCHLÄFLI, L.: Gesammelte mathematische Abhandlungen	56.15
SCHMID, E.V.: Ins Innere von Kunststoffen, Kunstharzen und Kautschuken, 2. erweiterte Auflage	19.25
MOSER, A.: Der Dampfbetrieb der Schweizerischen Eisenbahnen 1847—1947	31.20
THOMMEN, E.: Taschenatlas der Schweizer Flora	13.50
KALMUS, H.: Einfache Versuche mit Insekten	10.15
GYSEL, H.: Prozenttabellen organischer Verbindungen	125.—

* In Vorbereitung — * En préparation

** 2. Auflage in Arbeit — ** 2me édition en préparation

Verlangen Sie bitte Spezialprospekte

VERLAG BIRKHÄUSER AG. BASEL

Sämtliche Bücher können in den Buchhandlungen bezogen werden